EVALUATION OF A MICROPILE LATERALLY LOADED USING SEMIEMPIRICAL, ANALYTICAL AND COMPUTATIONAL MODELS FOR GEOTECHNICAL ENGINEERING PRACTICE

CASE OF STUDY: SABANETA

LUIS VILLEGAS NEGRETTE

Dissertation submitted as partial fulfillment of the requirements for the degree of Master in Engineering

SUPERVISOR: JORGE ALONSO PRIETO SALAZAR

MEDELLÍN

EAFIT UNIVERSITY

SCHOOL OF ENGINEERING

2017

Acceptance note

_____

_____

Chairman

_____

Examinator

_____

Examinator

_____

Medellín

01/12/2017

ACKNOWLEDGMENTS

First, I would like to express my gratitude and admiration to my bosses Pedro Salvá and Bernardo Vieco, thanks for allowing me to use the information consigned on this document for the development of this research. Their valuable advice and accurate guidelines have helped me to become the professional I am.

I want to thank my advisor Jorge Alonso Prieto for his mentoring and supervision. Without his comments, this could not be possible.

I deeply want to recognize the labor of the engineers Laura Sierra and Camilo Pérez, thanks to their commitment with this project, without that, this research could not be conducted.

Thanks to MIDAS Information Technology Co., Ltd. for allowing me to use a full license of its software MIDAS GTS NX during the development of this research, without its unconditional help and the support of the MIDAS LA team this could not have been conceivable. I want to highlight the huge collaboration from Katerine Hincapie and Angel F. Martínez, thank you for your patience and great attitude.

I would also like to thank my friends and colleagues Alejandro Velásquez, Carellys Vergara and Jaime A. Mercado for their comments and suggestion about the structure of this document and their unconditional support during this process.

I would finally like to express my deepest gratitude to both my relatives and friends, who have always encouraged me.

ABSTRACT

The Aburrá Valley's demographic increase has risen house offering. To tackle this local issue, recently the use of micropiles have spread widely, even though this system has proven to be a reliable alternative foundation to support vertical loads, its capacity to support lateral loads has always been a concern. Considering this, this research focuses in the evaluation of the behavior of a type D micropile's laterally loaded.

Two lateral load tests results are consigned and one of them is compared with results obtained from conventional methods used in practical engineering for lateral displacements estimation: semiempirical formulations, P-Y curves and three-dimensional finite element models.

The geotechnical parameters selection implications for the micropiles type D lateral displacement evaluation using semiempirical methods and P-Y curves are analyzed and briefly discussed. To recreate the triaxial tests stress-strain curves, some of the most practical constitutive soil models currently applied are revised. To evaluate the implications of the micropile injection process in the micropile lateral displacement estimation, a three-dimensional finite element model is used. Some alternative proposals for evaluation of the elastic behavior of a micropile laterally loaded are presented. Finally, conclusions are included, and some research topics are suggested.

KEYWORDS:

Micropile.
Lateral load.
Lateral deformation.
Semiempirical method.
P-Y curves.
Constitutive soil models.

RESUMEN

El incremento poblacional en el Valle de Aburrá ha llevado al aumento de la demanda de la vivienda. Para atender esto y los problemas locales, el uso de micropilotes como sistema de cimentación se ha extendido en los últimos años, y a pesar de que ha demostrado ser un sistema confiable para atender cargas verticales, su capacidad para atender solicitaciones horizontales siempre ha quedado en duda. Por eso, este trabajo se enfoca en la evaluación del comportamiento de un micropilote tipo D sometido a cargas laterales.

Se presentan los resultados de dos pruebas de carga lateral y uno de ellos se compara con los métodos convencionales usados en la ingeniería práctica para la estimación de desplazamientos laterales: formulaciones semiempíricas, curvas P-Y y modelos de elementos finitos en tres dimensiones.

Las implicaciones de la elección de los parámetros geotécnicos para la evaluación del comportamiento lateral de micropilotes tipo D usando métodos semiempíricos y curvas P-Y son analizadas y levemente discutidas. Para recrear las curvas de Esfuerzo-Deformación de los ensayos triaxiales, se revisaron algunos de los modelos constitutivos más prácticos aplicados en la actualidad. Uno modelo tridimensional de elementos finitos es usado para evaluar las implicaciones del proceso de inyección de los micropiles en la estimación del desplazamiento lateral. Se presentan algunas propuestas alternativas para la evaluación del comportamiento elástico de un micropilote lateralmente cargado. Finalmente, se dan las conclusiones y recomendaciones para futuras investigaciones.

PALABRAS CLAVE:

Micropilote.
Carga lateral.
Deformación lateral.
Método semiempírico.
Curvas P-Y.
Modelos constitutivos de suelo.

TABLE OF CONTENTS

LIST OF FIGURES

LIST OF TABLES

LIST OF ANNEXES

LIST OF SYMBOLS

T_L	Ultimate traction or compression micropile capacity
q_s	Ultimate grout to ground bond strength
$\mathrm{D_s}$	Average bond diameter
$\mathrm{L_s}$	Bond length
L_0	Depth of influence
E_p	Micropile's elasticity modulus
I_p	Micropile's inertia
E_s	Soil's elasticity modulus
P	Reaction intensity
k	Supporting medium stiffness
y	Beam's deflection
k_h	Coefficients of horizontal subgrade reaction
z	Depth of analysis below ground surface
d	Pile's width
γ	Effective unit weight
$\bar{k}_{s1}$	Basic coefficient of vertical subgrade reaction (for square area with width B = 30 cm)
q_u	Unconfined compressive strength
C_u, S_u	Undrained shear strength

ϕ’	Effective friction angle
ν	Poisson’s ratio
e	Void ratio
v_s	Shear wave velocities
L	Pile length
m	Coefficient
σ'	Vertical effective stress
y_u	Ultimate displacement
y_z	Lateral displacement
θ_z	Rotation
N_q, N_γ	Bearing capacity factors
N	Number of blows per foot (30 cm)
y/d	Normalized deflection
A, f, A_x, B_x, A_θ, B_θ, A_m, B_m, A_v, B_v, $A_{p\prime}$, B_p, A'_y, B'_y, A'_m, B'_m	Coefficients
M	Moment applied at pile head
M_z	Internal bending moment
V_z	Internal shear force
P_c	Characteristic load
M_c	Characteristic moment

T	Characteristic length of the soil-pile system
τ	Shear stress
G	Shear modulus
γ	Shear strain
F	Internal shear force
A	Transversal area where shear force is acting
ρ	Soil density
g	Gravity
t	Distance between micropile and slope crest
t_{lim}	Limit distance
r	Reduction coefficient
β	Slope angle

1 INTRODUCTION

Over the last decades the Aburrá Valley's population has grown significantly as it is presented by (Departamento Administrativo Nacional de Estadística 2017a), as a consequence, construction firms have been forced to intensify the housing offers and to improve their building practices in order to be more competitive and increase their income in a shorter period of time as it is inferred from the results of the (Departamento Administrativo Nacional de Estadística 2017b) buildings census.

To optimize the constructible areas, buildings of the Aburrá Valley are getting higher every day, what has resulted on a significant increase in service loads coming from the superstructure to the subsoil. For this reason, the need of a better understanding of subsoil conditions and the improvement of construction methods has become a constant.

Over the last 5 years, these construction firms have decided to buy micropile drilling rigs to reduce the direct cost of foundation systems, to avoid outsourcing and to have less time-consuming way to build foundations.

Even when the acquisition of micropile's construction equipment has been a profitable investment for construction firms, the Geotechnical design possibilities have been reduced almost exclusively to micropiles solutions and the wordiness about the reliability of this foundation system has become a constant.

Traditionally, micropiles are designed using some methodologies like (Lizzi 1982) and (Bustamante 1985), or design guidelines as (FHWA 2005), (Ministère de l'Équipement des Transports 1993) and (Dirección General de Carreteras 2005); nevertheless, these methodologies or guidelines are focused on the design of this element for vertical loads, and its lateral load resistance is lightly discussed or just neglected.

In concordance with the geological and geomorphological characteristics of the Aburrá Valley and its medium seismic hazard, most of the buildings of the Valley are constructed on places of moderate to very high slopes (Área Metropolitana del Valle de Aburrá 2012) and medium seismic risk (Ministerio de Ambiente Vivienda y Desarrollo Territorial 2010). These imply the presence of horizontal loads that must be supported by the structure of the building and its foundation system.

During a seismic event, deep foundations need to support lateral loads due to the initial lateral movements of the soil mass and the consequential interaction between foundation elements and the kinematic forces coming from the superstructure. This has been discussed by several authors like (Zeevaert 1983) and (Thilakasiri et al. 2009).

For the structural design of laterally loaded foundation elements, commonly, structural designers replace the soil by elastic equivalent springs. For certain conditions, this simplification can be considered correct (Day and Mucillo 2014), nevertheless; the reliability of the geotechnical methods to estimate these springs is the real concern, because there are a lot of methodologies to estimate them, but rarely the lateral expected behavior is confronted with the real one measured.

Currently, there are several methodologies developed to evaluate the lateral resistance and displacement of piles built on a specific type of soil and for specific pile conditions, however; these were not directly established for micropile elements; for which the construction method, small diameter and high reinforcement area are variables that are not considered on the actual lateral pile resistance formulation.

1.1 OBJECTIVES

To evaluate some current geotechnical methodologies used for lateral evaluation of deep foundations, analyzing their applicability to IRS micropiles built on the Aburrá Valley based on results of an IRS micropile laterally loaded.

- To perform a micropile lateral load test.
- To evaluate semiempirical moduli of subgrade reaction and their reliability.
- To calibrate a practical soil constitutive model to represent soils behavior.
- To simulate micropile lateral load test measurements.

1.2 SCOPE OF RESEARCH

The evaluation of the micropile laterally loaded is just for geotechnical purposes; considering specific site conditions and a construction method.

2 BACKGROUND

2.1 MICROPILES

Micropiles are a type of deep foundation solution conceived by (Lizzi 1950) as a technique for underpinning historical buildings affected by World War II.

The use of micropiles has extended from its original function. Nowadays, they are used to improve soils resistance and as foundation solution. Micropiles can be classified according to their use or construction grouting technique (FHWA 2005). Fig. 1 shows the (FHWA 2005) classification system.

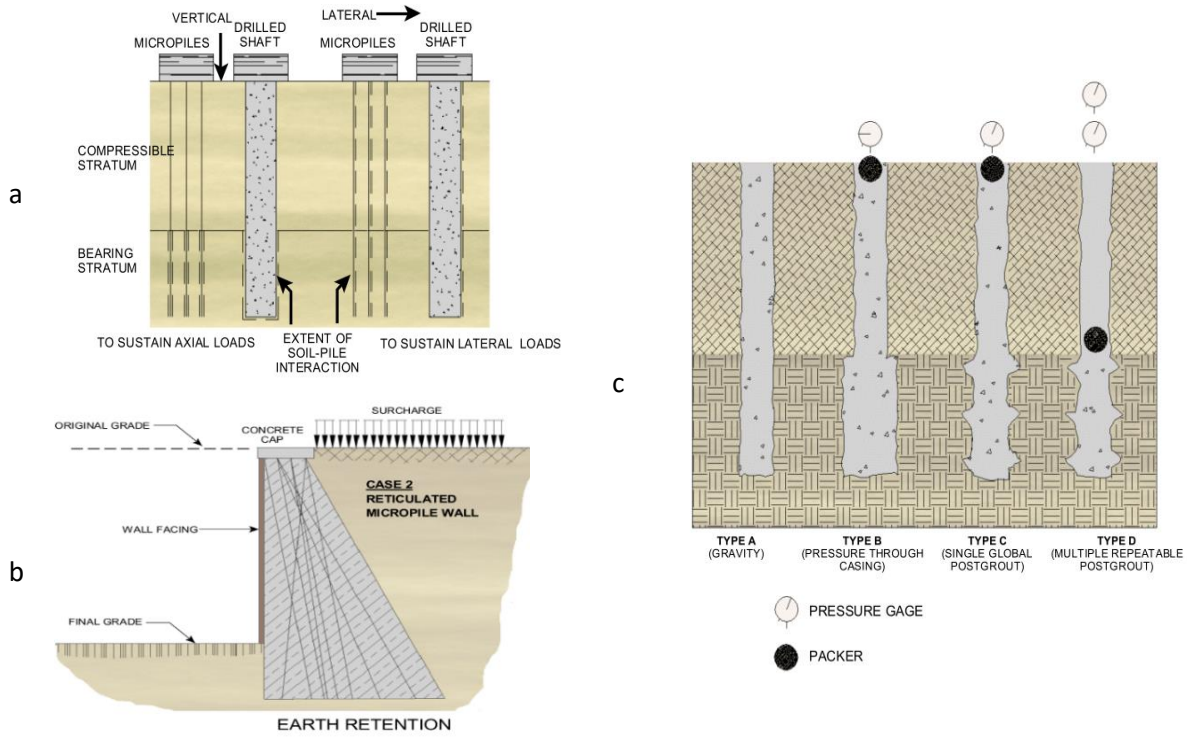

Fig. 1. Micropile classification system, a) Application classification Case 1, b) Application classification Case 2 and c) Types of grouting. After (FHWA 2005).

Case 1 micropiles are used to support vertical and lateral loads from the structure. Moreover, Case 2 micropiles are elements that work as a reticular arrangement to reinforce soil mass and improve its resistance.

The grouting (FHWA 2005) classification system is similar to DTU 13.2 used in France (L'École Nationale des Ponts et Chaussées 2004). The association and description of each classification system is shown below.

- Type A or II: foundation elements grouted by a sand-cement mortar or cement grout; placed by gravity head and non-injected.
- Type B or I: micropile's neat cement grout is placed into a pre-bored hole using injection pressure lower than in-situ lateral soil pressure to avoid hydrofracturing of surrounding soil. Typically, this injection pressure is lower than 1 MPa.
- Type C or III: is a two-stage procedure, the first stage, a micropile Type A is developed. In the second stage (15 to 25 minutes later), the grouting procedure is repeated applying a higher lateral injection pressure, which is close to the pressuremeter limit pressure and in all cases higher than 1 MPa. This kind of injection is worldwide known as IGU (Injection Globale et Unitaire).
- Type D or IV: as Type C, this methodology is a two-stage procedure. In the first one, a micropile Type B is constructed, and in the second one (after grouting has hardened), additional grout is injected using lateral pressures higher than pressuremeter limit pressure; commonly this pressure ranges between 2 to 8 MPa. This procedure can be performed several times as it is required and it is commonly known as IRS (Injection Répétitive et Sélective).

Another type of micropile that exists but is not classified yet, consists of a hollow steel bar that is employed as drilling rod during its installation and at the same time as a conduit for delivering the flushing fluid under pressure through the lost bit holes that is mounted on the tip of the bar, which allows the grouting to flush from the bottom of the borehole while drill is performed. This kind of micropile is commonly categorized as a Type B micropile, nevertheless; its construction procedure is totally different, for this reason some authors (Abd El-aziz 2012) have proposed to classify this micropile as Type E. In Fig. 2 a scheme of a Type E micropile is presented.

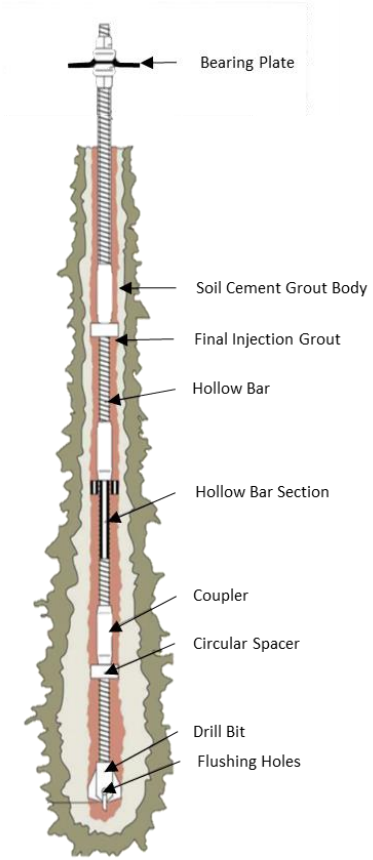

Fig. 2. Scheme of a hollow bar micropile. Adapted from (Abd El-aziz 2012).

Generally, a micropile is also characterized by its small diameter (less than 300 mm), slender ratios greater than 100 (L'École Nationale des Ponts et Chaussées 2004) and its mechanism of resistance.

Micropiles are usually designed to support vertical loads by considering only their lateral resistance capacity and neglecting their point capacity. The typical formulation used for the geotechnical design of these elements is shown on *(1)*.

$$T_L = \mathrm{q_s}\,\pi\,\mathrm{D}_s\,\mathrm{L_s} \quad (1)$$

where, T_L is the ultimate traction or compression capacity, q_s is the ultimate grout to ground bond strength, $\mathrm{D_s}$ is the average bond diameter, and $\mathrm{L_s}$is the bond length.

Some practical values and formulations i.e. (Bustamante 1985; Dirección General de Carreteras 2005; FHWA 2005) have been used to evaluate q_s. Nevertheless, this parameter is not just function of a specific soil type, installation grouting techniques used on its construction method are

important too. Taking into a count all these variables, load testing probes are commonly required to verify design assumptions.

On the other hand, for (FHWA 2005) one of the greatest limitations of micropiles is their lateral capacity. Sometimes, the main concern is just the vertical load, however, this conception is a mistake, particularly during a seismic event, where kinematic forces will result in a considerable lateral force requirement for the foundation system. As it is pointed out by (Richards and Rothbauer 2004), lateral load case often governs the design of micropiles and not just the vertical case.

Currently, lateral capacity of micropiles is estimated using theories developed for pile foundations, which do not consider the effect of the small diameter, the reinforcement controlling function and the installation method.

Sometimes, micropiles work as a group because they are connected by a cap to guarantee their unity. When a lateral solicitation exists, it is common to use a passive earth pressure resistance acting on the lateral side of the cap to verify its stability. Nevertheless, the ratio of displacement needed to develop a passive earth pressure on the cap can be excessive when it is compared to the elastic lateral displacement capacity of a micropile. Thus, a plastic hinge will be produced at certain depth. Consequently, micropiles will not be able to support the service loads coming from the superstructure.

To evaluate the influence of the lateral load on the micropile element, some formulations have been proposed. Equations *(2)* to *(4)* are some of the most used.

Author	**Equation**	
(FHWA 2005)	$L_0 = 20\mathrm{D_s}$	(2)
(Richards and Rothbauer 2004)	$L_0 = 2 \text{ to } 5 \text{ m}$	(3)
(L'École Nationale des Ponts et Chaussées 2004)	$L_0 = \sqrt[4]{\frac{4E_pI_p}{E_s}}$	(4)

where, L_0 is the depth of influence, E_p is the micropile's elasticity modulus, I_p is the micropile's inertia, and E_s is the soil modulus of elasticity

Generally, when groups of micropiles are used as foundation system lateral loads are supported by adding some battered micropiles at the cap. Nevertheless, (FHWA 2005) do not recommend this solution when ground will potentially settle around.

2.2 PILES LATERALLY LOADED

The evaluation of a pile laterally loaded can be performed based on its ultimate lateral resistance or by its allowable lateral displacement.

2.2.1 ULTIMATE LATERAL RESISTANCE

Some of the most common methodologies used to evaluate ultimate lateral resistance of soil were proposed by authors like (Brinch-Hansen 1961) and (Broms 1964a; b).

Brinch Hansen method assumes that the pile is rigid and no yield hinge can be developed, so the pile rotates as a rigid body at a certain point below the ground surface.

The above-mentioned assumptions consider that Rankine's passive earth pressure will be developed in front of the pile, and at the same time, behind the pile the active earth pressure will take place.

To develop passive earth pressure, lateral displacements are needed to be allowed, this displacement can be as large as a value close to 10% of a cantilever (pile's length), as it is shown on Fig. 3, where is presented the displacement needed to reach an earth pressure of a specific type of soil as a function of cantilever's height.

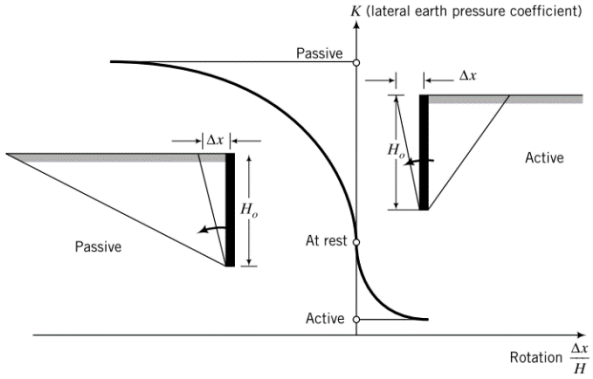

Retained soil	Stress state	Approximate displacement, Δx
Coarse-grained	Active	$0.001H_o$, (T, R)
	Passive	$0.05H_o$, (T) $> 0.1H_o$, (R)
Fine-grained	Active	$0.004H_o$, (T, R)
	Passive	unknown

T = translation, R = rotation

Fig. 3. Rotation required to mobilize active and passive earth resistance. After (Budhu 2015).

Brinch Hansen methodology can be used to estimate the ultimate lateral resistance of a pile-soil system, however, this method is not able to evaluate lateral displacements as is noted by (Ruigrok 2010).

Alternatively, Broms' formulation can be used to compute lateral deflections, ultimate lateral resistance and maximum bending moments for free head or restricted driven piles into saturated cohesive and cohesionless soils.

Broms proposed his formulation based on elastic theory to determine the behavior of pile element and soil's support reaction, he also considered that failure happens when pile's section ultimate stress or supporting soil ultimate stress is achieved.

To estimate the ultimate lateral resistance of soil, the author assumed that when a long pile is used a plastic hinge will take place at a certain depth, and that above it, the full passive resistance of soil will be developed.

Broms' method was established based on available lateral load test results, which at his time were limited, this is the reason why he recommended using his methodology with caution.

2.2.2 THEORY OF ELASTICITY

This theory expresses the elastic stress-strain relationship of a material based on Hooke's law as it is mentioned by (Timoshenko and Goodier 1951).

2.2.3 ELASTIC BEAM FOUNDATION

According to (Hetényi 1946) the elastic beam foundation methodology is based on (Winkler 1867) and (Zimmermann 1888) works. For this formulation, a perpendicular load is assumed to act along a beam member, the cross section is uniform and the element is supported by an elastic medium which will deflect as response of the applied load; therefore, a distributed reaction force will be produced on the supporting medium. The following equation was proposed to represent this behavior.

$$P = k\,y \tag{5}$$

Where, P is the reaction intensity, k is the supporting medium stiffness, and y is the beam's deflection.

Equation (5) involves that reacting medium is elastic; its constitutive material follows Hooke's law and k is a constant of proportionality that is just valid for the specific point of evaluation.

Using the elastic beam foundation formulation, a discretization of the element loaded, the flexural stiffness of a beam, equilibrium equations and differential procedures, is then possible to partially formulate equations to determine the internal forces of elements perpendicularly loaded. However, it is not possible to solve it directly and it will require the use of boundary conditions evaluations to find some integration constants. A detailed discussion of these formulations can be found on (Hetényi 1946).

2.2.4 SEMIEMPIRICAL FORMULATIONS

Several authors had formulated semiempirical coefficients of horizontal subgrade reaction (k_h) based on the elasticity theory and pile lateral load test literature reported or developed by them.

One of the first authors who proposed a semiempirical formulation was (Terzaghi 1955). He developed independent formulations for sands and clays.

For sands, he considered that k_h depends on the depth of analysis below ground surface (z), pile's width measured at right angles to the direction of projected lateral displacement (d), the effective unit weight (γ) and relative density of sand. As a result, the following formulation was proposed.

$$k_h = \frac{A\,\gamma\,z}{1.35\,d} \tag{6}$$

where, A is a coefficient, see Table 1.

Table 1. A values. After (Terzaghi 1955).

Relative density of sand	**Loose**	**Medium**	**Dense**
Range of values of A	100-300	300-1000	1000-2000
Adopted values of A	200	600	1500

Another form to present (6) is substituting $\frac{A\,\gamma}{1.35}$ value by n_h, what results in (7).

$$k_h = n_h \frac{z}{d} \tag{7}$$

For piles embedded in stiff clays, the k_h value is supposed to be constant with depth and is just function of pile's width. According to (Terzaghi 1955) this value can be estimated using (8).

$$k_h = \frac{\bar{k}_{s1}}{1.5\,d} \tag{8}$$

where, $\bar{k}_{s1}$ is the basic value of coefficient of vertical subgrade reaction (for square area with width B = 30 cm).

Suggested values proposed by (Terzaghi 1955), are shown on Table 2.

Table 2. Values of $\bar{k}_{s1}$ in kPa for square plates 30 cm x 30 cm and for long strips, 30 cm wide, resting on pre-compressed clay. Adapted from (Terzaghi 1955).

Consistency of clay	**Stiff**	**Very stiff**	**Hard**
Values of q_u (kPa)	95 – 191.5	191.5 - 383	> 383
Range for $\bar{k}_{s1}$, square plates	50 - 100	100 – 200	> 200
Proposed values, square plates	75	150	300

Various authors have used the same Terzaghi's formulation and have derivated n_h and k_h values for specific conditions. Some of the most common used on engineering practice are presented on the following table.

Table 3. k_h semiempircal formulations.

Formulation	**Equation**		
(Vesic 1961)	$k_h = \frac{0.65\,E_s}{d(1-\nu^2)}\sqrt[12]{\frac{E_s d^4}{E_p I_p}}$		(9)
(Francis 1964)	$k_h = 1885.08\gamma d N_\gamma + 3770.16\gamma z N_q$		(10)
(Broms 1964a)	$k_h = \frac{E_s}{m\,(1-\nu^2)\sqrt{L\,d}}$		(11)
	m values are shown on Table 4		
(Pise 1977)	$k_h = n_h z^{\frac{2}{3}}$		(12)
(Audibert and Nyman 1977)	$k_h = \frac{1}{A + By}$		(13)
	$A = \frac{0.145\,y_u}{yZN_q}$	$B = \frac{0.855}{yZN_q}$	

(Kishida and Nakai 1977)	$k_h = \frac{1.3\ E_s}{d(1-\nu^2)}\ \sqrt[12]{\frac{E_s d^4}{E_p I_p}}$		(14)
(Robinson 1979)	$k_h = 67\ \frac{S_u}{d}$		(15)
(Bhushan et al. 1981)	$\log lk_h = 0.82 + \log N - 0.62\ \log\frac{y}{d}$		(16)
	$k_h = 271.447\ (10^{0.82+\log N-0.62\ \log\frac{y}{d}})$		(17a)*
(Sogge 1981)	$k_h = 314.18\ to\ 4712.7\ \frac{z}{d}$		(18)
(Pyke and Beikae 1984)	$k_h = 2\frac{E_s}{d}$		(19)
(Habibagahi and Langer 1984)	$k_h = \frac{\sigma' N_q}{y}$		(20)
	$N_q = A + \sqrt{\frac{z}{d}}$	For 30°, A = 5,9,12 and 15 for y=2.54, 6.35, 12.7 and 25.4 mm	

where, E_s is the soil modulus of elasticity, E_p is the pile elasticity modulus, I_p is the pile inertia, ν is the Poisson's ratio, L is the pile length, m is the coefficient, see Table 4, σ' is the vertical effective stress, y_u is the ultimate displacement, N_q and N_γ are the bearing capacity factors, N is the SPT resistance over the embedded length of pile (blows/ft), y/d is the normalized deflection (%), and lk_h is the coefficient of subgrade reaction (lb/in^3).

*International System Adapted equation (kPa/m).

Table 4. Numerical values of m coefficient. After (Broms 1964a).

L/d	1.0	1.5	2	3	5	10	100
m	0.95	0.94	0.92	0.88	0.82	0.71	0.37

Even though several authors proposed some mathematical formulations for $k_h$like those shown on Table 3, others preferred to use intervals.

(Davisson 1970) suggested some n_h and k_h values based on his personal experience and literature reported values, see Table 5.

Table 5. Estimated values for k_h. Adapted from (Davisson 1970).

Soil type	**Value**
Granular soils	n_h ranges from 1.5 to 200 lb/in^3; is relative proportional to relativity density
Normally loaded organic silt	n_h ranges from 0.4 to 3 lb/in^3
Peat	n_h is approximately 0.2 lb/in^3

Cohesive soils	k_h is approximately $67\ C_u$

Based on field test data of lateral load test on timber piles in cohesionless soil, (Robinson 1979) suggested that k_h is independent from pile's width, and recommended the use of k_h and n_h values presented on Table 6.

Table 6. n_h and k_h values. Adapted from (Robinson 1979).

Soil Conditions			**Horizontal Subgrade Reaction**		
Soil description	**N**	**S_u, (kPa)**	**Horizontal movement (mm)**	**Type**	**Value Compute from Deflection (kPa)**
Amorphous peat	<1		26.42	k_h	689.47
3ft sand over amorphous peat			9.52	k_h	3447.38
				k_h	689.47
4ft gravelly clay over clayey silt		38.3	7.87	k_h	5102.12
	1.5	19.1		k_h	2551.06
5ft stiff clay over silt and peat	3	57.4	9.40	k_h	3447.38
	1	19.1		k_h	2068.43
Organic clay silt	<1	14.4	15.24	k_h	113.76
Layered silty sand and sandy silt	3		22.86	n_h	206.84
Layered sand and sandy silt	5		6.35	n_h	427.47
3.5ft sand over clayey silt	10		2.79	n_h	1765.06
	4				
Silty sand	5		6.09	n_h	689.47
Slightly organic silt	2		16.26	n_h	103.42
3ft organic silt over sandy silt	1		17.27	n_h	234.42
	3				

It is important to notice that some theories have been originally developed for vertical subgrade modulus, nevertheless, they are often used to estimate lateral behavior. Some of the most common used are (M.A.Biot 1937), (Skempton 1951) and (Broms 1964a).

2.2.5 NAVFAC METHOD

(NAVFAC 1986) procedure is based on the modulus of subgrade reaction and the idealized assumption that lateral loads do not exceed a third of ultimate lateral load capacity. For Granular

soils and normally consolidated cohesive soil k_h is assumed to increase linearly with depth, this is expressed by (21).

$$k_h = \frac{f * z}{d} \tag{21}$$

where, f is the coefficient of variation of lateral subgrade reaction (ton/ft^3), see Fig. 4.

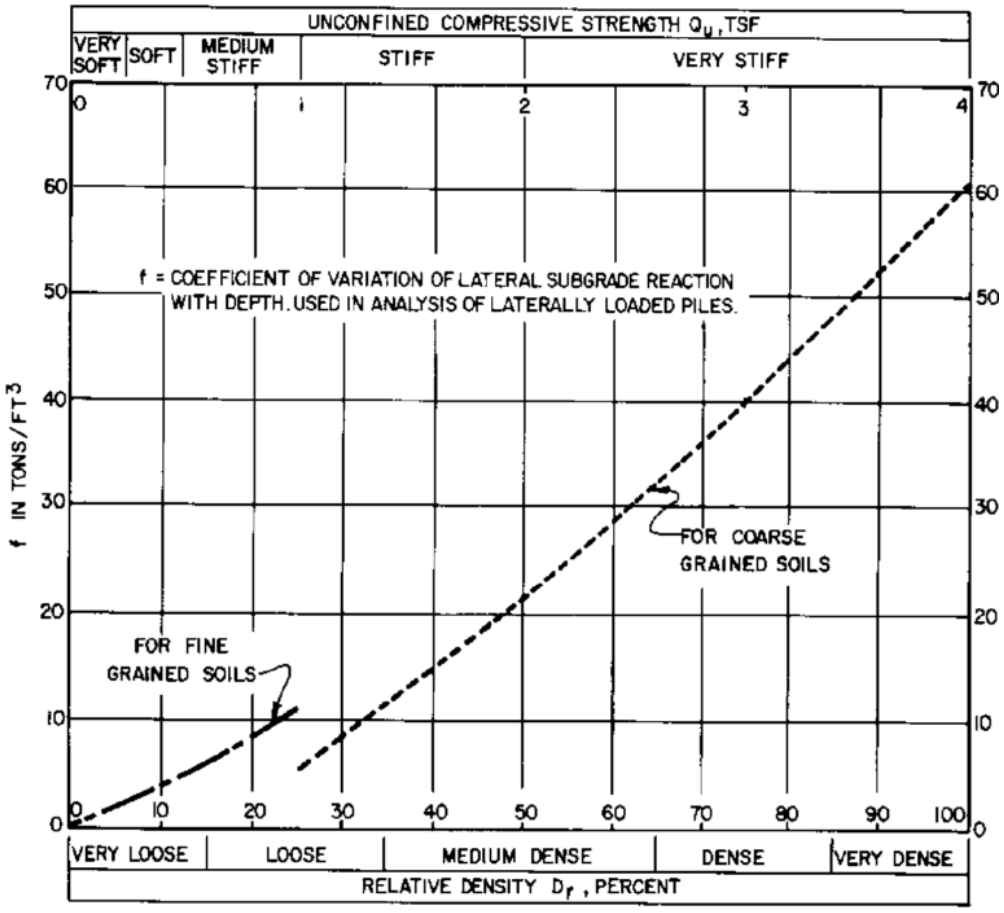

Fig. 4. Coefficient of variation of subgrade reaction. After (NAVFAC 1986).

For heavily consolidated cohesive soils the coefficient of lateral subgrade reaction is considered constant with depth. According to (NAVFAC 1986) the coefficient varies between 35 up to 70 C_u/d.

2.2.6 NONDIMENSIONAL CHARTS

This method derives from the differential equation for beam-column on a foundation given by (Hetényi 1946), the elasticity principles and some fundamental identities. Based on these principles the following equations can be defined for granular soils.

$$y_z = A_x \frac{PT^3}{E_p I_p} + B_x \frac{MT^2}{E_p I_p} \tag{22}$$

$$\theta_z = A_\theta \frac{PT^2}{E_p I_p} + B_\theta \frac{MT}{E_p I_p} \tag{23}$$

$$M_z = A_m PT + B_m M \tag{24}$$

$$V_z = A_v P + B_v \frac{M}{T} \tag{25}$$

$$p'_z = A_{p'} \frac{Q}{T} + B_{p'} \frac{M}{T^2} \tag{26}$$

where, A_x, B_x, A_θ, B_θ, A_m, B_m, A_v, B_v, $A_{p'}$, $B_{p'}$ are coefficients (see the table), M is the moment applied at pile head (kN*m), and T is the characteristic length of the soil-pile system.

$$T = \sqrt[5]{\frac{E_p I_p}{n_h}}$$

$$Z = \frac{z}{T}$$

Table 7. Coefficients for long piles in granular soils. Adapted from (Das 2002).

Z	A_x	A_θ	A_m	A_v	$A_{p'}$	B_x	B_θ	B_m	B_v	B_v
0.0	2.435	-1.623	0.000	1.000	0.000	1.623	-1.750	1.000	0.000	0.000
0.1	2.273	-1.618	0.100	0.989	-0.227	1.453	-1.650	1.000	-0.007	-0.145
0.2	2.112	-1.603	0.198	0.956	-0.422	1.293	-1.550	0.999	-0.028	-0.259
0.3	1.952	-1.578	0.291	0.906	-0.586	1.143	-1.450	0.994	-0.058	-0.343
0.4	1.796	-1.545	0.379	0.840	-0.718	1.003	-1.351	0.987	-0.095	-0.401
0.5	1.644	-1.503	0.459	0.764	-0.822	0.873	-1.253	0.976	-0.137	-0.436
0.6	1.496	-1.454	0.532	0.677	-0.897	0.752	-1.156	0.960	-0.181	-0.451
0.7	1.353	-1.397	0.595	0.585	-0.947	0.642	-1.061	0.939	-0.226	-0.449
0.8	1.216	-1.335	0.649	0.489	-0.973	0.540	-0.968	0.914	-0.270	-0.432
0.9	1.086	-1.268	0.693	0.392	-0.977	0.448	-0.878	0.885	-0.312	-0.403
1.0	0.962	-1.197	0.727	0.295	-0.962	0.364	-0.792	0.852	-0.350	-0.364
1.2	0.738	-1.047	0.767	0.109	-0.885	0.223	-0.629	0.775	-0.414	-0.268
1.4	0.544	-0.893	0.772	-0.056	-0.761	0.112	-0.482	0.688	-0.456	-0.157
1.6	0.381	-0.741	0.746	-0.193	-0.609	0.029	-0.354	0.594	-0.477	-0.047
1.8	0.247	-0.596	0.696	-0.298	-0.445	-0.030	-0.245	0.498	-0.476	0.054
2.0	0.142	-0.464	0.628	-0.371	-0.283	-0.070	-0.155	0.404	-0.456	0.140

3.0	-0.075	-0.040	0.225	-0.349	0.226	-0.089	0.057	0.059	-0.213	0.268
4.0	-0.050	0.052	0.000	-0.106	0.201	-0.028	0.049	-0.042	0.017	0.112
5.0	-0.009	0.025	-0.033	0.015	0.046	0.000	-0.011	-0.026	0.029	-0.002

For cohesive soils

$$y_z = A'_x \frac{PR^3}{E_p I_p} + B'_x \frac{MR^2}{E_p I_p} \quad (27)$$

$$M_z = A'_m PR + B'_m M \quad (28)$$

where, A'_y, B'_y, A'_m, B'_m are coefficients (see the following figure)

$$R = \sqrt[4]{\frac{E_p I_p}{k}}$$

k, see equation (9)

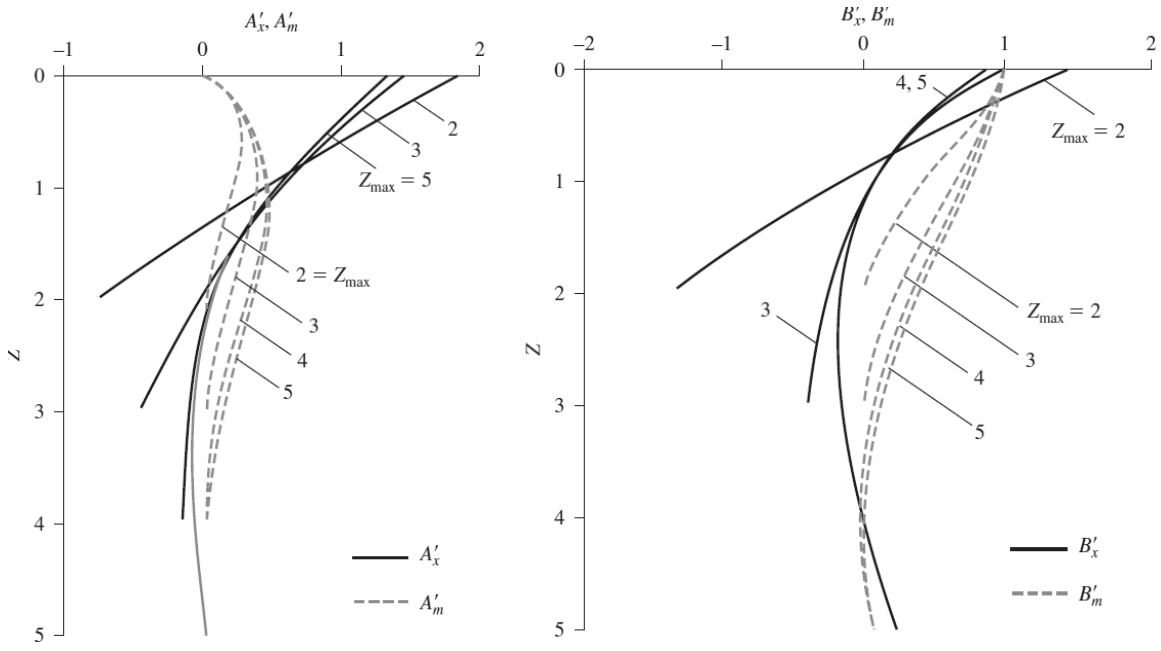

Fig. 5. Coefficients for long piles in cohesive soils. Adapted from (Das 2002).

2.2.7 P-Y CURVES

This method is based on results of pile lateral load tests instrumented with strain gauges along its depth for different specific soil conditions and pile geometries.

The relationship between applied lateral load and deflection along pile's depths can be obtained by two steps integrations of the moment curves recorded by strain gauges and the settle of points of control at ground line where lateral load, pile's deflection and its slope are well known.

Some of the first researchers that defined the p-y curves concept were (McClelland and Focht 1958); after them, numerous studies were done to evaluate the lateral behavior of several kind of piles under different subsoil conditions. Even though all that information was available, there was not a clear procedure to analyze the lateral behavior of piles laterally loaded under specific soil conditions, that's why, all that information was gathered and analyzed by several authors i.e. (Matlock 1970), (Welch and Reese 1972), (Reese et al. 1974), (Reese and Welch 1975), (Murchinson 1983), and others. They developed step by step methodologies to simulate P-Y curves for specific conditions. These detailed procedures are used by commercial software e.g. LPile, PileLAT 2014, PyPile, ALLPILE and others; detailed information can be found on (Reese et al. 2002) or in software's technical manuals.

2.2.8 CHARACTERISTIC LOAD METHOD

As a practical approach, (Duncan et al. 1994) proposed the Characteristic Load Method which is a simplification of P-Y curves results, which is based on pile's geometry, pile's head restrictions, pile's material properties; and soil's resistance.

Using dimensionless axes charts, lateral deflection and bending moments can be assessed as a function of characteristic load (P_c) and the characteristic moment (M_c).

Based on (Duncan et al. 1994) the charts are suitable to be used as a hand computation; however, this method is limited to piles and drilled shafts piles, and should not be used to estimate the lateral behavior of deep foundations in stiff clay subjected to cyclic loadings.

2.2.9 COMPUTATIONAL MODELS

Before the improvement and the accessibility to computational tools, the analysis and design of engineering problems were based almost exclusively on empirical considerations or restricted to solutions of simplified mathematical equations as it is mentioned by (Desai and Zaman 2013). Nevertheless, these simplified methodologies were not able to consider complex geometrics, load cases, or further conditions.

Thanks to the advances on computational methods, many additional variants can be considered to evaluate their significance into an engineering problem. This particularity reveals the advantages of computational models to be used as a tool to evaluate what if scenarios.

The user of a computational tool must consider the mathematical restrictions and implications involved in the use of a software of Finite Elements or Finite Differences, or a Plain Strain Model, Axisymmetric Model or a 3D Model.

Even when the computational knowledge is required, if the final user concerning is about a geotechnical simulation, he also may understand the hypothesis, advantages, limitations and how the get the parameter of the constitutive soil model available.

According to (Brinkgreve 2005) the most commonly used geotechnical models for practical purposes are Hooke's law (LE), the Mohr-Coulomb model (MC), the Drucker-Prager model (DP), the Duncan-Chang model or Hyperbolic model (DC), the Cam-Clay model (CC), the Soft Soil (Creep) model (SS(c)) and the Hardening Soil model (HS).

As it is mentioned by (Brinkgreve 2005), these models have the advantage that can be easily implemented with a discrete geotechnical parametric characterization. In some cases, they can even be inferred based on correlations or just estimated according to experience. The estimation methodologies to get the parameters needed for models presented are summarize on the following table.

Table 8. Overview of model parameters and selection methods. Adapted from (Brinkgreve 2005).

Parameters	Models	Oedometer	CRS	CD	CU	UU	DSS	Torvane	SPT	CPT	PM	DMT	Vane test	Classification	Tables, rules
C'	MC, DP, DC, SS(C), HS			D	D		D			C					C
Φ'	MC, DC, SS(C), HS			D	D		D			C					C
M (friction)	DP, CC			I	I		I			I					I
S_u	MC, DP, DC, HS					D		D	C	C			D	C	C
Ψ	MC, HS			D											C
E	LE, MC, DP	I	I	I	I	I	I		C	C		C		C	C
E_{50}^{ref}	DC, HS	I	C	D	I	D	I		I	I				C	C
E_{ur}^{ref}	DC, HS	(D)		(D)	(I)	(D)				I					C
E_{oed}^{ref}	HS	D	D				I		I	I	I	C		C	C
λ (*)	CC, SS(C)	D	I							C	I	I		C	C
K (*)	CC, SS(C)	(D)	I							C				I	C
μ *	SSC	(D)	D												C
V	LE, MC, DP, DC	I		D											C
V_{ur}	CC, SS(C), HS	(I)													C
m (power)	DC, HS	D	I	D	D									C	C
K_o^{nc}	SS(C), HS	(D)												C	C
R_f	DC, HS														C

where, D means directly, (D) means directly and recalculation is needed, I means indirectly, (I) means indirectly and recalculation is needed, and C means correlation.

The parameters for most of the constitutive soil models mentioned on the previous table can also be obtained from triaxial tests. These tests may be performed and instrumented in coherence with the characteristics that are going to be evaluated.

To understand each of the hypothesis, restrictions, advantages and the soil parameters needed for each soil constitutive model, it is necessary to refer to their original publications. i.e. for the Hardening Soil Model, (Schanz et al. 1999) mention that the basis idea of the model is the hyperbolic relationship between the deviatoric stress and the vertical strain from the primary triaxial loading. When this happens, soil presents a decreasing stiffness before the plastic strain occurs. This relationship, allows this model to represent in a more reliable way, the behavior of loose sands and normally consolidated clays during a drained triaxial test.

The model failure criterion is the Mohr-Coulomb, then, its strength parameters are needed (ϕ' and C'). As the model has a hyperbolic relationship, a failure ratio (R_f) must be defined.

For the primary loading, the confining stress dependent secant stiffness modulus for primary loading (E_{50}) is needed. To relate it to different stress values, this modulus is a function of a stress referenced modulus (E_{50}^{ref}), normally referenced to a 100 kPa stress (p^{ref}). In addition to this, a power coefficient is used (m) to consider its stress dependency as a logarithmic function. The m value will depend of the level of stress used and the material.

The same function is applied for the unloading and reloading stress paths, but, the modulus that ought to be applied for this stress paths (E_{ur}^{ref}) is the Young's modulus; therefore, the unloading and reloading stress path is elastic. Due to it, the Hooke's law must be satisfied, and the elastic strains computed using the Poisson's ratio for the unloading and reloading (ν_{ur}) strain estimation.

The plastic potential function adopted for the flow rule involves the use of the dilatancy angle (Ψ). On the other hand, the plastic strain originated from the yield cap is controlled by the tangent stiffness modulus for primary oedometer loading (E_{oed}^{ref}) and the coefficient of earth pressure at-rest for normally consolidated conditions (K_0^{NC}).

2.3 MICROPILES LATERALLY LOADED

After the results of eight lateral tests reported by (Plumelle and Raynaud 1996), the concern about the small lateral capacity of micropiles has become a constant. For that reason, the analysis of micropile laterally tested literature has increased.

Ten lateral load tests were conducted by (Long et al. 2004) to compare the behavior predicted using P-Y curves computed by LPILE software and the measures recorded on laterally loaded micropile field tests. As a result, he concluded that predicted and measured was in reasonably good agreement and that differences between measured and predicted was about $\pm$10 percent.

(Richards and Rothbauer 2004) performed twenty lateral load tests on eight different project places and compared their results with LPILE, NAVFAC and Characteristic Load Method estimations. The

results of those tests exposed that deflections can be overestimated by these methods, but they correspond to a conservative approach.

In both works, these authors agree with the importance of a good parameter identification of the upper 5 m and highlight the influence of the flexural stiffness in the behavior of the laterally loaded micropile.

In North Carolina, (Babalola 2011) installed sixteen micropiles which were prescribed on a depth of rock to perform nine single lateral load tests and a micropile group load test. He compared his results with the P-Y curves generated by FB-MultiPier software and analyzed the sensitivity of input parameters used.

Different types of vertical and lateral tests were performed by (Abd El-aziz 2012) on hollow bar micropiles built on a superficial thick layer of overconsolidated clayey silt to silty clay soil, overlying a compact sand deposit; within those tests, two monotonic lateral load tests were performed to compare them to predicted behavior by mean of P-Y curves computed by LPILE. Thus, the research concluded that some adjustments are needed on the parameters used to compute the P-Y curve to represent the measurements. These adjustments involved the use of parameter values not even reported on the original formulation of P-Y curves for the type of soil of the site of study.

As an extension of (Abd El-aziz 2012) works, (Osama F. 2013) resolved to conduct eight lateral tests on micropiles built on cohesive soils to compare his results with LPILE estimated behavior. He built two of the eight micropiles using 18 cm of diameter and the other six with 23 cm of diameter. As result of his research, P-Y curves fitted better for the highest diameter micropile.

(Kershaw and Luna 2014) analyzed the effect of vertical loads on the performance of lateral load tests of single micropiles installed at a clay and shale site. According to their results, the vertical load has a minimal effect on the lateral behavior of micropiles installed in stiff clay.

(Rabab'ah et al. 2014) used a 2D Finite Element Analysis to evaluate the effect of micropiles installation in the performance of an existing bridge abutment wall and its foundations, previous to its renovation. Based on lateral evaluations using LPILE and a plain strain model using a commercial

2D finite element (FE) software and a Mohr Coulomb Model, they concluded that P-Y curves overestimate the lateral displacement and that a good agreement can be obtained using a FE model.

3 CASE STUDY

3.1 DESCRIPTION

The case study is in Sabaneta, Colombia; close to Sabaneta's downtown as it is presented in Fig. 6 (see project's pin). The project is a residential complex of 10 buildings with 28-stories, vertical service loads at foundation level between 6.7 and 15.6 MN and lateral seismic loads of 6 MN per support. Both loads were obtained using the NSR-10 guideline.

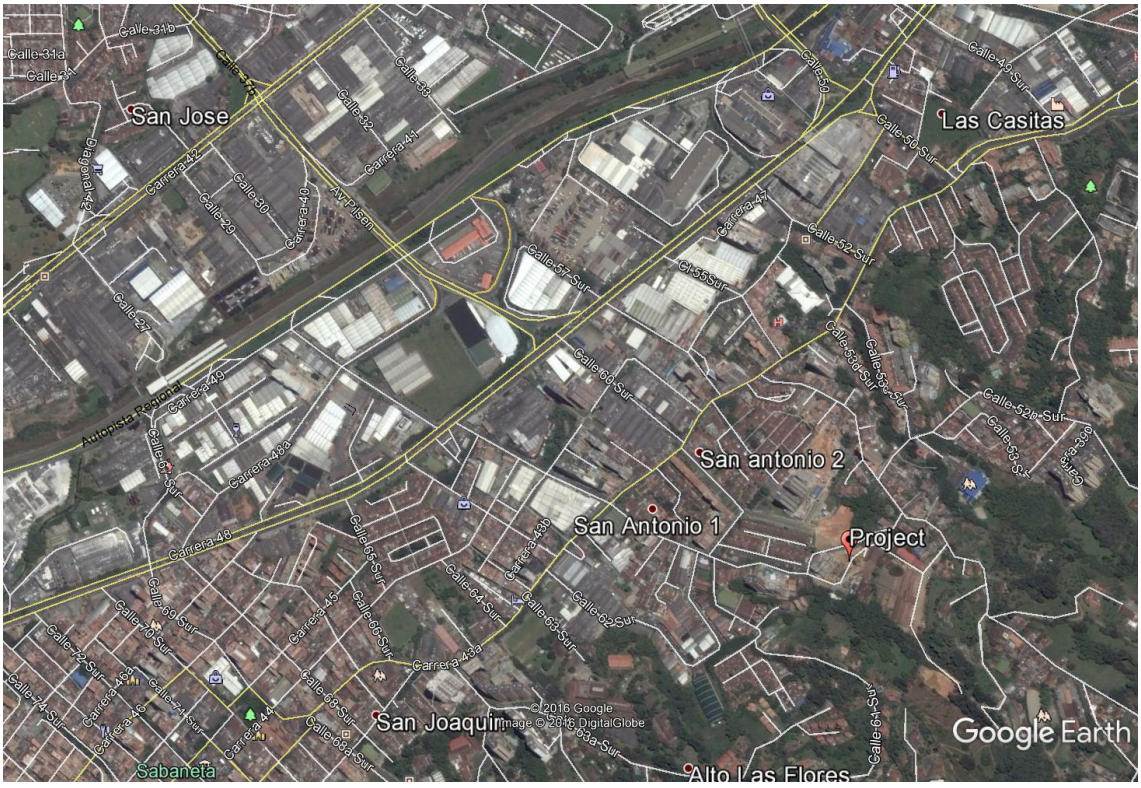

Fig. 6. Project location. After Google Earth 2016.

This research focuses on the evaluation of methodologies frequently used in geotechnical practice to analyze the lateral behavior of micropiles and their reliability to reproduce measurements obtained from a lateral load test performed on an IRS micropile regularly used in Aburrá Valley.

3.2 GEOLOGICAL CHARACTERISTICS

According to (Área Metropolitana del Valle de Aburrá 2007), the geological units that surround the project site are soils derived from rocks that belong to Grupo El Retiro in the Complejo Cajamarca, which is composed by Esquistos de Cajamarca (TReC) and Migmatitas de Puente Peláez (TTmPP).

At the same time, there are different types of soil deposits: alluvial (Qal or Qat) and mudflow with debris (NQFll), and in some places, are anthropic fills (Qll). This is illustrated on Fig. 7.

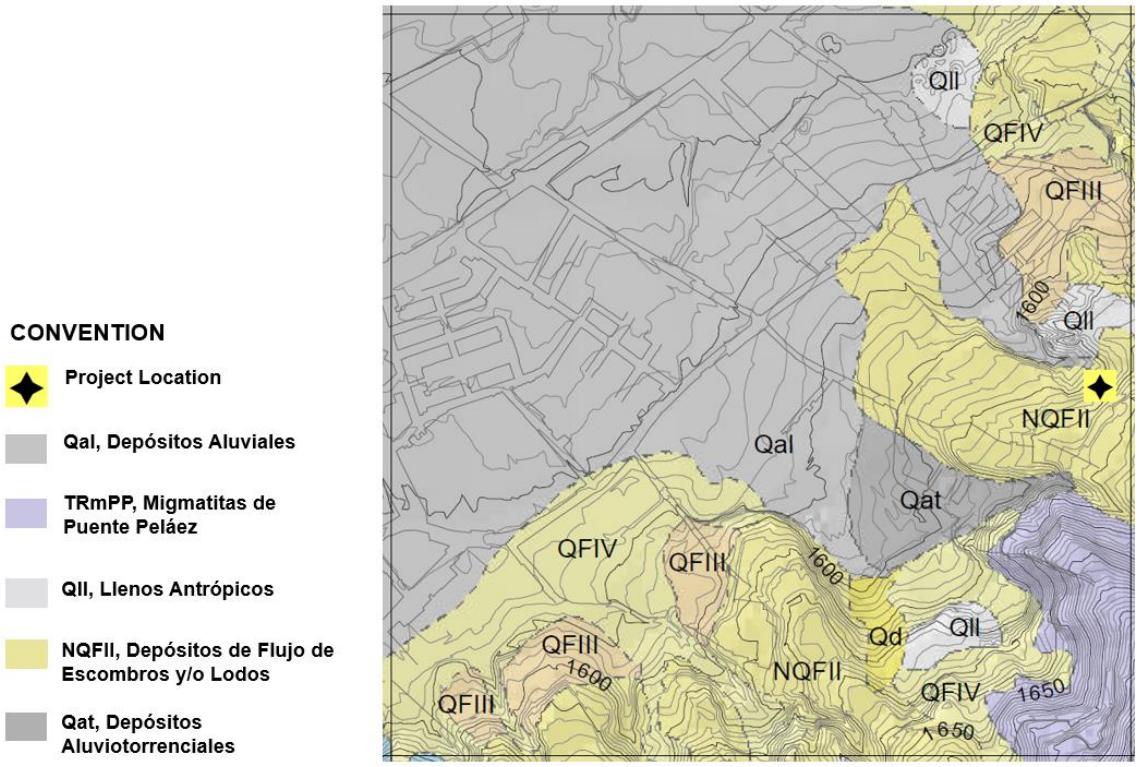

Fig. 7. Regional geology. After (A.M.V.A 2007).

3.2.1 MIGMATITAS DE PUENTE PELÁEZ (TRMPP)

This geological unit corresponds to soils derivate from migmatite rocks, which are characterized by their compositional banding and shales. These rocks are principally constituted by quartz, feldspar and micas, they have a migmatite structure which presents several white and white-yellow bands, due to leucosome's present, and dark grey bands by melanosome.

3.2.2 DEPÓSITOS DE FLUJO DE LODOS Y/O ESCOMBROS (NQFII)

Corresponds to soils deposited with variable thickness (around two meters) which are mud-flows mud-supported with sub-angular boulders of gneiss, shales and quartz.

3.3 GEOTECHNICAL CHARACTERISTICS

To identify the geotechnical characteristics of the underlaying soil, a geotechnical survey program had been done for 5 of the 10 buildings projected. The survey involved 28 (22 in the original site conditions and 6 posteriors to excavations) Standard Penetration Tests (SPT), 6 Down Holes (DH) and 8 geophysical linear arrays of seismic analysis of surface wave (SASW) methods (1 of theses was performed after micropiles construction and beside them). These field tests were located as shown in Fig. 8.

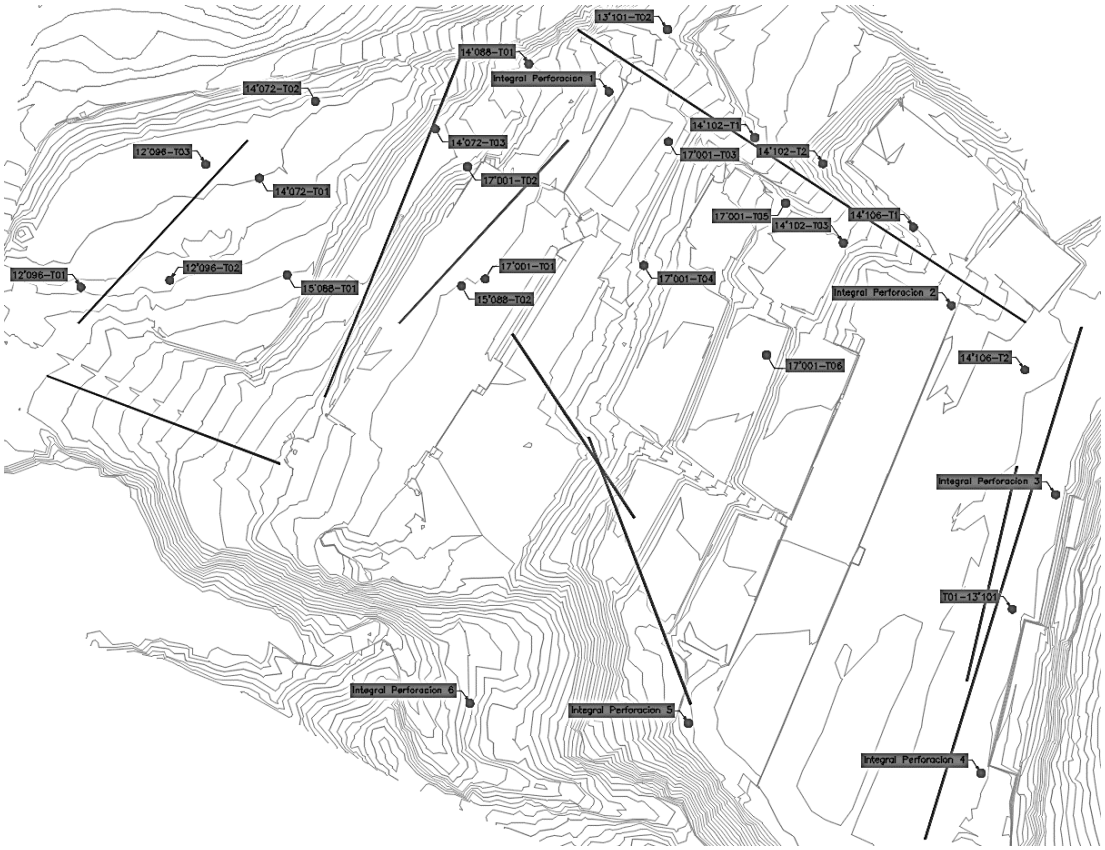

Fig. 8. Geotechnical survey location on the original terrain conditions.

Based on field test results, visual inspection of samples and some laboratory test results, it was possible to identify the geotechnical characteristics of each of the materials that constitute the soil profile.

Each sample obtained from SPT was visually described and some of them were chosen for laboratory tests. Disturbed samples were used to make a basic geotechnical characterization based on water contents, density, specific gravity, the Unified Soil Classification System (USCS), and gravimetric and volumetric relationships. On the other hand, undisturbed samples were selected to determine their undrained and drained soil resistance parameters using unconfined compression tests, consolidated drained direct shear tests and consolidated undrained compressional triaxial test with pore pressure record.

3.3.1 SURVEY RESULTS

Micropiles vertically (M-PC-V) and horizontally tested (M1-PC-H and M2-PC-H) were located as it is shown in Fig. 9. It is also shown in this figure, the location of the closest field tests which are: SPT 14’088-T01, SPT 13’101-T02, SPT Integral 01 and DH Integral 01; and 3 geophysical linear arrays (the dashed one was performed after micropiles construction).

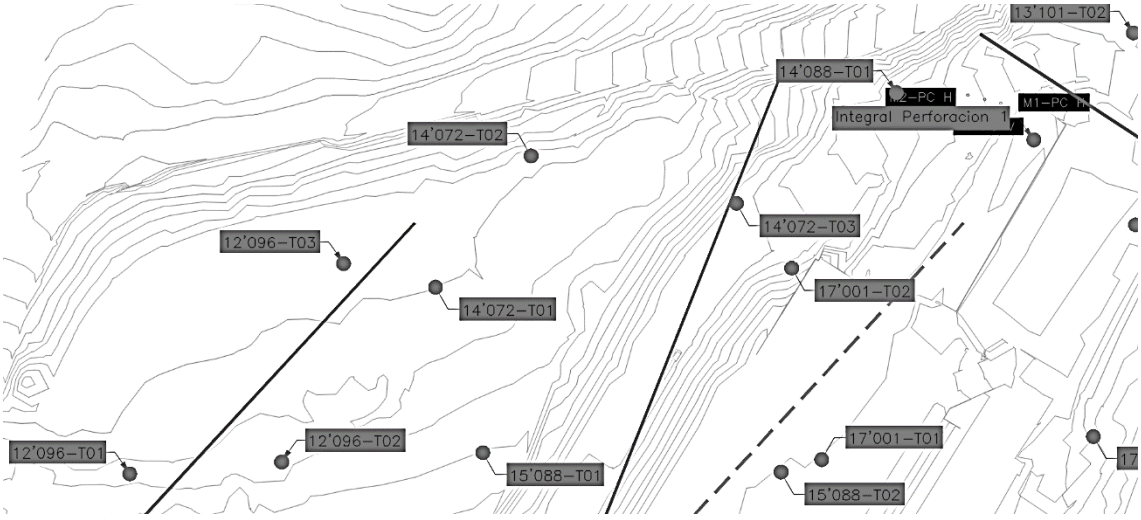

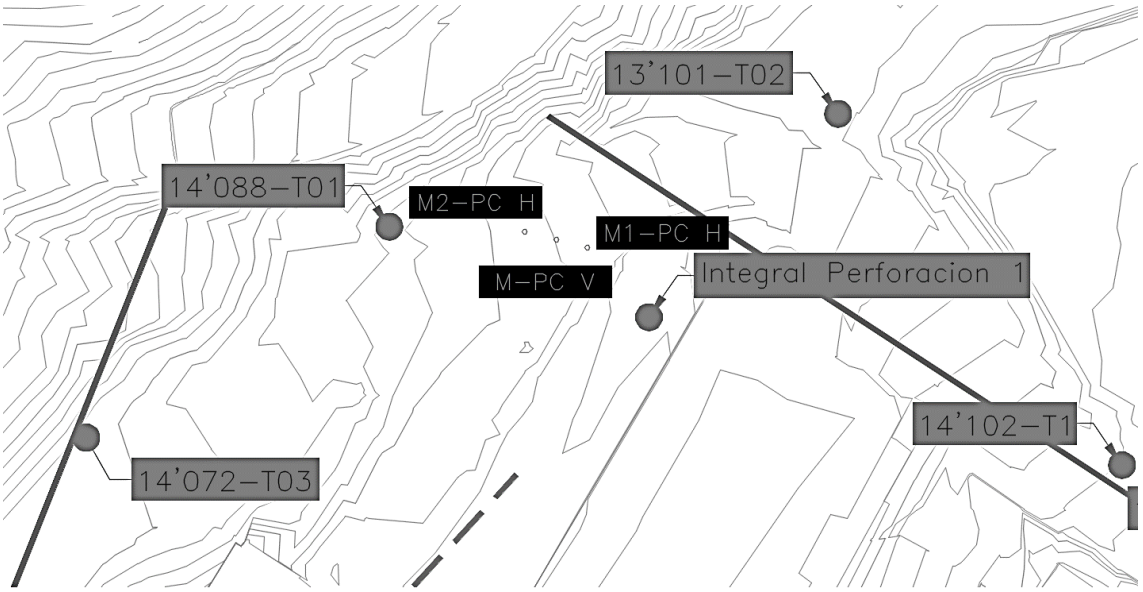

Fig. 9. Location of field tests and micropiles vertically and horizontally tested.

Even though not all the triaxial tests were done on the field tests shown in the previous figure, they were made on the same material. These laboratory tests will be used in the following chapters, then a brief discussion will take place there.

Fig. 10 summarizes the results of index laboratory tests including classification based on the USCS, content of fines, void ratio, dry and total densities and water content. Fig. 11 supplements the index laboratory tests with the soil resistance parameters obtained from laboratory tests, field exploration program results (shear wave velocities previous to micropiles construction - v_s-P- and after micropiles construction - v_s-A, and SPT blow counts) and the adopted soil profile.

Fig. 12 presents the SPT blow counts corrected by energy, sampler diameter, sampling method and overburden pressure to get the (N60) values, (Kishida 1967) correlation applied to get the effective friction angle (ϕ') and compared it with consolidated direct shear tests (DST) results. Also, there is the E_s evaluated using N60 and shear wave velocities (v_s) values according to (GCO 2006) and (Mayne 2006) formulations respectively.

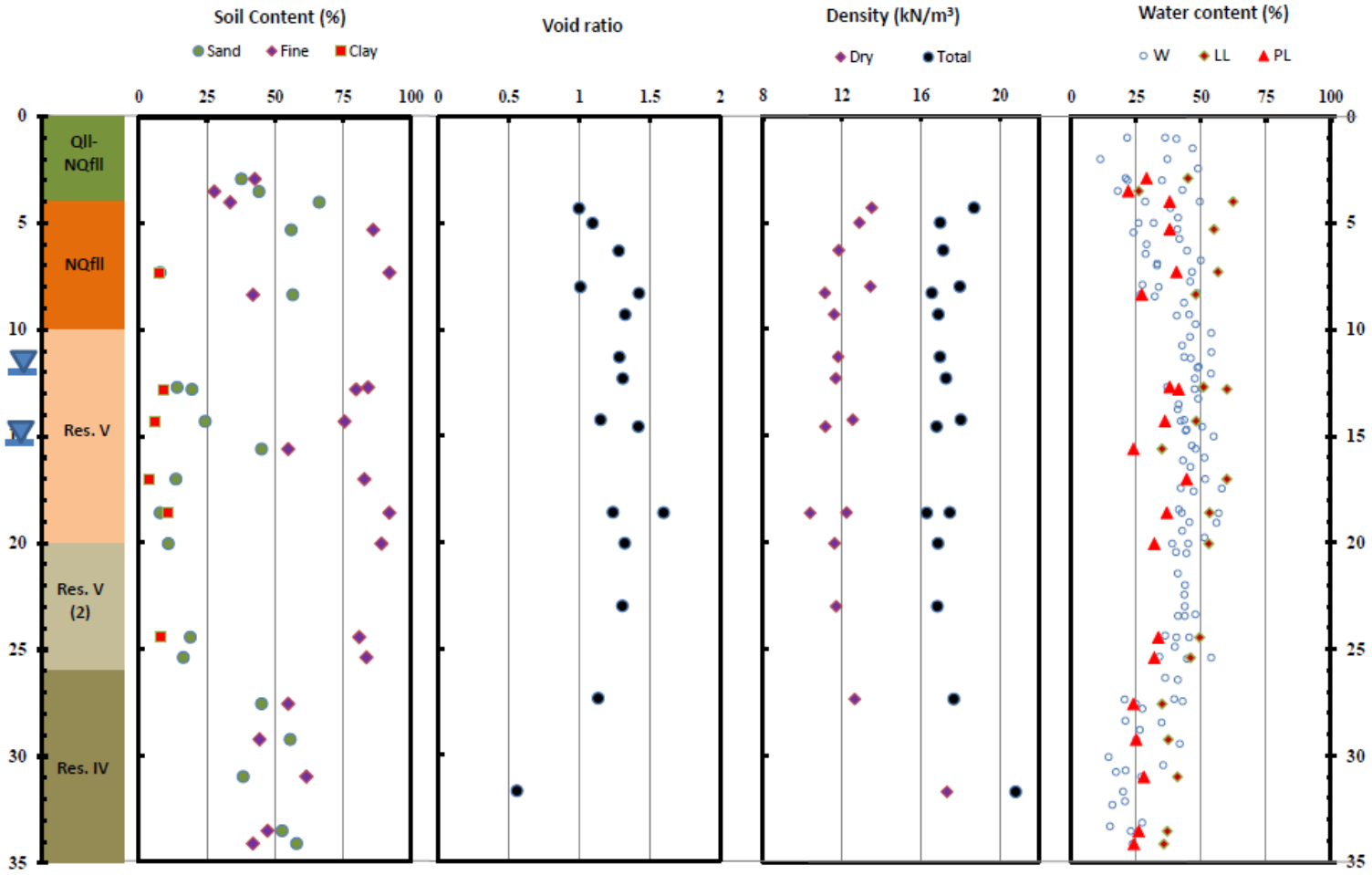

Fig. 10. Summary of basic characterization laboratory tests.

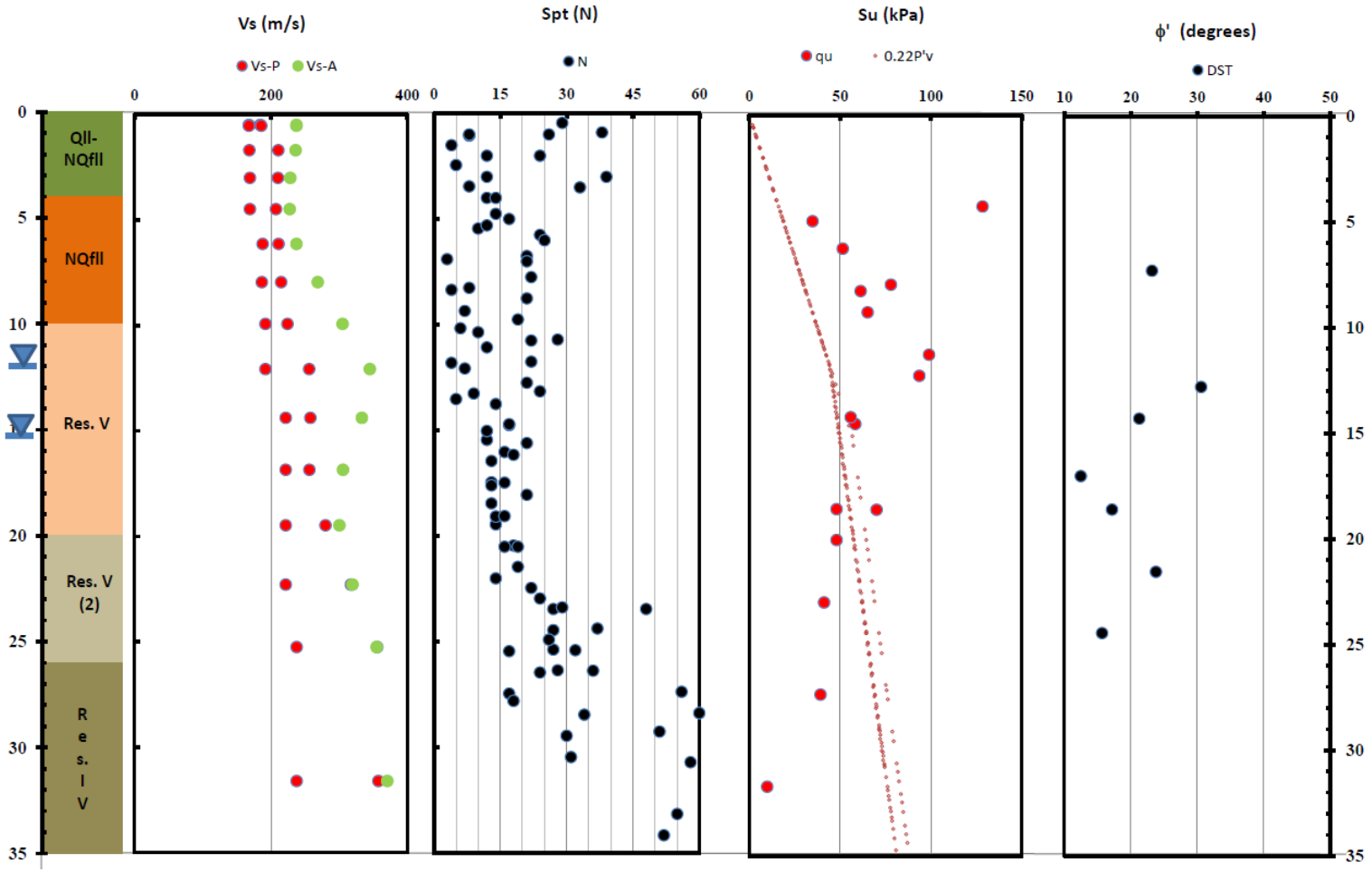

Fig. 11. Summary of field tests and mechanical soil resistance based on some laboratory tests.

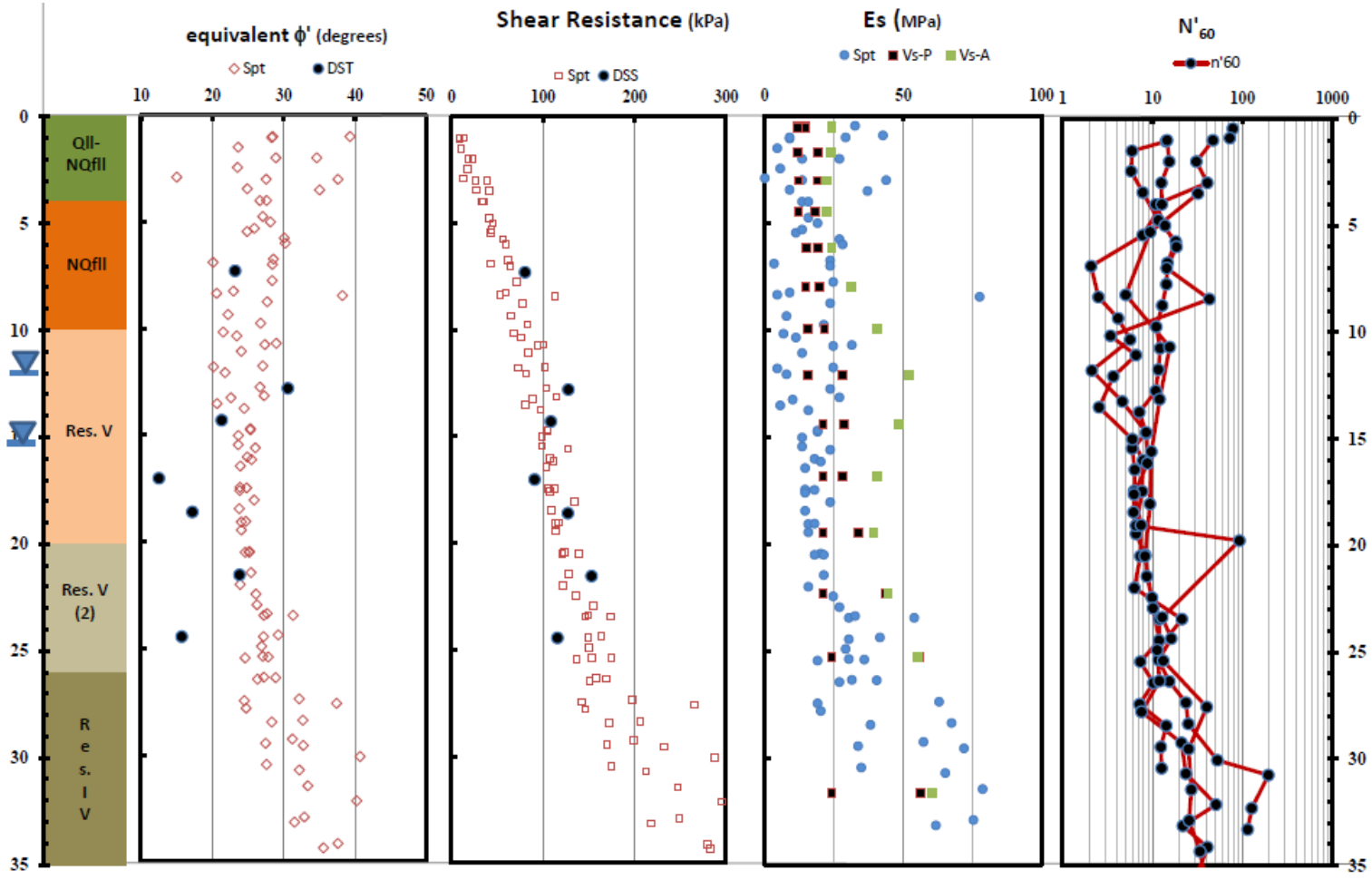

Fig. 12. Summary of soil parameters.

The most superficial layer of the simplified geotechnical profile corresponds to man-made fills conformed during the construction of existing buildings that were located on project site. This layer, was entirely removed during construction of current project execution, therefore it will not be further discussed.

NQfll layer is a heterogeneous material with boulders as those shown on Fig. 13 and a soil matrix classified as silty sands and silty clays as is illustrated on Fig. 10.

Fig. 13. NQfll's boulder.

Under this layer, a residual soil profile is easily identified by its characteristic texture derived from parental rock, the reduction of soil's water content, the increase of soil's resistance directly associated with the SPT blow count, and the decrease of void ratio and the rise of soil's density. If this soil profile is associated to (Fookes 1997) residual's soil description, it is quite simple to relate each soil layer to specifics horizons. In this survey, three differentiable soil layers were found under NQfll layer, these ones were classified as part of the horizons V and IV. In the following figure, the first two materials which are below NQfll layer are presented.

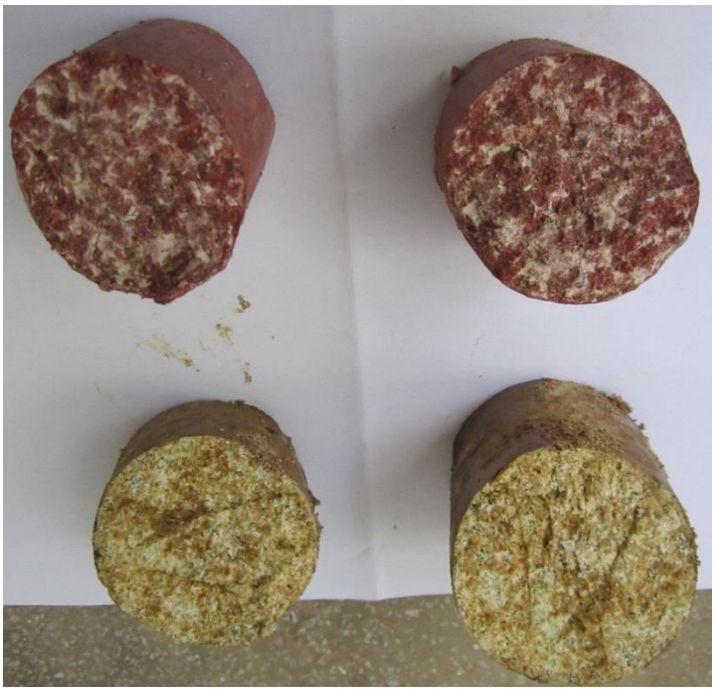

Fig. 14. Res. V and Res. V (2) materials.

In the following table, a summary of the index and the resistance Mohr coulomb's soil parameters for each layer is presented.

Table 9. Basic Index and soil's resistance parameters.

Layer	e		W (%)		γ (kN/m³)		Su (kPa)		C' (kPa)		Φ' (°)		E_s (kPa)	
	Min (m)	Max (M)	m	M	m	M	m	M	m	M	m	M	m	M
NQfll	0.9	1.4	18	50	16	19	34	128	11	27	20	38	3	35
Res. V	1.0	1.6	42	58	16	18	48	99	4	53	20	29	4	52
Res. V (2)	0.7	1.3	32	54	17	19	39	41	30	34	23	31	12	55
Res. IV	0.6	0.6	14	41	20	20	-	-	0	0	24	41	19	82

3.4 MICROPILES LOAD TESTS

As it was mentioned previously, three load tests were performed at project site, those were performed following the guidelines of as per ASTM D 1143 and ASTM D 3966. The results of these tests are presented and briefly discussed on next paragraphs; but it is important to mention that:

- 4 m were cut before tests were carried out, then fills layer were removed.
- Micropiles were 27 m length and their initial diameter was 20 cm.
- Micropiles classified as Type D (FHWA 2005).
- Micropiles were built using an IRS method, and pressure varied between 700 to 1100 kPa, increasing at depth.
- Longitudinal micropiles' reinforcement was 4 #10 steel bars.
- Transversal micropiles' reinforcement used steel stirrups each 0.15 m.
- Final average micropiles' diameter after injection varied between 30 and 35 cm, in correspondence with construction registers and exhumated measurements.

Some illustrative pictures of site conditions and micropiles built are presented on next figures.

Fig. 15. Site conditions and micropile's reinforcement.

Fig. 16. Exhumed micropiles.

3.4.1 VERTICAL LOAD TEST

The test was performed according to ASTM D 1143 guidelines, this test consisted of a hydraulic jack, 7 extensometers (5 in the central micropile and 1 in each of the reaction micropiles) and three micropiles: two reaction micropiles, set at the sides and one central, where the hydraulic jack is located. Test arrangement and its results can be seen in the following figure.

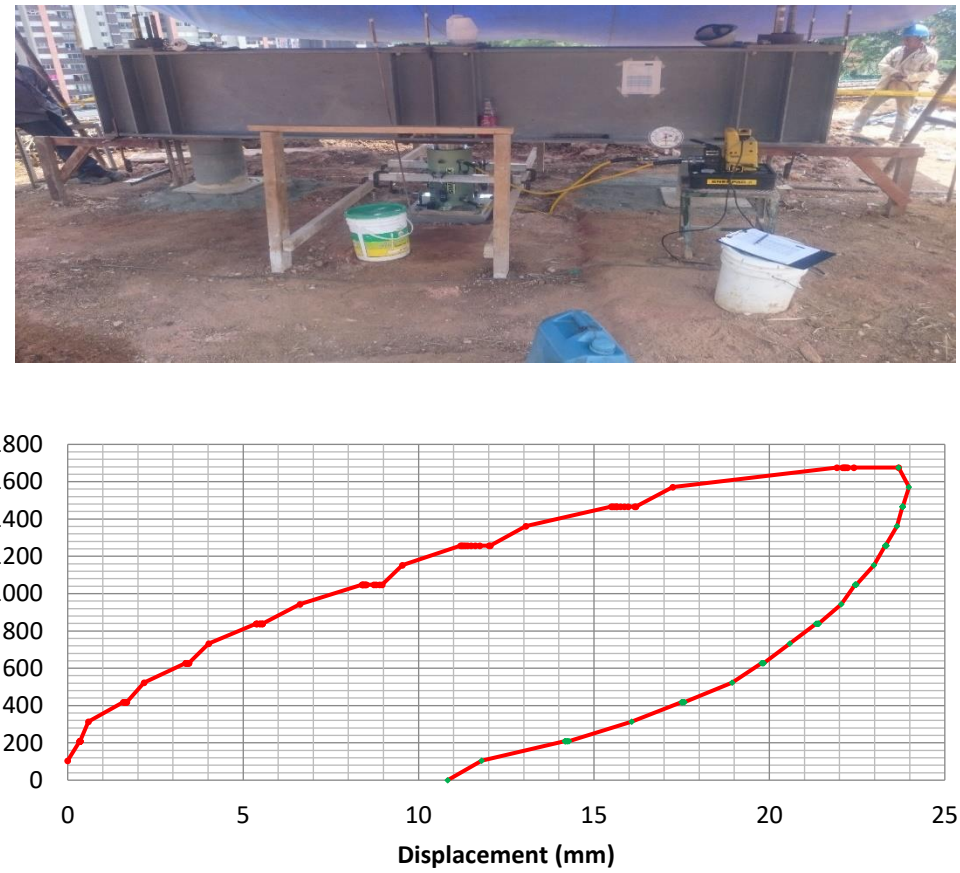

Fig. 17. Vertical load test - M-PC-V.

The curve shown above illustrates that the micropile behaved approximately linearly until 1570 kN load, where 17 mm vertical displacement were measured, after that, the slope of this curve changed and deformations enlarged without any significant increment of load.

Considering that reinforcement bars were 4 #10 conventional steel bars, it is expected that yielding point load be reached at 350 kN per bar, so, for the 4 steel bars the total yielding point load could be 1400 kN, based on that, it is considered that soil did not fail and reinforcement did.

3.4.2 LATERAL LOAD TEST

After three months that vertical load test ended, the reaction micropiles were used for the lateral load tests.

The lateral load test procedure was designed to fulfill the ASTM D3966-07 requirements. The basic concept of this test is to set a reaction support, then, apply a lateral load using a hydraulic jack between the reaction and the micropile tested, finally, record each lateral displacement in the reaction and the micropile and the load applied. The features of each of the elements used during tests were:

- Reactions: a concrete deadman of 0.6 m width, 0.6 m length and 0.5 m depth.
- Hydraulic Jack: Enerpac RCH-202.
- A hydraulic hand pump.
- A pressure gauge.
- Two bearing plates.
- Electronic displacement indicators: two Mitutoyo ABSOLUTE Digimatic Indicator ID-U SERIES 575-123.
- A reference beam.
- Two wirelines, four mirrors and two scales.

The arrangement and the results of the tests are presented on the following pictures.

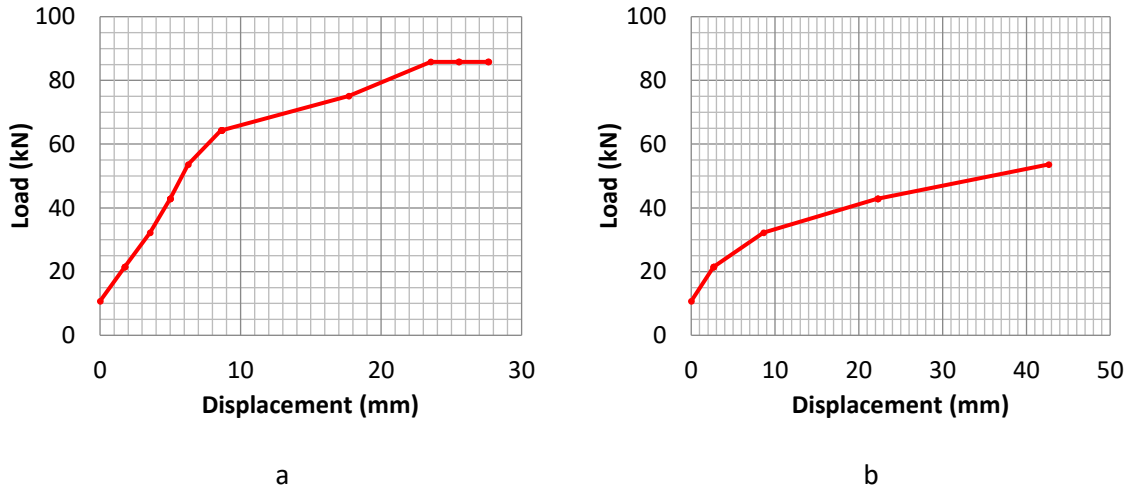

Fig. 18. Lateral Load tests. a) M1-PC-H and b) M2-PC-H results.

The analyses of the behavior of the micropile laterally loaded is the purpose of the following chapter. However, it is important to notice the difference between both results. This is due to the micropiles proximity to the slopes of the road as can be inferred from Fig. 9. M1-PC-H is 7 m to the crest of the slope, while M2-PC-H is just 2.4 m to 4.4 m to the crest of the slope which inclination varies from 18° to 40° respectively.

4 ANALYSES

4.1 CURRENT PRACTICAL USED MODELS

In structural practice engineering it is common to model soil as springs (modulus of subgrade reaction) and foundation elements like beams. These springs are considered linear perfectly elastic and are commonly used for all stages and load combinations as a constant without considering soils spatial variation, its resistance degradation due to cyclic load, the effect of construction techniques, special boundary conditions and soils variation of stiffness for the stress changes during construction and operation process.

From this point of view, geotechnical engineers must define which springs should be used for structural analysis, considering all previous mentioned variables.

For practical engineering purposes, it is common to use semiempirical formulations or P-Y curves limited to a specific lateral deformation at foundation element's upper part, to define these springs.

It is important to notice that semiempirical formulations or P-Y curves have their own limitations and cannot be used for all conditions. For example, P-Y curves were developed for large piles and not for smaller once as it is mentioned by (Reese et al. 2002), as a consequence, it is possible to get a good approach to piles' internal solicitations, but if the lateral displacements are the concern, it will not be a consistent method.

A lateral load test is rarely performed to check theoretical spring values used and ultimate lateral displacement, for this reason, it is important to evaluate the reliability of methods commonly used in practical engineering and try to recreate the measurements obtained from large scale tests.

4.2 MODELING

In the following paragraphs, the evaluation of micropile M1-PC-H will be presented using semiempirical methods, P-Y curves and computational geotechnical modelling.

4.2.1 BEAM ON ELASTIC FOUNDATION USING SEMIEMPIRICAL FORMULATIONS

To evaluate the lateral behavior of micropile M1-PC-H, the range of parameters presented in Fig. 10 to Fig. 12, and Table 9 were applied to equations (9) to (20), and were assigned to an elastic beam element.

Table 10 to Table 12 present the moduli of subgrade reaction computed for the lowest, the average and the highest NQfll soil's parameters respectively. The remainder subgrade reaction moduli evaluation can be consulted on annexes Annex 1 to Annex 6.

Table 10. NQfll layer moduli of subgrade reaction - semiempirical formulations - Lowest case.

Formulation	k_h (kPa/m)	Parameters
(Vesic 1961)	4391	E_s=3 MPa, v=0.3, d=0.3 m, I_p=3.97E-4 m^4, E_p=33GPa
(Francis 1964)	1184060	Z=3m, γ=16kN/m^3, ϕ=20°, $N_γ$=2.9, N_q=6.4, d=0.3m
(Broms 1964a)	3131	E_s=3 MPa, v=0.3, d=0.3 m, L=27 m, m=0.37
(Audibert and Nyman 1977)	100987	Z=3m, γ=16kN/m^3, ϕ=20°, N_q=6.4, y_u=6mm, y=2.54mm
(Kishida and Nakai 1977)	8781	E_s=3 MPa, v=0.3, d=0.3 m, I_p=3.97E-4 m4, E_p=33GPa
(Robinson 1979)	7593	S_u=34kPa, d=0.3m
(Bhushan et al. 1981)	69109	N=2, d=0.3m, Y=2.54mm
(Sogge 1981)	3142	Z=3m, d=0.3m
(Pyke and Beikae 1984)	20000	E_s=3 MPa, d=0.3 m
(Habibagahi and Langer 1984)	154248	Z=3m, σ'=48kPa, γ=16kN/m^3, ϕ=20°, A=5, d=0.3m, y=2.54mm

Table 11. NQfll layer moduli of subgrade reaction - semiempirical formulations - Intermediate case.

Formulation	k_h (kPa/m)	Parameters
(Vesic 1961)	19003	E_s=12MPa, v=0.3, d=0.3 m, I_p=3.97E-4 m^4, E_p=33GPa
(Francis 1964)	10849512	Z=3m, γ=19.5kN/m^3, ϕ=37.6°, $N_γ$=59.2, N_q=46.2, d=0.3m
(Broms 1964a)	12523	E_s=12MPa, v=0.3, d=0.3 m, L=27 m, m=0.37
(Audibert and Nyman 1977)	889204	Z=3m, γ=19.5kN/m^3, ϕ=37.6°, N_q=46.2, y_u=6mm, y=2.54mm
(Kishida and Nakai 1977)	38005	E_s=12MPa, v=0.3, d=0.3 m, I_p=3.97E-4 m4, E_p=33GPa
(Robinson 1979)	4556	S_u=20.4kPa, d=0.3m

(Bhushan et al. 1981)	172772	N=5, d=0.3m, Y=2.54mm
(Sogge 1981)	3142	Z=3m, d=0.3m
(Pyke and Beikae 1984)	80000	E_s=12MPa, d=0.3 m
(Habibagahi and Langer 1984)	187989	Z=3m, σ'=58.5kPa, γ=19.5kN/m^3, ϕ=37.6°, A=5, d=0.3m, y=2.54mm

Table 12. NQfll layer moduli of subgrade reaction - semiempirical formulations - Highest case.

Formulation	**k_h (kPa/m)**	**Parameters**
(Vesic 1961)	60596	E_s=35MPa, v=0.3, d=0.3 m, I_p=3.97E-4 m^4, E_p=33GPa
(Francis 1964)	11204182	Z=3m, γ=19kN/m^3, ϕ=38°, $N_γ$=64.1, N_q=48.9, d=0.3m
(Broms 1964a)	36524	E_s=35MPa, v=0.3, d=0.3 m, L=27 m, m=0.37
(Audibert and Nyman 1977)	916986	Z=3m, γ=19kN/m^3, ϕ=38°, N_q=48.9, y_u=6mm, y=2.54mm
(Kishida and Nakai 1977)	121191	E_s=35 MPa, v=0.3, d=0.3 m, I_p=3.97E-4 m4, E_p=33GPa
(Robinson 1979)	28587	S_u=128kPa, d=0.3m
(Bhushan et al. 1981)	1382176	N=40, d=0.3m, Y=2.54mm
(Sogge 1981)	3142	Z=3m, d=0.3m
(Pyke and Beikae 1984)	233333	E_s=35MPa, d=0.3 m
(Habibagahi and Langer 1984)	183169	Z=3m, σ'=57kPa, γ=19kN/m^3, ϕ=38°, A=5, d=0.3m, y=2.54mm

It is worth noting that for these evaluations, pile's modulus of elasticity was computed using the equivalent modulus of the composed micropile section (33 GPa), the bearing capacity factors were calculated using (Meyerhof 1963) formulation, the ultimate lateral deflection was assumed as 6 mm and admissible lateral deflection was considered as 2.54 mm.

SAP 2000 models use the beam elastic foundation principle, so, equivalent springs are necessary to evaluate lateral displacement and internal solicitations. The moduli of subgrade reaction presented in previous tables were multiplicated by their afferent area to convert it into an equivalent spring. In the following figure, the SAP 2000 model used is introduced.

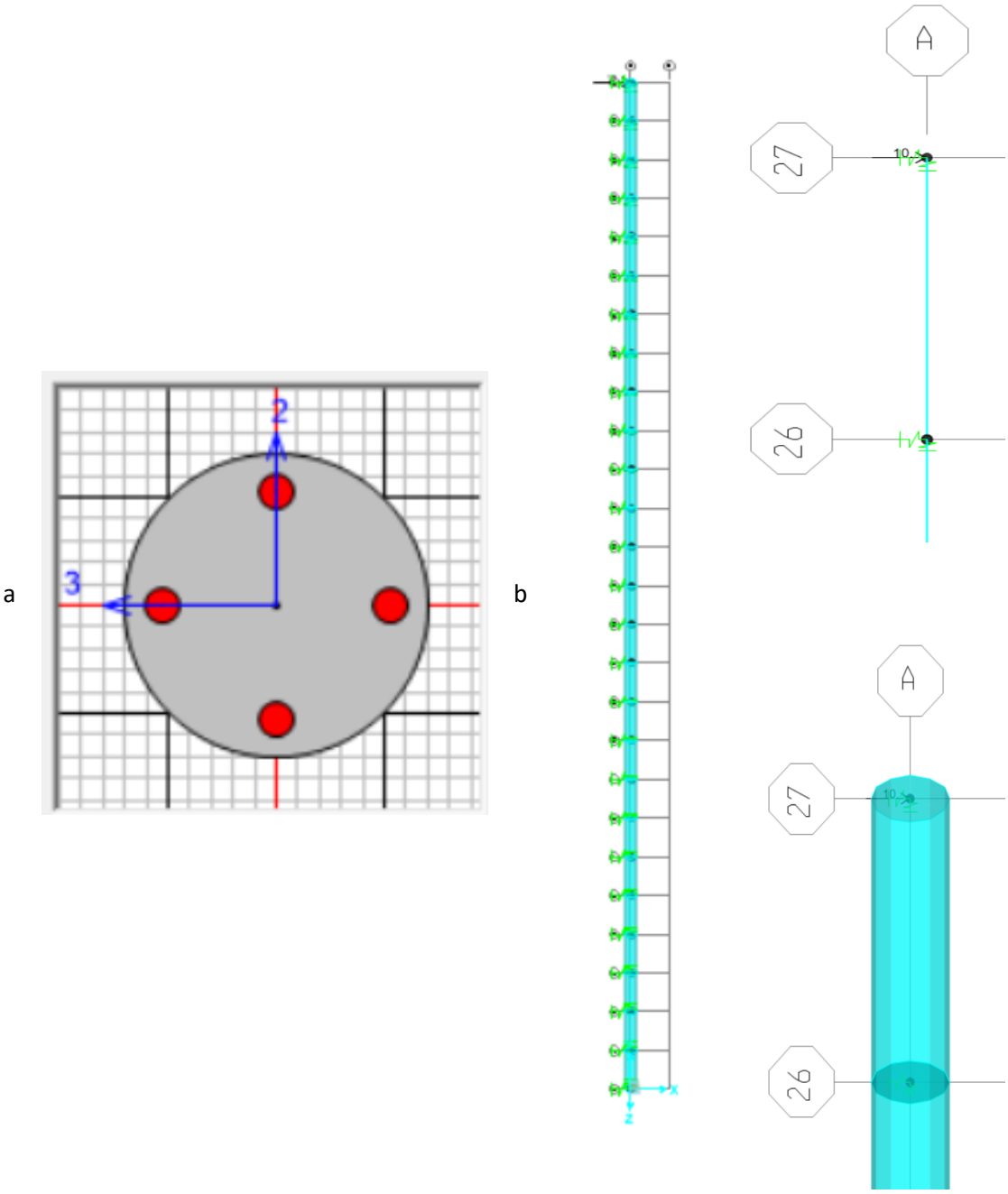

Fig. 19. SAP 2000 model. a) Micropile cross section, and b) 3D model.

The results of the lateral evaluation using the equivalent springs obtained from the semiempirical formulations and the model presented in Fig. 19 are shown in the following group of figures, where

computed lateral deflection is directly compared with lateral load test measured deflection at micropile's head.

a

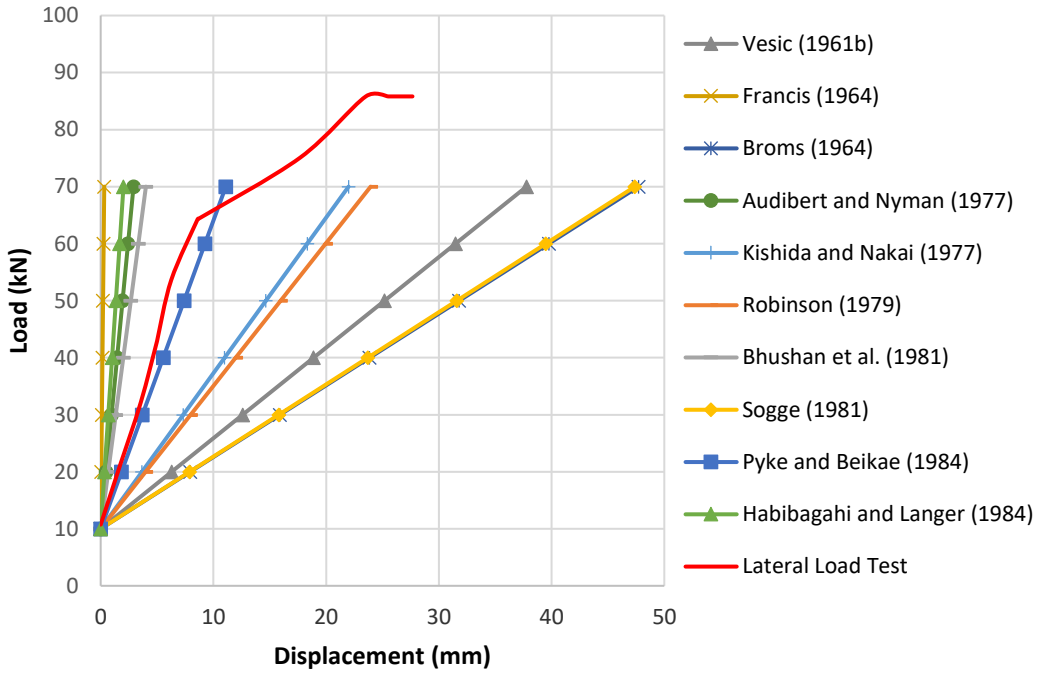

b

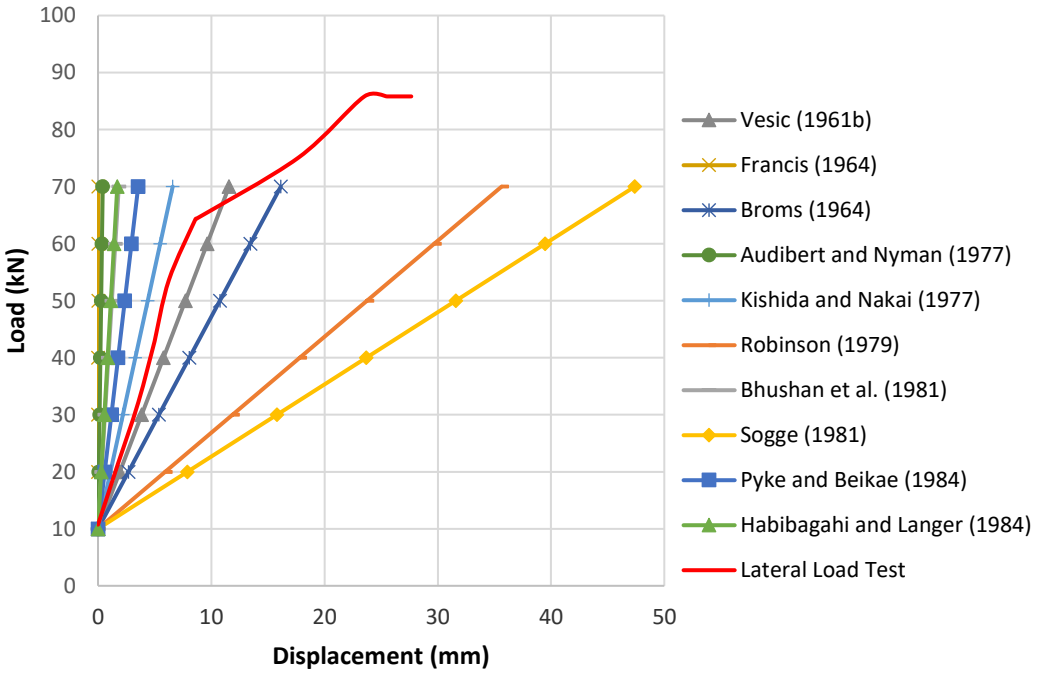

c

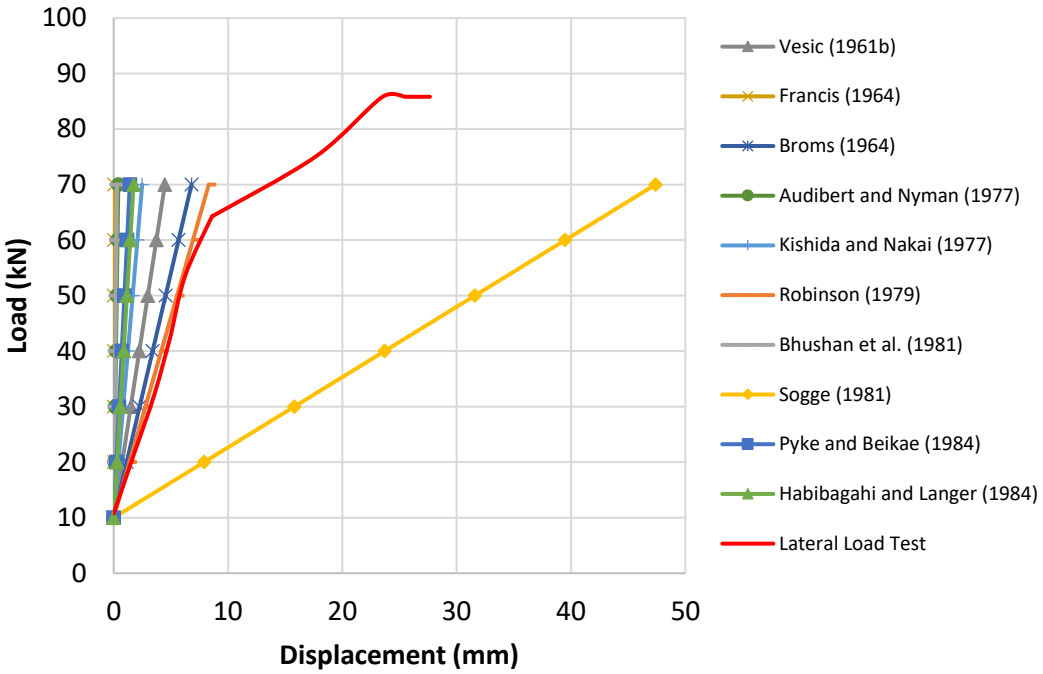

Fig. 20. Comparison between lateral load test result against lateral response of a beam on elastic foundation using semiempirical methodologies for: a) the lowest soil's parameters, b) average soil's parameters, and c) the highest soil's parameters.

Based on direct comparison of the predicted displacements and measured once, it is evident that the predicted lateral displacement using semiempirical models fits relatively well in some cases, nevertheless, it is not reliable, because it depends too much on the soil parameters used which will depend in some cases on the designers' experience, reliability and wisdom.

4.2.2 P-Y CURVES

To evaluate the lateral displacement of the micropile's head M1-PC-H using P-Y curves method, the software ALLPILE was implemented. In the following figure, the micropile characteristics and soils parameters used are shown.

a

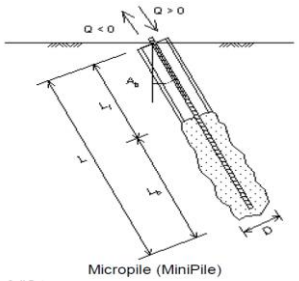

Loads:
Load Factor for Vertical Loads= 1.0
Load Factor for Lateral Loads= 1.0
Loads Supported by Pile Cap= 0 %
Shear Condition: Static

(with Load Factor)
Vertical Load, Q= 0.0 -kN
Shear Load, P= 90.0 -kN
Moment, M= 0.0 -kN-m

Profile:
Pile Length, L= 27.0 -m
Top Height, H= 0.000 -m
Slope Angle, As= 0
Batter Angle, Ab= 0

Pile Data:

Depth -m	Width -cm	Area -cm2	Per. -cm	I -cm4	E -MPa	Weight -kN/m
0.0 27.0	30	706.9	94.2	39760.8	20683	1.668

b

Soil Data:

Depth -m	Gamma -kN/m3	Phi	C -kN/m2	K -MN/m3	e50 or Dr %	Nspt
0	16	20	11	25.9	1.4	2
6	16	20	4	59.3	1.6	2
10	6	20	4	61.7	1.6	2
16	7	23	30	109.2	1.3	2
22	10	24	0	29.4	0.6	12

c

Soil Data:

Depth -m	Gamma -kN/m3	Phi	C -kN/m2	K -MN/m3	e50 or Dr %	Nspt
0	19.5	37.6	11.5	25.9	1.20	5
6	17.9	16.0	52.2	59.3	0.99	8
10	7.9	16.0	52.2	61.7	0.99	8
16	9.7	16.0	29.7	109.2	0.78	12
22	10.0	35.0	0.0	29.4	54.06	20

d

Soil Data:

Depth -m	Gamma -kN/m3	Phi	C -kN/m2	K -MN/m3	e50 or Dr %	Nspt
0	19	38	27	25.9	0.9	40
6	18	29	53	59.3	1	15
10	8	29	53	61.7	1	15
16	9	31	34	109.2	0.7	35
22	10	41	0	29.4	0.6	45

Fig. 21. ALLPILE Model. a) micropile characteristics, b) the lowest soil's parameters, c) average soil's parameters, and d) the highest soil's parameters.

In accordance with soil conditions presented on Fig. 21, the P-Y curves obtained at the middle of each soil layer are presented on the following figures.

a

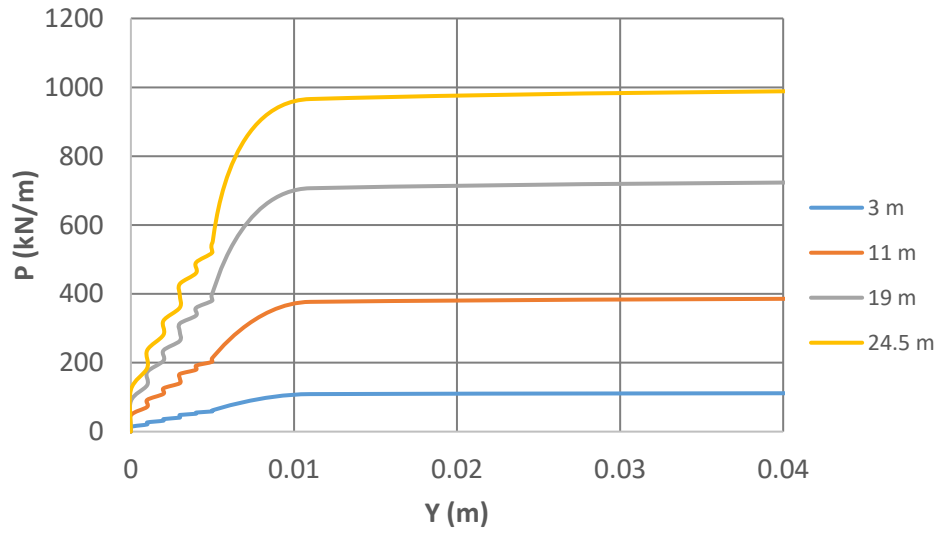

b

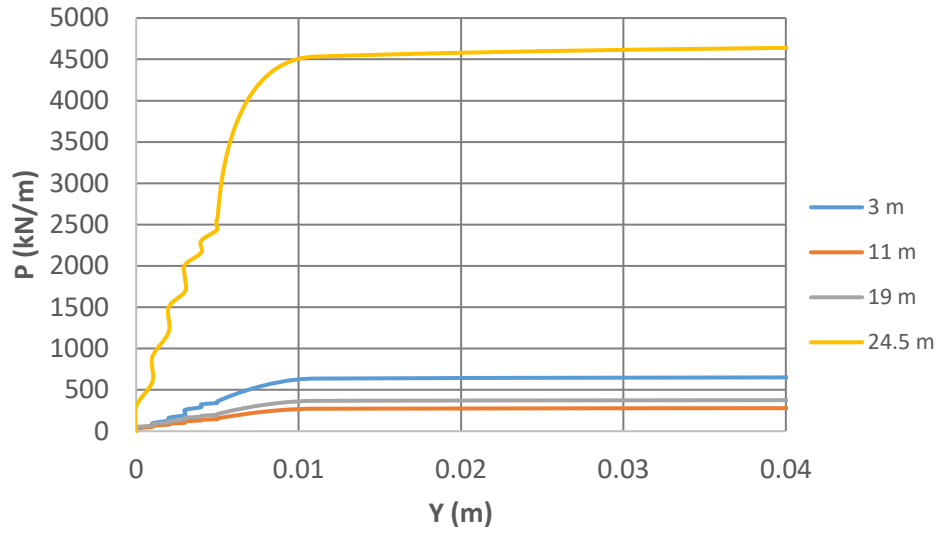

c

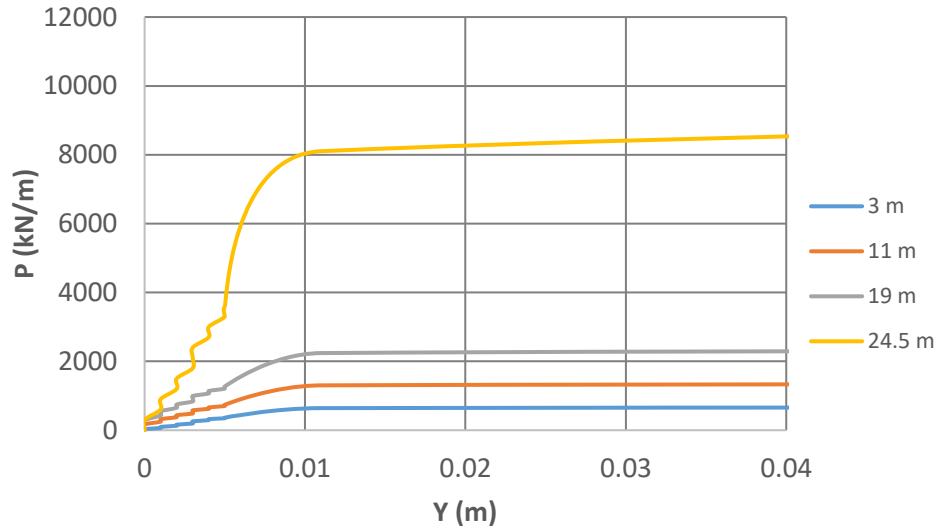

Fig. 22. P-Y curves for: a) the lowest soil's parameters, b) average soil's parameters, and c) the highest soil's parameters.

Based on the elastic foundation principles and the equivalent spring for non-linear conditions; P-Y curves previously shown, are used to compute lateral displacements of the micropile of study. In the next group of figures, lateral load test result is directly compared against the lateral displacement calculated for each of the scenarios previously introduced for semiempirical evaluation. Detailed information of these evaluations can be consulted on annexes Annex 7 to Annex 9.

a

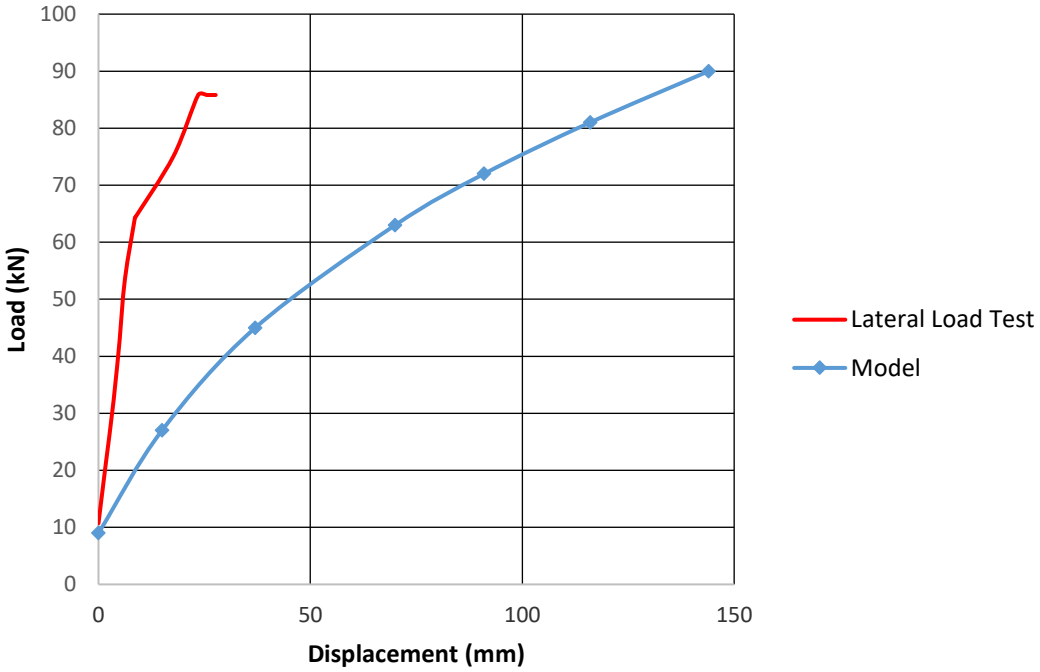
100
90
80
70
60
50
40
30
20
10
0
Load (kN)
0
50
100
150
Displacement (mm)
Lateral Load Test
Model

b

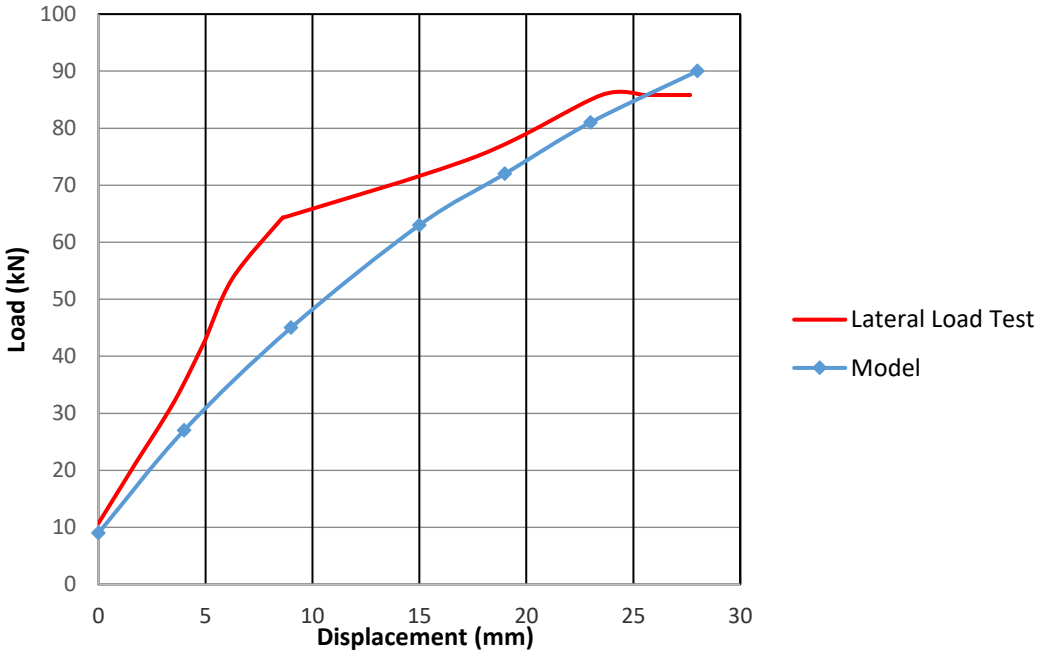
100
90
80
70
60
50
40
30
20
10
0
Load (kN)
0
5
10
15
20
25
30
Displacement (mm)
Lateral Load Test
Model

c

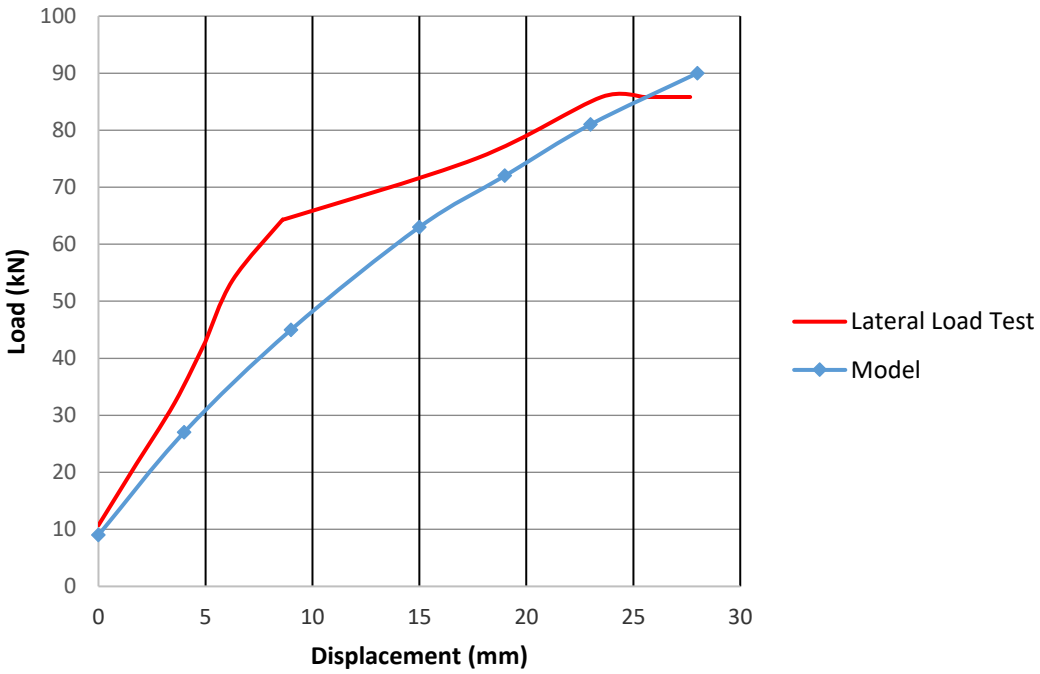

Fig. 23. Comparison between lateral load test result against lateral response of a beam on elastic foundation using P-Y curves method for: a) the lowest soil's parameters, b) average soil's parameters, and c) the highest soil's parameters.

According to results, it is evident that P-Y curves can be used, nevertheless, the micropile lateral displacement estimation can be overpredicted regardless which soil parameters are used (even if the highest ones are applied), which means a conservative approach for displacement evaluations as it was pointed out by (Long et al. 2004; Rabab'ah et al. 2014; Richards and Rothbauer 2004).

4.2.3 COMPUTATIONAL MODEL

In the following paragraphs, a brief discussion of the soil constitutive models that must be used is presented. After that, analyses are performed and discussed.

4.2.3.1 CONSTITUTIVE MODELS EVALUATION

To define which constitutive soil model ought to be used, some of the models presented on Table 8 were evaluated using the SoilTest module of the software MIDAS GTS NX version 2.1. Results obtained from simulation were confronted against stress-strain tri-axial test results for the three upper soil layers, the evaluation for the NQfll layer is presented in the following figures, the other ones can be found on annexes.

a

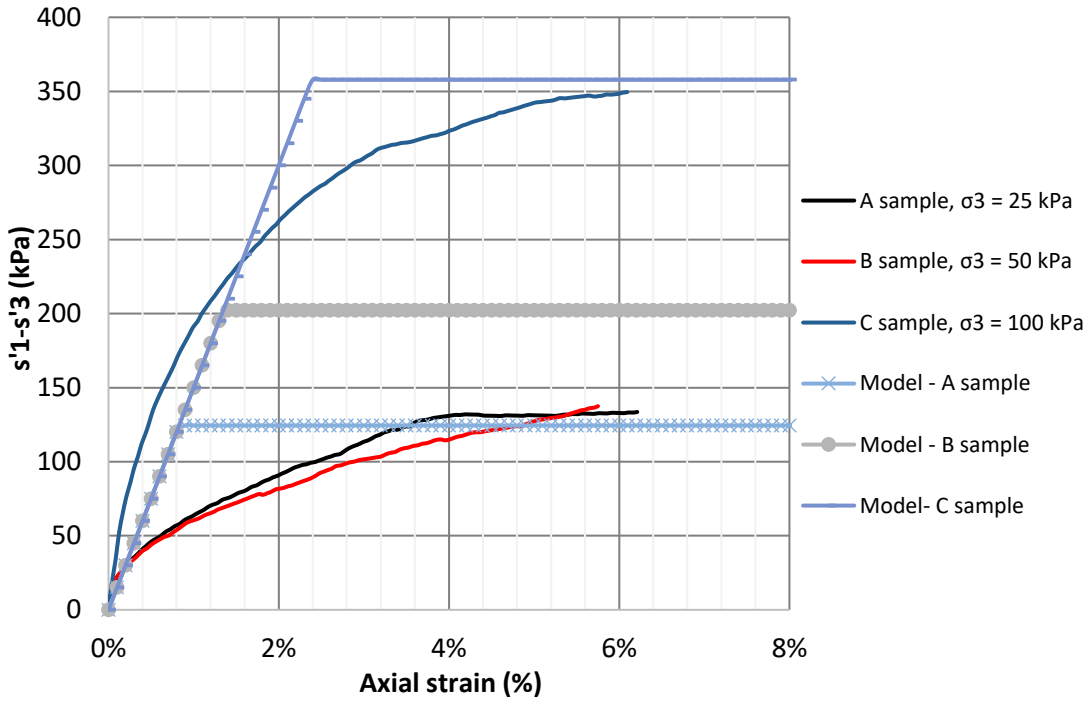

b

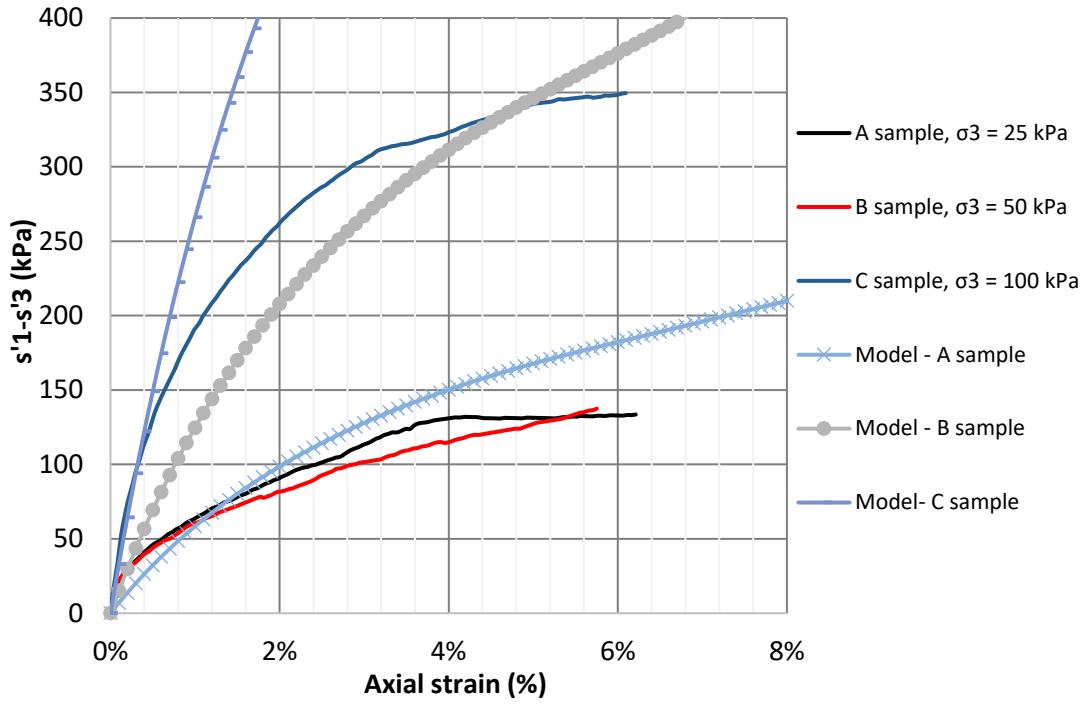

c

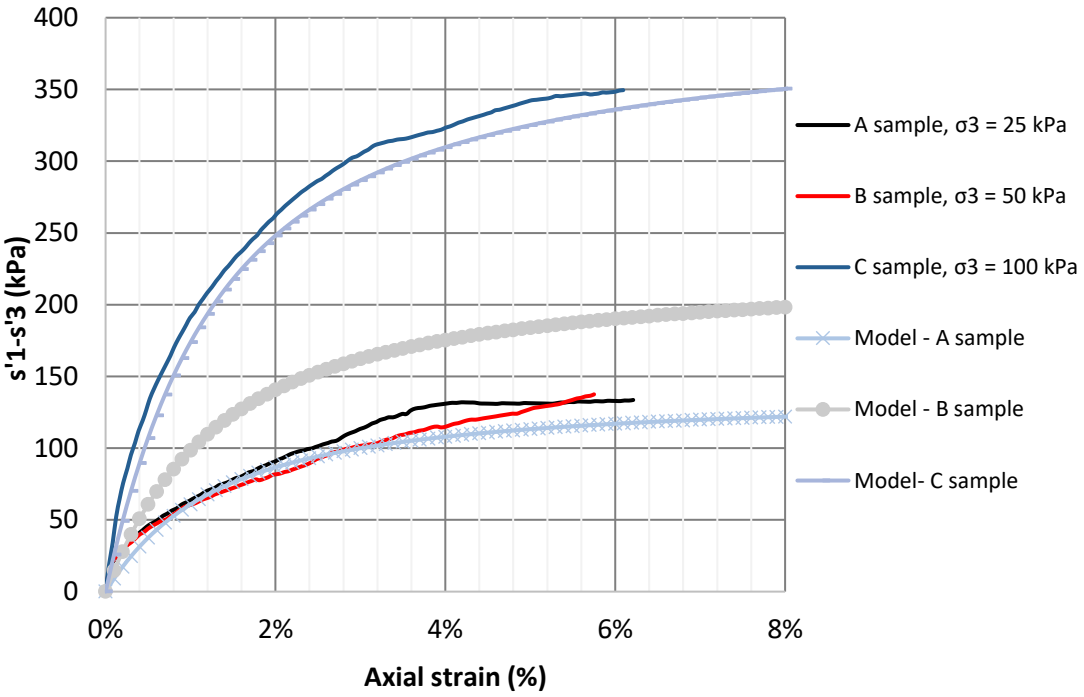

Fig. 24. NQfll constitutive model evaluation. a) Mohr Coulomb model, b) Duncan-Chang model and c) Hardening Soil model.

According to Fig. 24, the best model to represent the soil test behavior is the Hardening Soil Model. Considering this, it will be used to simulate the soil behavior of the three upper layers, and for the bottom one, a Mohr Coulomb model will be employed.

The model and the parameters used to represent each soil layer are summarized in the following tables.

Table 13. Constitutive soil parameters for each soil layer modeled with HS.

Parameter	NQfll	Res. V	Res. V (2)
γ (kN/m^3)	19.5	17.9	19.7
γ_d (kN/m^3)	15	12.8	15.6
ν	0.35	0.35	0.35
C' (kPa)	11.50	-	-
Φ' (°)	37.57	-	-
C (kPa)	-	52.5	30
Φ (°)	-	16	16
Ψ (°)	-	-	-
E_{50}^{ref} (kPa)	20700	5770	4230
E_{oed}^{ref} (kPa)	20700	5770	4230
E_{ur}^{ref} (kPa)	62100	17310	12690
P_{ref} (kPa)	100	100	100
m (power)	1	1	1
K_o^{nc}	0.39	0.72	0.72
R_f	0.9	0.9	0.9

Table 14. Constitutive soil parameters for each soil layer modeled with MC.

Parameter	Res. IV
γ (kN/m^3)	20
γ_d (kN/m^3)	17
ν	0.3
C' (kPa)	0
Φ' (°)	35
Ψ (°)	-
E (kPa)	82000

4.2.3.2 LATERAL BEHAVIOR

After calibration of the HS model for the three first layers and the assumption of the MC model for the bottom one, the 3D model was settled as is shown in the following figure.

a

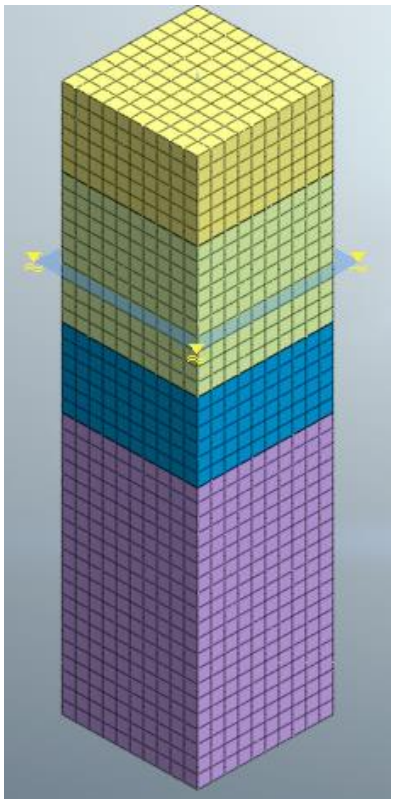

b

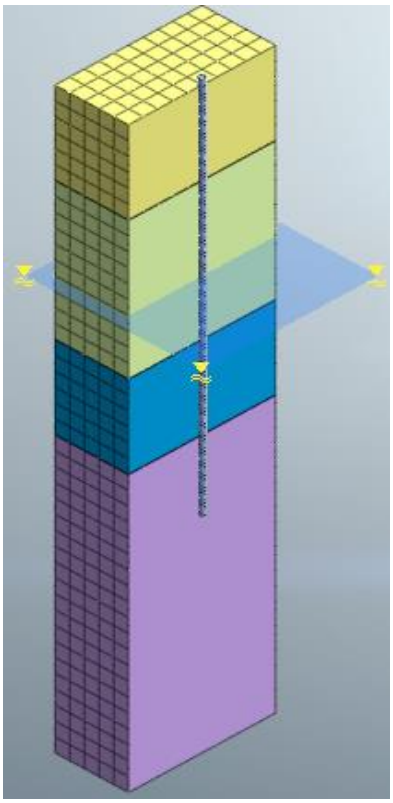

Fig. 25. 3D model. a) soil layer and b) micropile element.

Soil parameters used for each soil layer were established on Table 13 and Table 14. First layer (NQfll) thickness is 6 m, second one (Res. V) is 10 m, the third one (Res. IV(2)) is 6 m and the last one (Res. IV) is 20 m. Phreatic level position is 12 m below top layer surface. The micropile element is considered as a beam element directly connected to each soil layer mesh (without using interfaces). Micropile properties are presented on the following figure.

a

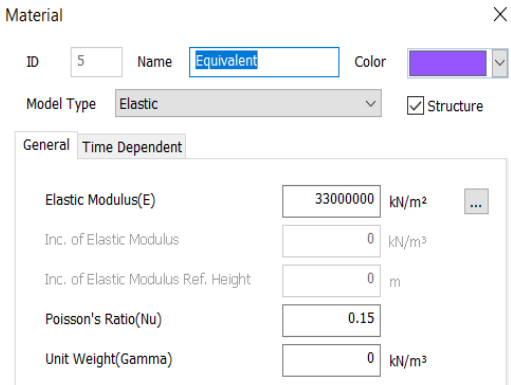

b

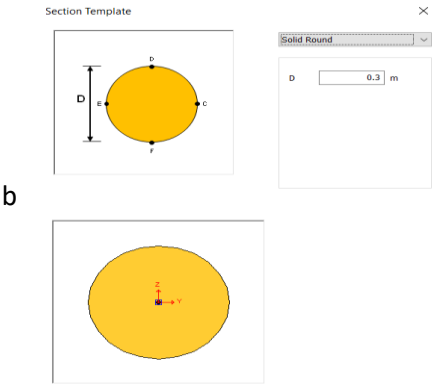

Fig. 26. Micropile characteristics. a) equivalent material properties and b) cross section.

It is important to notice that the equivalent resistance was used to consider the composite section of micropile element as it was done on previous evaluations.

The dimensions of the model were 10 m wide, 10 m long and 42 m high. The meshing elements used were rectangular finite elements the size of 1 m. The boundary conditions at the lateral sides corresponded to horizontal translational constraints and in the bottom of the model a vertical displacement constraint. The micropile element was restricted to rotation on its vertical axis.

For the lateral evaluations of the micropile this was laterally loaded by means of a point load placed at its head. This load was increased by stages. For these evaluations, three scenarios were considered:

- First one: soil parameters of Table 13 and Table 14 are used.
- Second one: moduli of elasticity and Over Consolidation Ratio (OCR) are scaled.
- Third one: a Mohr Coulomb model is used and moduli of elasticity are determined based on (Mayne 2006) methodology and post micropile construction Vs measurements shown in Fig. 11 as Vs-A.

For these scenarios, the geometry of the model and the micropile are kept as a constant, and just soil properties are changed.

4.2.3.2.1 Initial conditions (1^{s} scenario)

Using directly the calibrated soil models to evaluate the lateral behavior of a micropile type IV will get results like those presented on the following figure.

a

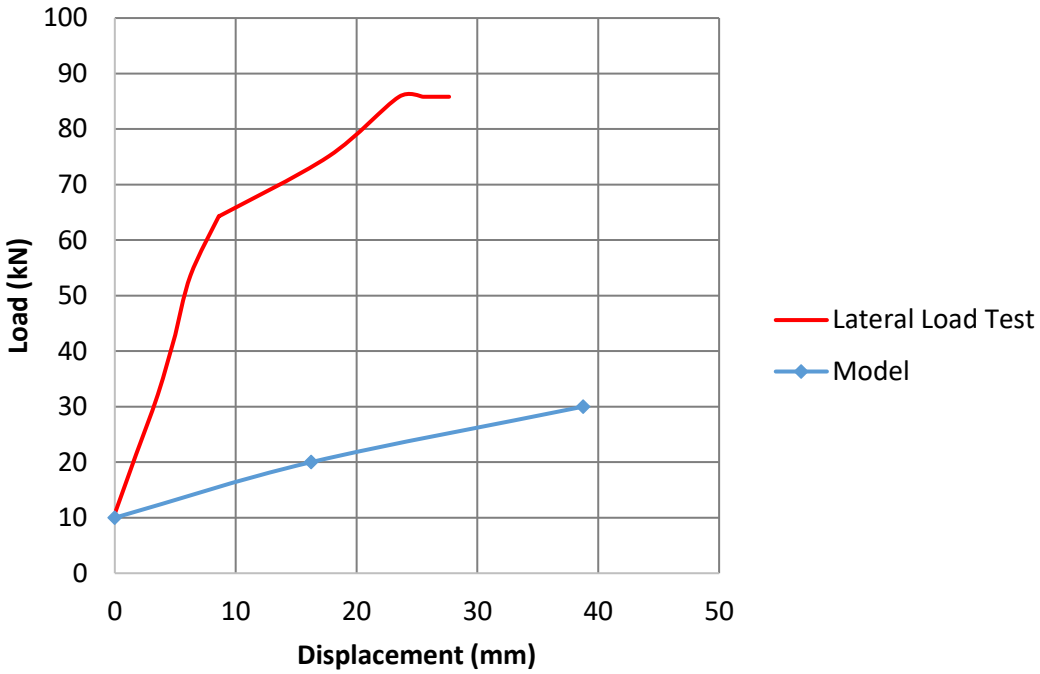

b

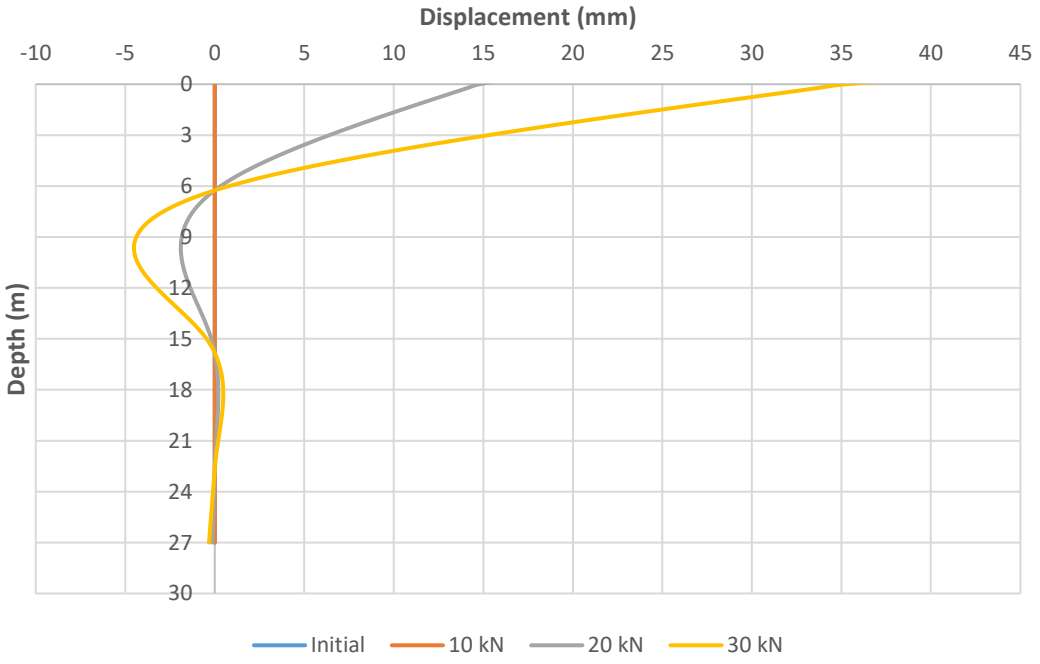

Fig. 27. Lateral displacement evaluation at: a) micropile's head and b) along micropile's depth.

It is important to notice that the model did not converged because the soil resistance was too low, nevertheless, from the previous figure is quite notable that at 6 m depth is presented a slope change in the micropile deformation shape, this implies an inflection point and possibly a plastic hinge. This

result presents a good agreement with Table 15. Considering this, then, the lateral behavior of the micropile is primarily defined by the first soil layer.

Table 15. Evaluation of equations (2) to (4).

Author	Equation	
(FHWA 2005)	$L_0 = 20 * 0.3\ \mathrm{m} = 6\ \mathrm{m}$	(29)
(Richards and Rothbauer 2004)	$L_0 = 2 \text{ to } 5\ \mathrm{m}$	(30)
(L'École Nationale des Ponts et Chaussées 2004)	$L_0 = \sqrt[4]{\frac{4 * 33\ GPa * 3.97E^{-4}\ m^4}{20.7\ MPa}} = 1.3\ m$	(31)

4.2.3.2.2 Scaled stress (2[d] scenario)

To consider the effect of the soil improvement based on the micropile injection procedure, then, taking account, the discussion presented on the previous section, for the first soil layer the reference soil modulus for primary loading was scaled to the pressure of injection used at surface (1000 kPa) and the OCR to 50 (ratio between the average insitu horizontal effective stress and the injection pressure applied on the first layer – it is between 45 to 50).

a

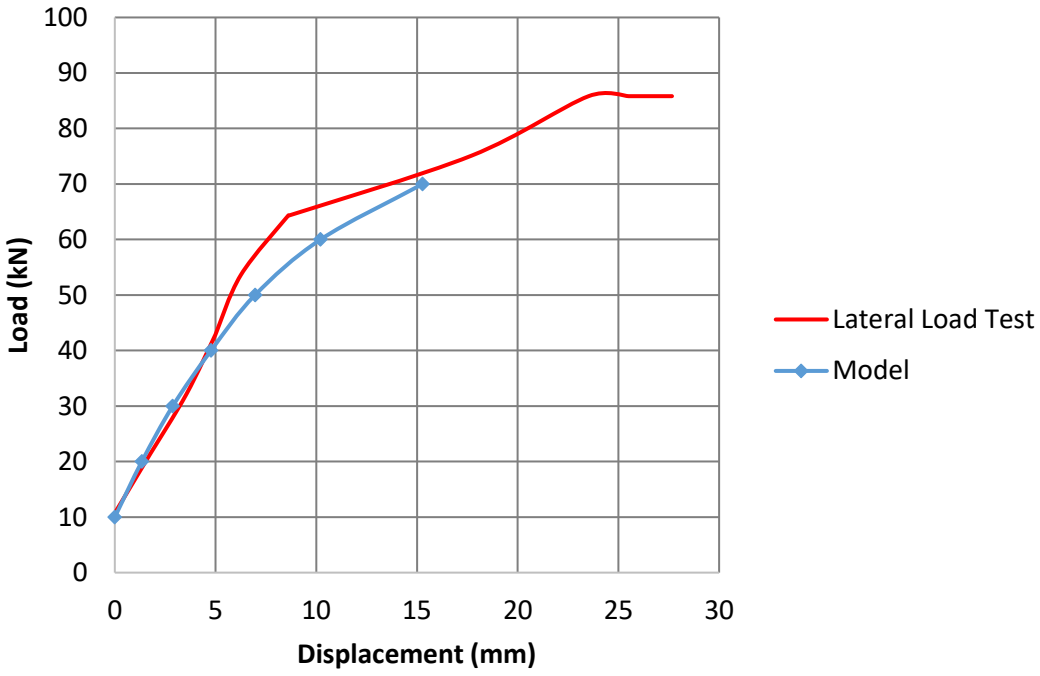

b

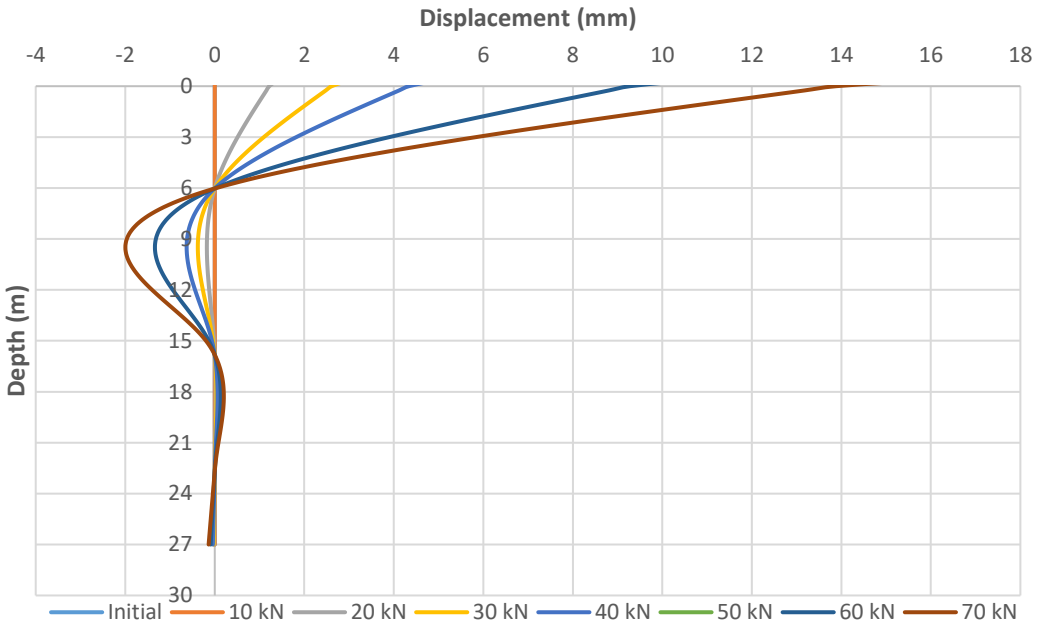

Fig. 28. Lateral displacement evaluation with NQfll's reference modulus and OCR scaled. a) micropile's head and b) along micropile's depth.

Results obtained from the model after considering the increased effect of soil's stiffness and resistance due to injection pressure used to build the micropile, show a decent agreement with lateral load test measurements. This implies that modelling must consider the use of a soil constitutive model that could be able to reproduce laboratory tests concerning characteristic as good as possible, the construction techniques used and to scale stress and resistance due to soil's disturbances.

4.2.3.2.3 Second approach (3^{d} scenario)

As an alternative to evaluate the lateral behavior of the micropile of interest, a Mohr Coulomb model was used for the first soil layer (NQfll), nevertheless, the soil modulus used (E_{50}) to consider the effect of the injection procedure was computed with the Vs measured after the injection procedure. The modulus used for the evaluation was the highest one for NQfll layer after some micropiles were constructed (see Fig. 12).

a

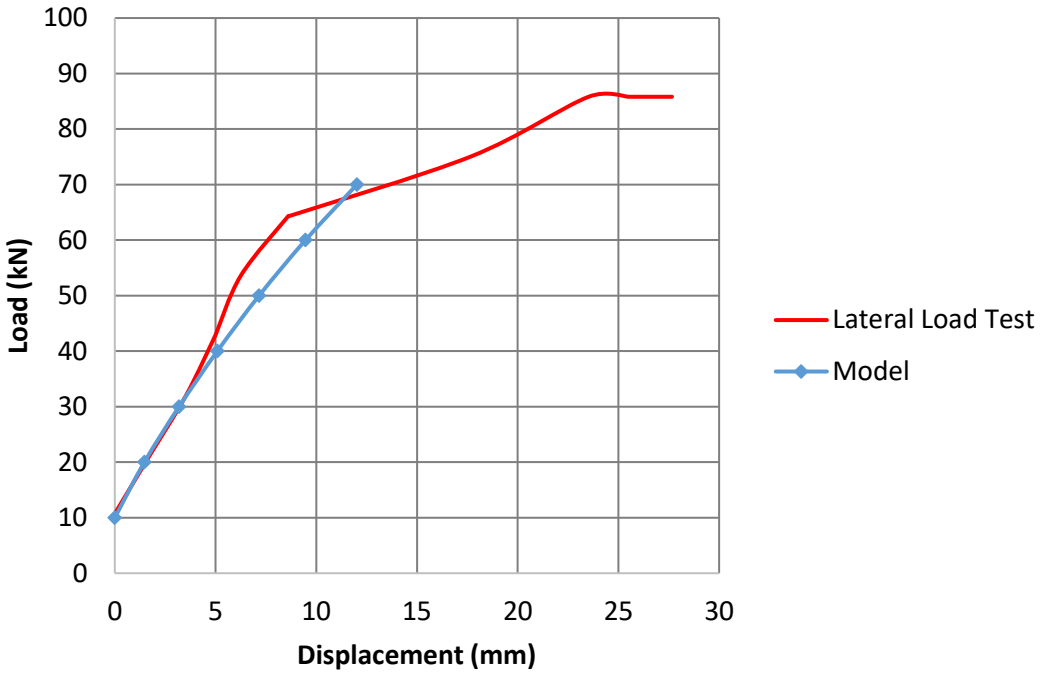

b

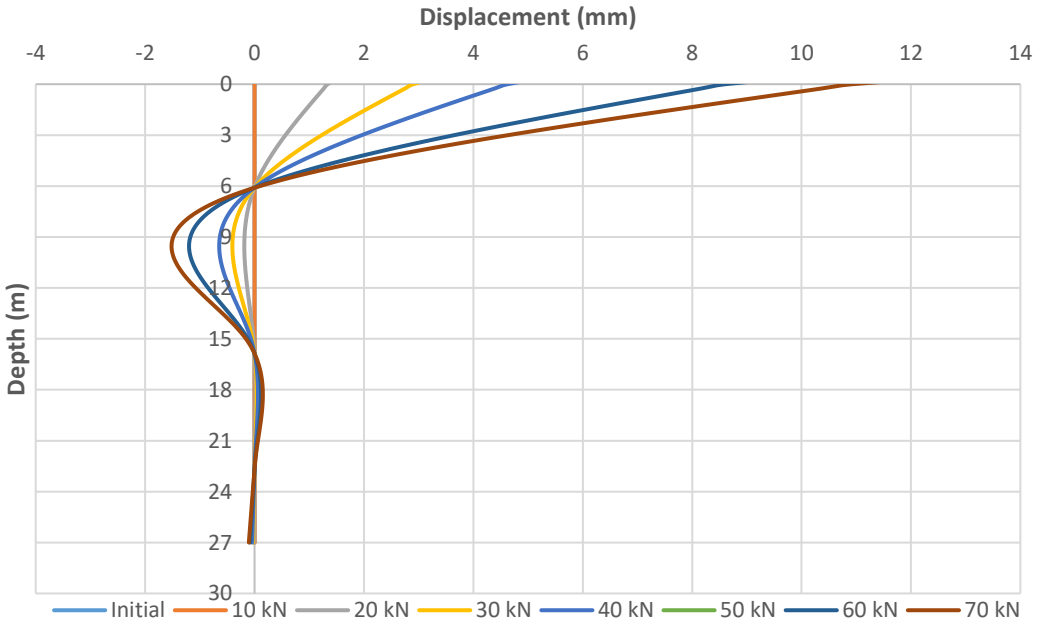

Fig. 29. Lateral displacement evaluation with NQfll Mohr Coulomb model using soil's modulus after injection. a) micropile's head and b) along micropile's depth.

The MC model seems to be enough to consider elastic part behavior of the soil and the lateral load test result. Nonetheless, it is just usable if complementary geotechnical surveys after micropiles

have been entirely built is performed and if a limited lateral displacement value of 1 cm is considered as a boundary condition.

5 ADDITIONAL APPROACH

Considering the increase of geophysical exploration methods used nowadays and some of their results -shear wave velocity (Vs). It could be reasonable to expect an approach to compute the modulus of subgrade reaction derived directly from Vs results. A brief discussion about a proposed formulation is presented in the following paragraphs.

The shear stress (τ) is:

$$\tau = G\,\gamma \tag{32}$$

where, G is the shear modulus and γ is the shear strain.

Also:

$$\tau = \frac{F}{A} \tag{33}$$

where, F is the internal shear force and A is the area of the section where shear force is acting.

By definition:

$$v_s = \sqrt[2]{\frac{G}{\rho}} \tag{34}$$

where ρ is the soil density.

Replacing G from (34) into (32) it results into:

$$\tau = {v_s}^2\,\rho\,\gamma \tag{35}$$

And (33) in (35):

$$\frac{F}{A} = {v_s}^2\,\rho\,\gamma \tag{36}$$

Based on (5):

$$\frac{k\,y}{A} = {v_s}^2\,\rho\,\gamma \tag{37}$$

Then, leaving k from (37):

$$k = \frac{{v_s}^2\,\rho\,\gamma\,A}{y} \tag{38}$$

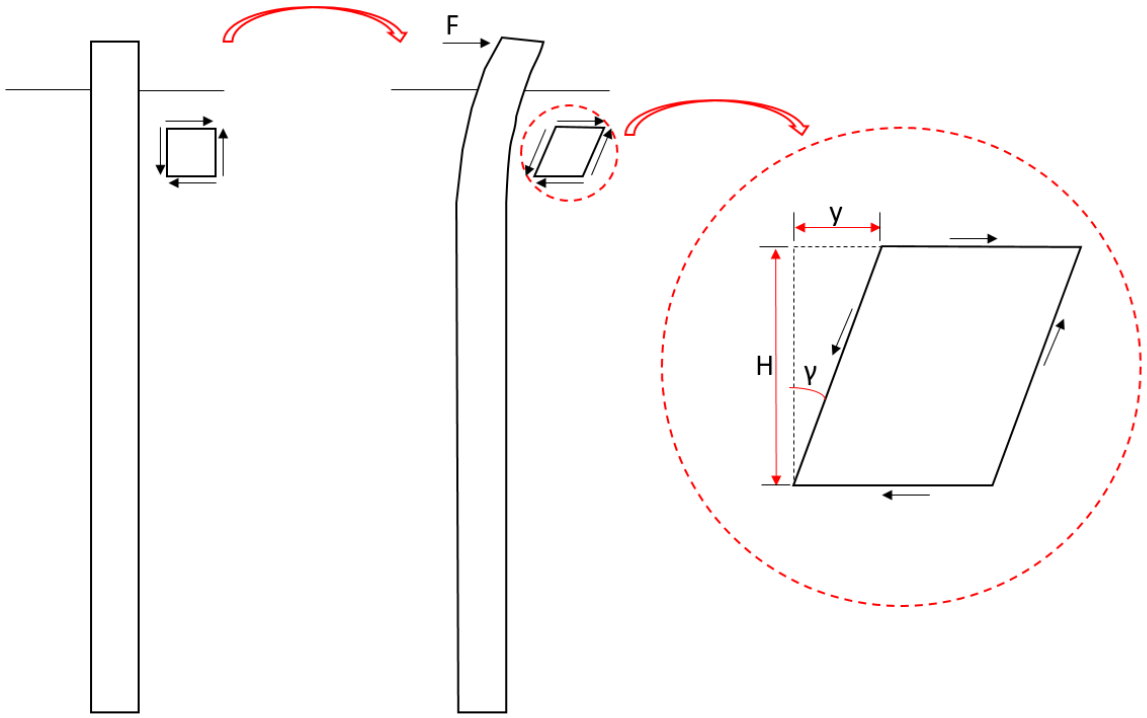

Fig. 30. Soil shear stress conditions during a lateral load test.

As it is inferred from Fig. 30, $\gamma = \frac{y}{H}$ and $A = Micropile\ Diameter\ (d) * 1m.$ Considering these variables values, then:

$$k = \frac{{v_s}^2\ \rho\ \ d * 1m}{H} \tag{39}$$

If (39) is multiplied and divided by gravity (g), then:

$$k = \frac{{v_s}^2\ \gamma\ \ d * 1m}{H\ g} \tag{40}$$

It is important to mention that this equation is based on elasticity theory, consequently, it can be used just to represent soil's elastic response. Using equation (40), the following results were obtained to represent the elastic part of the load test.

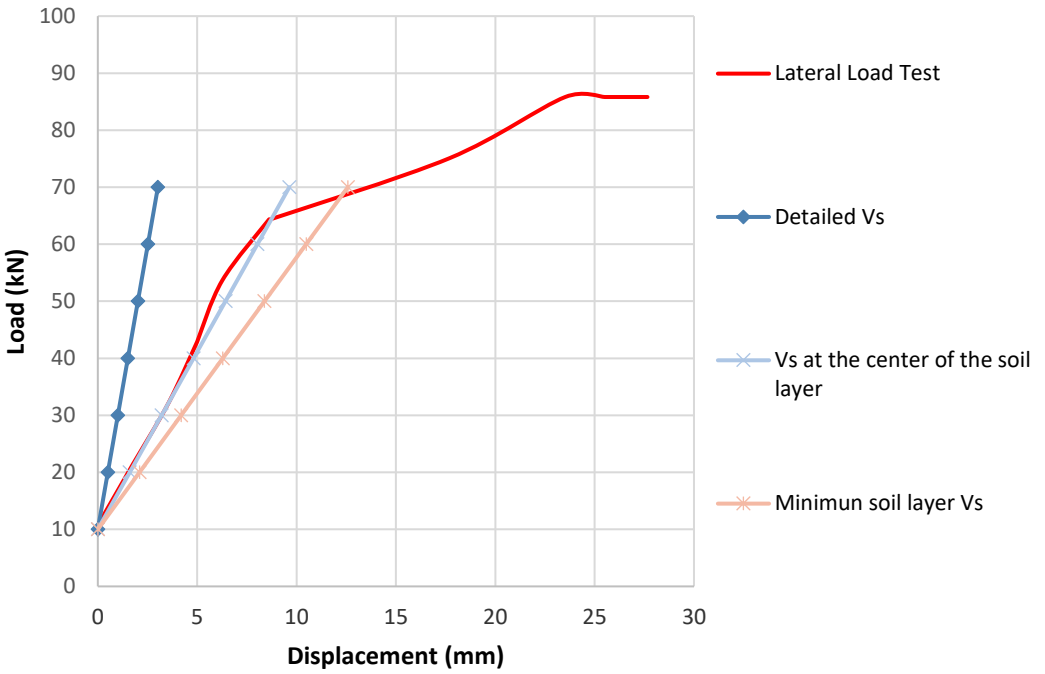

Fig. 31. Evaluation of M1-PC-H lateral load test result again proposed formulation for the elastic part.

The most fitted results were obtained using the middle height of each soil layer and its correspondent shear wave velocity. The value of k used for each soil layer is shown in Table 16.

Table 16. Moduli of subgrade reaction using proposed formulation for springs each meter along micropile element.

Soil layer	Vs (m/s)	K (kN/m)
NQfll	218	7153
Res. V	239	6666
Res. V (2)	283	15490
Res. IV	298	19843

As an additional effort to evaluate the reliability of equation (40), the M2-PC-H lateral load test result is compared with the latest results, but this time influenced by the coefficients of reduction proposed by (Mezazigh 1995). For this evaluation, the conditions mentioned on3.4.2 are used to obtain the reduction coefficients and the result of this is presented on Table 17.

Table 17. Evaluation of coefficients of reduction due to slope proximity using (Mezazigh 1995).

t (m)	2.4	4.4
B or D (m)	0.3	
β (°)	18	40

t_{lim} (m)	1.14	4.84
r	1.30	0.72
$t \leq t_{lim}$	No	Yes

Based on Table 17 results, the reduction coefficient is 0.72. Then, the new moduli of subgrade reaction are:

Table 18. Moduli of subgrade reaction using proposed formulation and (Mezazigh 1995) methodology.

Soil layer	Reduction coefficient	K (kN/m)
NQfll	0.727	5205
Res. V		4851
Res. V (2)		11273
Res. IV		14441

Using these new values, the displacement obtained is compared against the recorded M2-PC-H lateral load test as is shown in the next figure.

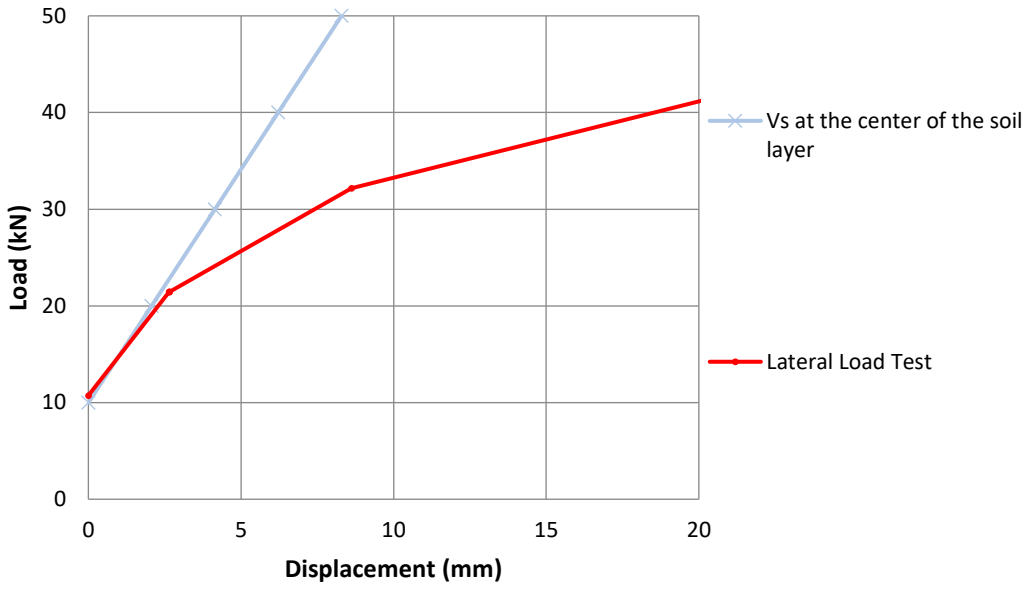

Fig. 32. Evaluation of M2-PC-H lateral load test result compared to proposed formulation for the elastic part and affected by (Mezazigh 1995).

It is important to note that the upper 6 m of soil controls the lateral behavior of the micropile, then, it will be necessary to perform additional instrumented tests to verify the truthfulness of this

proposed method. Tentatively, this elastic method must be restricted to micropiles lateral head displacement not larger than 1 cm. To represent the plastic part of the micropile behavior, maybe the use of degradation curves could be used.

A comparison between the semi-empirical methods that consider the elasticity modulus as a main parameter and the proposed formulation can be performed if (Mayne 2006) methodology is applied to degrade the initial shear modulus and transform it into the equivalent soil modulus as it is pointed out by (Salvá 2014).

To do this degradation, an hyperbolic function is applied using a safety factor between 1.5 and 3 (as it is normally used for foundation systems), a g value of 0.3 (the most feasible results are found using g values varying between 0.2 and 0.4), a F value of 1 (this is suggested by (Mayne 2006)) and taking into account that the most fitted results were obtained using (40) with H equal to 3 m, then, the proposed formulation will result in the following equation.

$$k = 3.3 * \frac{Es * d}{(1+v)} \; to \; 1.3 * \frac{Es * d}{(1+v)} \tag{41}$$

This new equation could be compared with those presented on Table 3, and easily identify that it is similar to (Vesic 1961), (Kishida and Nakai 1977) and (Broms 1964a), nevertheless, this proposal could be used from direct measurements of the shear wave velocity, what means an advantage because it reduces subjectivity.

6 CONCLUSIONS AND RECOMMENDATIONS

Based on results shown on previous chapters, the following conclusions and recommendations are drawn from the evaluation of lateral response of a micropile type IV (IRS) laterally loaded.

6.1 CONCLUSIONS

1. As references and for practical engineering approaches, the ultimate lateral load of a micropile can be considered at least as 4% of the ultimate vertical load.
2. The use of semiempirical formulations to evaluate lateral displacement of a micropile may result in an over or underestimation of the lateral displacement depending of the parameters and the formulation applied. It will be the responsibility of the geotechnical engineer designer to evaluate which of these formulations ought to be used, based on his professional experience and parametrical reliability.
3. Lateral displacements estimation using P-Y curves for silts will result in a conservative approach independently of which geotechnical parameters are implemented.
4. Even though geotechnical engineers have calibrated constitutive soil models that can accurately represent the characteristics that will be evaluated (displacements, pore pressures, etc.), it is important to consider the effects on the stress conditions of soil according to the construction techniques that are used. If this is not taken into account, the lateral displacements evaluated will be overpredicted.
5. If it is not possible to calibrate advanced soil constitutive models, alternatively, a Mohr Coulomb soil model can be used if a post-grouted injection survey can be performed with at least a geophysical field test to evaluate the increase in the soil modulus of elasticity as consequence of the soil's densification effect of the injections. However, this evaluation method will be just valid for the elastic range of the soil and reliable for lateral displacements lower than 1 cm.

6.2 RECOMMENDATIONS

A. As a complementary condition of evaluation, it is necessary to compute the reduction of the lateral resistance by the presence of slopes near the micropile. This is quite evident in the comparison of the results of Fig. 18.
B. This research focused on the analysis of response of a single micropile, nevertheless it could be interesting to evaluate the performance of a group of micropiles laterally loaded and the effect of the separation between elements.
C. To supply the horizontal resistance of micropiles installed vertically, the use of battered micropiles or anchors in the micropile group's cap will be desirable.
D. To verify the representativeness of the numerically evaluated deformed shape, it will be necessary to perform another test, but this time instrumented with strain gauges along its length.
E. Considering that the main concern about lateral loads results from external sources like earthquakes and wind forces, it will be necessary to evaluate the soil's resistance degradation by the effect of cyclic loads.
F. It would be highly recommended to use steel cases as reinforcement for the first 6 m of the micropile, this will help to improve the stiffness of the element and may help to increase lateral resistance.

7 REFERENCES

Abd El-aziz, A. Y. (2012). “Performance of Hollow Bar Micropiles Under Axial and Lateral Loads in Cohesive Soils.” Western University.

Área Metropolitana del Valle de Aburrá. (2007). *Microzonificación y evaluación del riesgo sísmico del Valle de Aburrá*.

Área Metropolitana del Valle de Aburrá. (2012). “Directrices y Lineamientos para la Elaboración de los Estudios Geológicos, Geomorfológicos, Hidrológicos, Hidráulicos, Hidrogeológicos y Geotécnicos para Intervenciones en Zonas de Ladera, en eb.” Medellín.

Audibert, J. M. E., and Nyman, K. J. (1977). “Soil restraint against horizontal motion of pipes.” *Journal of the Geotechnical Engineering Division*, ASCE, 103(10), 1119–1142.

Babalola, M. R. (2011). “Evaluation of the Lateral Response of Micropiles via Full Scale Load Testing.” The University of North Carolina at Charlotte.

Bhushan, K., Lee, L. J., and Grime, D. B. (1981). “Lateral load tests on drilled piers in sand.” *Drilled Piers and Caissons:*, ASCE, 114–131.

Brinch-Hansen, J. (1961). “The Ultimate Resistance of Rigid Piles Against Transversal Forces.” *Bulletin No. 12, Geoteknisk Institut (The Danish Geotechnical Institute)*, (12), 5–9.

Brinkgreve, R. B. J. (2005). “Selection of Soil Models and Parameters for Geotechnical Engineering Application.” 69–98.

Broms, B. (1964a). “Lateral Resistance of Piles in Cohesive Soils.” *Soil Mechanics and Foundations Division*, 27–63.

Broms, B. (1964b). “Lateral Resistance of Piles in Cohesionless Soils.” *Journal of the Soil Mechanics and Foundations Division*, 90, 123–156.

Budhu, M. (2015). *Soil Mechanincs and Foundations*. *Statewide Agricultural Land Use Baseline 2015*.

Bustamante, M. (1985). “Une méthode pour le calcul des tirants et des micropieux injectés.” 75–92.

Das, B. M. (2002). *Principles of Foundation Engineering*. *McGraw-Hill handbooks*.

Davisson, M. T. (1970). “Lateral Load Capacity of Piles.” 104–112.

Day, R., and Mucillo, J. (2014). “Use and Abuse of Springs to Model Foundations.”

Departamento Administrativo Nacional de Estadística, D. (2017a). “No Title.” *ESTIMACIONES DE POBLACIÓN 1985 - 2005 Y PROYECCIONES DE POBLACIÓN 2005 - 2020 TOTAL MUNICIPAL POR ÁREA*, <http://www.dane.gov.co/files/investigaciones/poblacion/proyepobla06_20/Municipal_area_1985-2020.xls>.

Departamento Administrativo Nacional de Estadística, D. (2017b). “Censo Edificaciones -Ceed.” Bogotá D.C.

Desai, C. S., and Zaman, M. (2013). *Advanced Geotechnical Engineering: Soil-Structure Interaction using Computer and Material Models*. CRC Press.

Dirección General de Carreteras. (2005). *Guía para el Proyecto y la Ejecución de Micropilotes en Obras de Carretera*.

Duncan, J., Jr, L. E., and Ooi, P. (1994). “Lateral load analysis of single piles and drilled shafts.” *Journal of geotechnical …*, 120(5), 1018–1033.

FHWA. (2005). *Micropile Design and Construction - Reference Manual*.

Fookes, P. G. (1997). “Tropical residual soils: A Geological Society Engineering Group working party revised report.” Geological Society of London.

Francis, A. J. (1964). “Analysis of pile groups with flexural resistance.” *Journal of Soil Mechanics & Foundations Div*, 90(Proc. Paper 3887).

GCO. (2006). “Foundation design and construction.” *Geo Publication*, (1).

Habibagahi, K., and Langer, J. (1984). “Horizontal subgrade modulus of granular soils.” *Laterally loaded deep foundations: Analysis and performance*, 21–34.

Heténi, M. (1946). *Beams on Elastic Foundation: Theory with Applications in the Fields of Civil and Mechanical Engineering*. University of Michigan press.

Kershaw, K. a., and Luna, R. (2014). “Full-Scale Field Testing of Micropiles in Stiff Clay Subjected to Combined Axial and Lateral Loads.” *Journal of Geotechnical and Geoenvironmental Engineering*, 140(1), 255–261.

Kishida, H. (1967). “Ultimate bearing capacity of piles driven into loose sand.” *Soils and Foundations*, 公益社団法人地盤工学会, 7(3), 20–29.

Kishida, H., and Nakai, S. (1977). “Large deflection of a single pile under horizontal load.” *Proc. Specialty Session*, 87–92.

L’École Nationale des Ponts et Chaussées. (2004). *FOREVER - Synthèse des résultats et recommandations du Projet national sur les micropieux*.

Lizzi, F. (1950). “First Patent on Root Piles and Reticulated Root Piles.” Fondedile, Naples.

Lizzi, F. (1982). “The pali radice (root piles).” *Symposium on Soil and Rock Improvement Techniques including Geotextiles, Reinforced Earth and Modern Piling Methods, Bangkok, Paper D-3*.

Long, J., Maniaci, M., Menezes, G., and Ball, R. (2004). “Results of Lateral Load Tests on Micropiles.” *GeoSupport 2004: Drilled Shafts, Micropiling, Deep Mixing, Remedial Methods, and Specialty Foundation Systems*, 122–133.

M.A.Biot. (1937). “On bending of an infinite beam on an elastic Foundation.” *Journal of Applied Mathematics and Mechanics*, 22(5), 984–988.

Matlock, H. (1970). “Correlations for design of laterally loaded piles in soft clay.” *Offshore Technology in Civil Engineering’s Hall of Fame Papers from the Early Years*, 77–94.

Mayne, P. W. (2006). “In-situ test calibrations for evaluating soil parameters.” *Characterisation*

and Engineering Properties of Natural Soils–Proceedings of the Second International Workshop on Characterisation and Engineering Properties of Natural Soils: Taylor & Francis, 1601–1652.

McClelland, B., and Focht, J. A. (1958). "Soil modulus for laterally loaded piles." *Transactions of the American Society of Civil Engineers*, ASCE, 123(1), 1049–1063.

Meyerhof, G. G. (1963). "Some recent research on the bearing capacity of foundations." *Canadian Geotechnical Journal*, NRC Research Press, 1(1), 16–26.

Mezazigh, S. (1995). *Etude expérimentale de pieux chargés latéralement: proximité d'un talus et effet de groupe*.

Ministère de l'Équipement des Transports. (1993). "Règles techniques de conception et de calcul des fondations des ouvrages de génie civil."

Ministerio de Ambiente Vivienda y Desarrollo Territorial. (2010). *Reglamento Colombiano de Construcción Sismo Resistente NSR-10*. *Diario Oficial*, Colombia, 444.

Murchinson, J. (1983). "An evaluation of py relations in Sands." University of Houston: American Petroleum Institute.

NAVFAC. (1986). "7.02: Foundations & Earth Structures." NAVFAC, Washington, D.C.

Osama F., E. H. D. (2013). "Investigation of Hollow Bar Micropiles in Cohesive Soil." The University of Western Ontario.

Pise, P. J. (1977). "Experimental Coefficients for Laterally Loaded Piles." *Int. Symp. On Soil Struct. Interact. India Univ. of Roorkee*, 327–333.

Plumelle, C., and Raynaud, D. (1996). *Essais de Chargement des Micropieux Isolés et des Groupes. Rapport du Projet National de Recherche FOREVER, N: FO/95/03*.

Pyke, R., and Beikae, M. (1984). "A new solution for the resistance of single piles to lateral loading." *Laterally Loaded Deep Foundations: Analysis and Performance*, ASTM International.

Rabab'ah, S. R., Niedzielski, J. C., and Elsayed, A. A. (2014). "Analysis and design of Micropile-Supported Wall to Resist Lateral Deflection of Existing Railroad Bridge Abutment." 3102–3111.

Reese, L. C., Cox, W. R., and Koop, F. D. (1974). "Analysis of laterally loaded piles in sand." *Offshore Technology in Civil Engineering Hall of Fame Papers from the Early Years*, 95–105.

Reese, L. C., Van Impe, W., and Holtz, R. (2002). *Single Piles and Pile Groups Under Lateral Loading*. CRC Press.

Reese, L. C., and Welch, R. C. (1975). "Lateral loading of deep foundations in stiff clay." *Journal of Geotechnical and Geoenvironmental Engineering*, 101(ASCE# 11456 Proceeding).

Richards, T. D., and Rothbauer, M. J. (2004). "Lateral Loads on Pin Piles (Micropiles)." *GeoSupport 2004: Drilled Shafts, Micropiling, Deep Mixing, Remedial Methods, and Specialty Foundation Systems*, 158–174.

Robinson, K. E. (1979). "Horizontal Subgrade Reaction Estinnated from Lateral Loading Tests on Tinnber Piles." 520–536.

Ruigrok, J. A. T. (2010). "Laterally Loaded Piles." TU Delft.

Salvá, P. J. (2014). "Comportamiento Mecánico de Suelos Saprolíticos para el Diseño de Cimentaciones Profundas." Universidad EAFIT.

Schanz, T., Vermeer, P. A., and Bonnier, P. G. (1999). "The hardening soil model : Formulation and verification." 1–16.

Skempton, A. W. (1951). "The bearing capacity of clays."

Sogge, R. L. (1981). "Laterally loaded pile design." *Journal of Geotechnical and Geoenvironmental Engineering*, 107(ASCE 16510).

Terzaghi, K. (1955). "Evaluation of Coefficient of Subgrade Reaction." *Geotechnique, London*, 5(4), 41–50.

Thilakasiri, H. S., Potts, D. M., Kontoe, S., and Zdravkovic, L. (2009). “Earthquake Induced Kinematic Forces on Pile Foundations in Layered Medium.” *Engineer: Journal of the Institution of Engineers, Sri Lanka*, 42(4), 56–64.

Timoshenko, S., and Goodier, J. N. (1951). *Theory of Elasticity*. *Journal of Elasticity*.

Vesic, A. B. (1961). “Beams on Elastic Subgrade and the Winkler’s Hypothesis.” *Proceedings, 5th International Conference on Soil Mechanics and Foundation Engineering*, 1, 845–850.

Welch, R. C., and Reese, L. C. (1972). *Lateral load behavior of drilled shafts*. University of Texas at Austin.

Winkler, E. (1867). “Die Lehre von der Elasticitaet und Festigkeit (The Theory of Elasticity and Stiffness).” Pague, 182.

Zeevaert, L. (1983). *Foundation Engineering for difficult subsoil conditions*. Van Nostrand Reinhold Company Inc.

Zimmermann, H. (1888). *Die Berechnung des Eisenbahnoberbaues*. Berlin.

8 ANNEXES

Semiempirical evaluations

Formulation	Kh (kPa/m)	Parameters
(Vesic 1961)	5780	E_s=4MPa, v=0.3, d=0.3 m, I_p=3.97E-4 m^4, E_p=33GPa
(Francis 1964)	4272283	Z=11m, γ=16kN/m^3, ϕ=20°, $N_γ$=2.9, N_q=6.4, d=0.3m
(Broms 1964a)	4174	E_s=4MPa, v=0.3, d=0.3 m, L=27 m, m=0.37
(Audibert and Nyman 1977)	370284	Z=11m, γ=16kN/m^3, ϕ=20°, N_q=6.4, y_u=6mm, y=2.54mm
(Kishida and Nakai 1977)	11560	E_s=4MPa, v=0.3, d=0.3 m, I_p=3.97E-4 m4, E_p=33GPa
(Robinson 1979)	10720	S_u=48kPa, d=0.3m
(Bhushan et al. 1981)	69109	N=2, d=0.3m, Y=2.54mm
(Sogge 1981)	11520	Z=11m, d=0.3m
(Pyke and Beikae 1984)	26667	E_s=4MPa, d=0.3 m
(Habibagahi and Langer 1984)	722512	Z=11m, σ'=166kPa, γ=16kN/m^3, ϕ=20°, A=5, d=0.3m, y=2.54mm

Annex 1- Res. V layer moduli of subgrade reaction - semiempirical formulations – Lowest case

Formulation	Kh (kPa/m)	Parameters
(Vesic 1961)	93047	E_s=52MPa, v=0.3, d=0.3 m, I_p=3.97E-4 m^4, E_p=33GPa
(Francis 1964)	12409533	Z=11m, γ=18kN/m^3, ϕ=29°, $N_γ$=13.2, N_q=16.4, d=0.3m
(Broms 1964a)	54265	E_s=52MPa, v=0.3, d=0.3 m, L=27 m, m=0.37
(Audibert and Nyman 1977)	1070380	Z=11m, γ=18kN/m^3, ϕ=29°, N_q=16.4, y_u=6mm, y=2.54mm
(Kishida and Nakai 1977)	186095	E_s=52MPa, v=0.3, d=0.3 m, I_p=3.97E-4 m4, E_p=33GPa
(Robinson 1979)	22110	S_u=99kPa, d=0.3m
(Bhushan et al. 1981)	518316	N=15, d=0.3m, Y=2.54mm
(Sogge 1981)	11520	Z=11m, d=0.3m
(Pyke and Beikae 1984)	346667	E_s=52MPa, d=0.3 m
(Habibagahi and Langer 1984)	818266	Z=11m, σ'=188kPa, γ=18kN/m^3, ϕ=29°, A=5, d=0.3m, y=2.54mm

Annex 2. Res. V layer moduli of subgrade reaction - semiempirical formulations -Highest case.

Formulation	Kh (kPa/m)	Parameters
(Vesic 1961)	38451	E_s=23MPa, v=0.3, d=0.3 m, I_p=3.97E-4 m^4, E_p=33GPa
(Francis 1964)	11148767	Z=20m, γ=17kN/m^3, ϕ=23°, $N_γ$=4.8, N_q=8.7, d=0.3m
(Broms 1964a)	24002	E_s=23MPa, v=0.3, d=0.3 m, L=27 m, m=0.37
(Audibert and Nyman 1977)	968144	Z=20m, γ=17kN/m^3, ϕ=23°, N_q=8.7, y_u=6mm, y=2.54mm
(Kishida and Nakai 1977)	76902	E_s=23MPa, v=0.3, d=0.3 m, I_p=3.97E-4 m4, E_p=33GPa

(Robinson 1979)	8710	S_u=39kPa, d=0.3m
(Bhushan et al. 1981)	241881	N=2, d=0.3m, Y=2.54mm
(Sogge 1981)	20945	Z=20m, d=0.3m
(Pyke and Beikae 1984)	153333	E_s=23MPa, d=0.3 m
(Habibagahi and Langer 1984)	1243934	Z=20m, σ'=240kPa, γ=17kN/m^3, ϕ=23°, A=5, d=0.3m, y=2.54mm

Annex 3. Res. V (2) layer moduli of subgrade reaction - semiempirical formulations - Lowest case.

Formulation	**Kh (kPa/m)**	**Parameters**
(Vesic 1961)	98877	E_s=55MPa, v=0.3, d=0.3 m, I_p=3.97E-4 m^4, E_p=33GPa
(Francis 1964)	29756397	Z=20m, γ=19kN/m^3, ϕ=31°, N_y=18.6, N_q=20.6, d=0.3m
(Broms 1964a)	57395	E_s=55MPa, v=0.3, d=0.3 m, L=27 m, m=0.37
(Audibert and Nyman 1977)	2577408	Z=20m, γ=19kN/m^3, ϕ=31°, N_q=20.6, y_u=6mm, y=2.54mm
(Kishida and Nakai 1977)	197753	E_s=55 MPa, v=0.3, d=0.3 m, I_p=3.97E-4 m4, E_p=33GPa
(Robinson 1979)	9157	S_u=41kPa, d=0.3m
(Bhushan et al. 1981)	1209404	N=35, d=0.3m, Y=2.54mm
(Sogge 1981)	20945	Z=20m, d=0.3m
(Pyke and Beikae 1984)	366667	E_s=55MPa, d=0.3 m
(Habibagahi and Langer 1984)	1451256	Z=20m, σ'=280kPa, γ=19kN/m^3, ϕ=31°, A=5, d=0.3m, y=2.54mm

Annex 4. Res. V (2) layer moduli of subgrade reaction - semiempirical formulations - Highest case.

Formulation	**Kh (kPa/m)**	**Parameters**
(Vesic 1961)	31262	E_s=19MPa, v=0.3, d=0.3 m, I_p=3.97E-4 m^4, E_p=33GPa
(Francis 1964)	17081628	Z=23.5m, γ=20kN/m^3, ϕ=24°, N_y=5.7, N_q=9.6, d=0.3m
(Broms 1964a)	19828	E_s=19MPa, v=0.3, d=0.3 m, L=27 m, m=0.37
(Audibert and Nyman 1977)	1483906	Z=23.5m, γ=20kN/m^3, ϕ=24°, N_q=9.6, y_u=6mm, y=2.54mm
(Kishida and Nakai 1977)	62524	E_s=19MPa, v=0.3, d=0.3 m, I_p=3.97E-4 m4, E_p=33GPa
(Robinson 1979)	0	S_u=0kPa, d=0.3m
(Bhushan et al. 1981)	414653	N=12, d=0.3m, Y=2.54mm
(Sogge 1981)	24611	Z=23.5m, d=0.3m
(Pyke and Beikae 1984)	126667	E_s=19MPa, d=0.3 m
(Habibagahi and Langer 1984)	1826754	Z=23.5m, σ'=335kPa, γ=20kN/m^3, ϕ=24°, A=5, d=0.3m, y=2.54mm

Annex 5. Res. IV layer moduli of subgrade reaction - semiempirical formulations - Lowest case.

Formulation	**Kh (kPa/m)**	**Parameters**
(Vesic 1961)	152405	E_s=82MPa, v=0.3, d=0.3 m, I_p=3.97E-4 m^4, E_p=33GPa
(Francis 1964)	132232692	Z=23.5m, γ=20kN/m^3, ϕ=41°, N_y=114, N_q=73.9, d=0.3m
(Broms 1964a)	85571	E_s=82MPa, v=0.3, d=0.3 m, L=27 m, m=0.37

(Audibert and Nyman 1977)	11418463	Z=23.5m, γ=20kN/m^3, ϕ=41°, N_q=73.9, y_u=6mm, y=2.54mm
(Kishida and Nakai 1977)	304810	E_s=82MPa, v=0.3, d=0.3 m, I_p=3.97E-4 m4, E_p=33GPa
(Robinson 1979)	0	S_u=0kPa, d=0.3m
(Bhushan et al. 1981)	1554948	N=45, d=0.3m, Y=2.54mm
(Sogge 1981)	24611	Z=23.5m, d=0.3m
(Pyke and Beikae 1984)	546667	E_s=82MPa, d=0.3 m
(Habibagahi and Langer 1984)	1826754	Z=23.5m, σ'=335kPa, γ=20kN/m^3, ϕ=41°, A=5, d=0.3m, y=2.54mm

Annex 6. Res. IV layer moduli of subgrade reaction - semiempirical formulations - Highest case.

P-Y curves:

LATERAL ANALYSIS

Figure 2

Loads:
Load Factor for Vertical Loads= 1.0
Load Factor for Lateral Loads= 1.0
Loads Supported by Pile Cap= 0 %
Shear Condition: Static

(with Load Factor)
Vertical Load, Q= 0.0 -kN
Shear Load, P= 90.0 -kN
Moment, M= 0.0 -kN-m

Profile:
Pile Length, L= 27.0 -m
Top Height, H= 0.000 -m
Slope Angle, As= 0
Batter Angle, Ab= 0

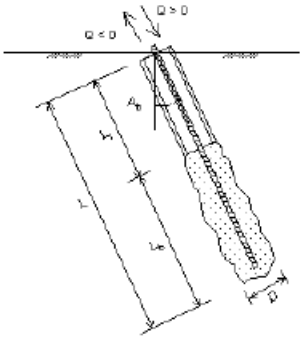

Soil Data:

Depth -m	Gamma -kN/m3	Phi	C -kN/m2	K -MN/m3	e50 or Dr %	Nspt
0	16	20	11	25.9	1.4	2
6	16	20	4	59.3	1.6	2
10	6	20	4	61.7	1.6	2
16	7	23	30	109.2	1.3	2
22	10	24	0	29.4	0.6	12

Pile Data:

Depth -m	Width -cm	Area -cm2	Per. -cm	I -cm4	E -MPa	Weight -kN/m
0.0	30	706.9	94.2	39760.8	20683	1.668
27.0						

Single Pile Lateral Analysis:
Top Deflection, yt= 14.70000-cm
Max. Moment, M= 166.00-kN-m
Top Deflection Slope, St= -0.05990
N/G! Top Deflection, 14.7000-cm, Exceeds the Allowable Deflection= 2.50-cm

Note: If the program cannot find a result or the result exceeds the upper limit. The result will be displayed as 99999.
The Max. Moment calculated by program is an internal force from the applied load conditions. Structural engineer has to check whether the pile has enough capacity to resist the moment with adequate factor of safety. If not, the pile may fail under the load conditions.

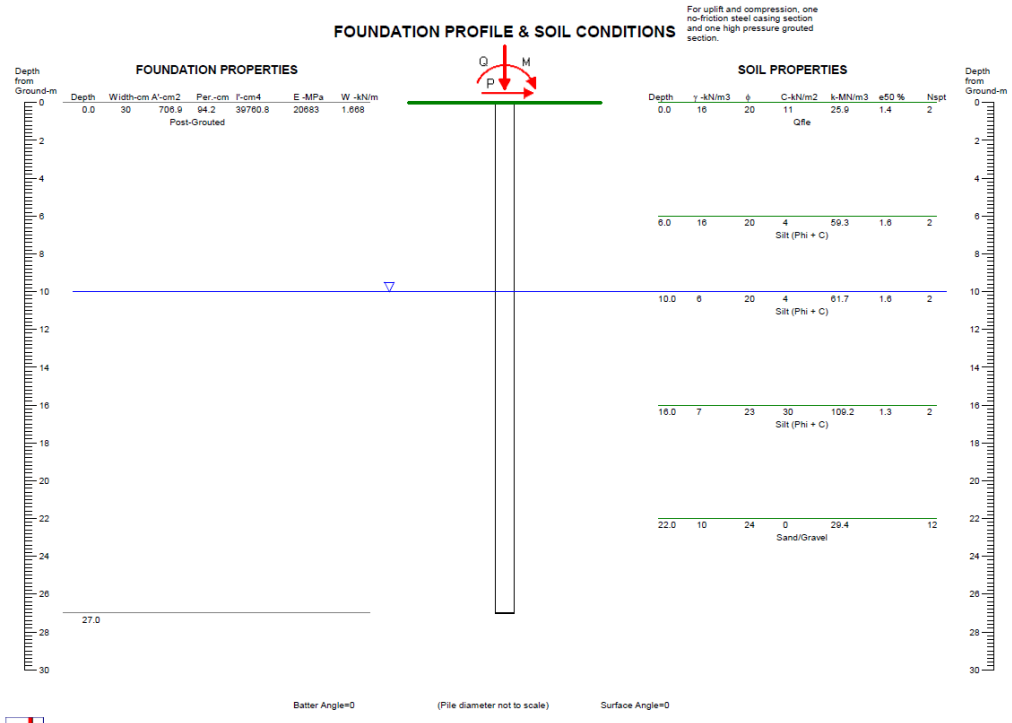

Figure 1

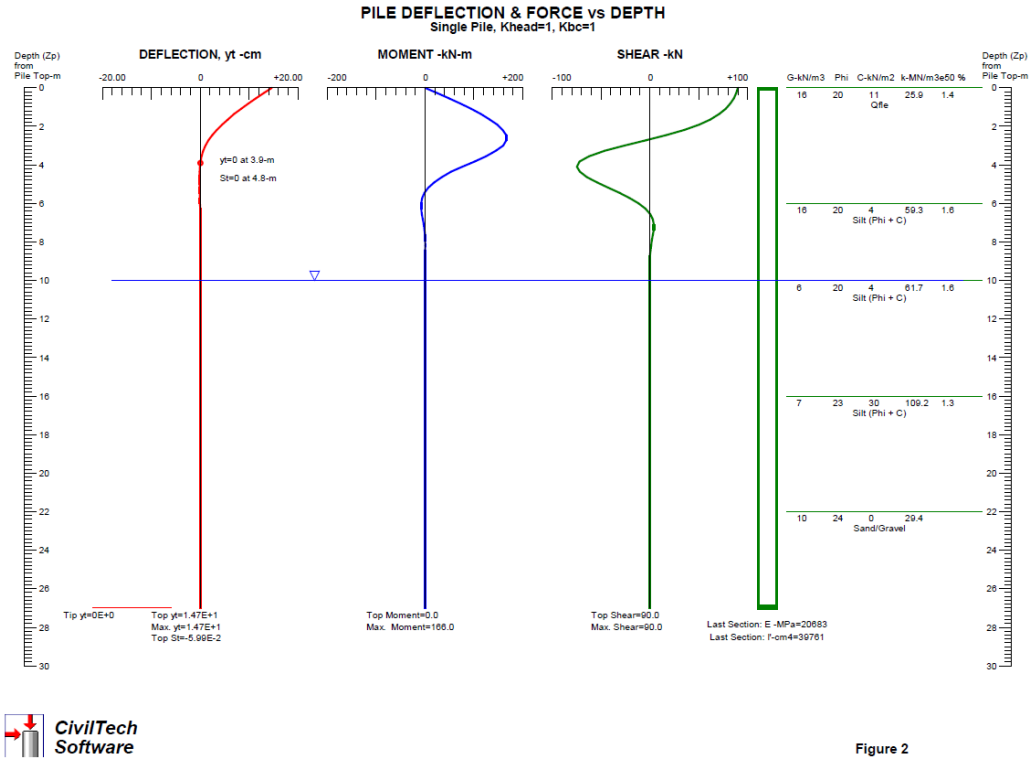

Figure 2

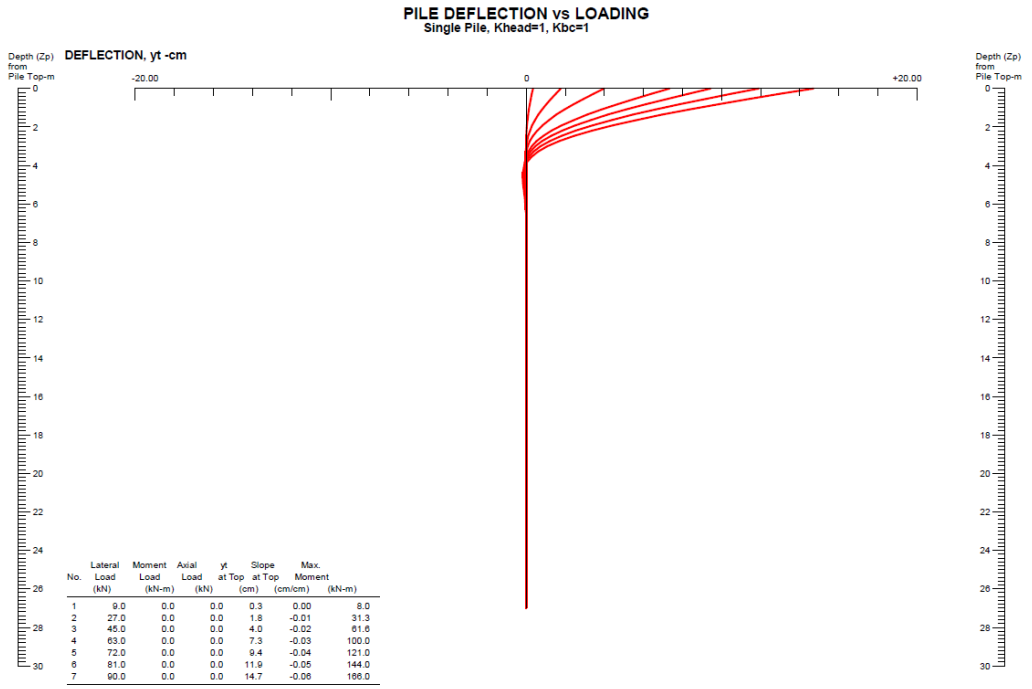

No.	Lateral Load (kN)	Moment Load (kN-m)	Axial Load (kN)	yt at Top (cm)	Slope at Top	Max. Moment (kN-m)
1	9.0	0.0	0.0	0.3	0.00	8.0
2	27.0	0.0	0.0	1.8	-0.01	31.3
3	45.0	0.0	0.0	4.0	-0.02	61.6
4	63.0	0.0	0.0	7.3	-0.03	100.0
5	72.0	0.0	0.0	9.4	-0.04	121.0
6	81.0	0.0	0.0	11.9	-0.05	144.0
7	90.0	0.0	0.0	14.7	-0.06	166.0

CivilTech Software

Figure 2

LATERAL LOAD vs DEFLECTION & MAX. MOMENT

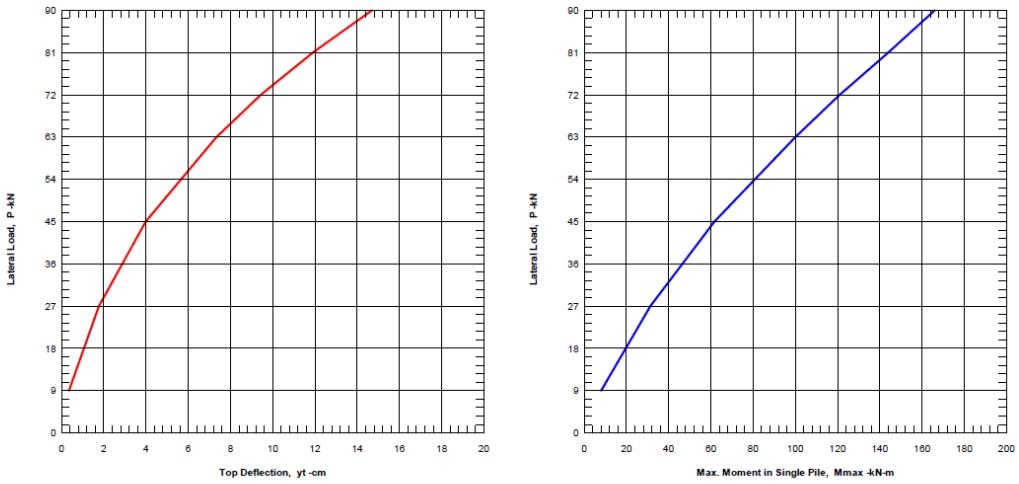

CivilTech Software

Figure 2

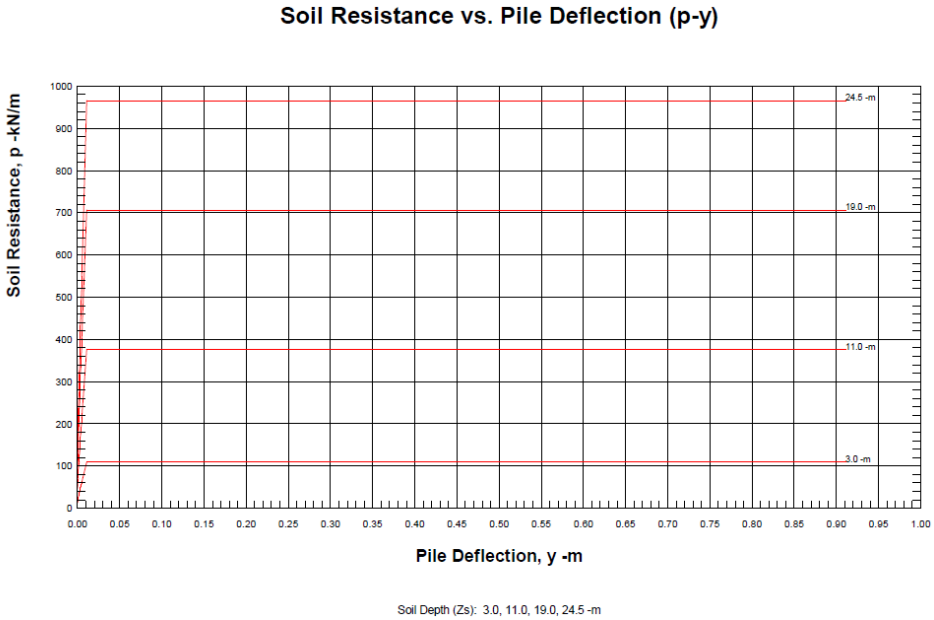

CivilTech Software

Figure 2

0Load_L

Soil Resistance vs. Pile Deflection (p-y)

Zs -m	p -kN/m	y -m
3.00	0.0	0.000
3.00	13.7	0.000
3.00	20.8	0.001
3.00	26.7	0.001
3.00	31.8	0.002
3.00	36.4	0.002
3.00	40.6	0.003
3.00	44.6	0.003
3.00	48.4	0.003
3.00	52.0	0.004
3.00	55.4	0.004
3.00	58.7	0.005
3.00	61.9	0.005
3.00	109.0	0.011
3.00	109.0	0.311
3.00	109.0	0.611
3.00	109.0	0.911
11.00	0.0	0.000
11.00	47.3	0.000
11.00	72.0	0.001
11.00	92.2	0.001
11.00	109.8	0.002
11.00	125.8	0.002
11.00	140.5	0.003
11.00	154.3	0.003
11.00	167.4	0.003
11.00	179.8	0.004
11.00	191.7	0.004
11.00	203.1	0.005
11.00	214.1	0.005
11.00	376.9	0.011
11.00	376.9	0.311
11.00	376.9	0.611
11.00	376.9	0.911
19.00	0.0	0.000
19.00	88.7	0.000
19.00	135.1	0.001
19.00	172.9	0.001
19.00	206.0	0.002
19.00	235.9	0.002
19.00	263.5	0.003
19.00	289.4	0.003
19.00	313.9	0.003
19.00	337.2	0.004
19.00	359.5	0.004
19.00	381.0	0.005
19.00	401.7	0.005
19.00	706.9	0.011
19.00	706.9	0.311
19.00	706.9	0.611
19.00	706.9	0.911
24.50	0.0	0.000
24.50	121.1	0.000
24.50	184.6	0.001
24.50	236.3	0.001
24.50	281.4	0.002
24.50	322.3	0.002
24.50	360.1	0.003
24.50	395.5	0.003
24.50	428.9	0.003
24.50	460.7	0.004
24.50	491.2	0.004
24.50	520.5	0.005
24.50	548.8	0.005
24.50	965.9	0.011
24.50	965.9	0.311
24.50	965.9	0.611
24.50	965.9	0.911

Zs - Depth from Soil Top
p - Soil Resistance
y - Pile Deflection

Annex 7. Lateral evaluation using P-Y curves - lowest case.

LATERAL ANALYSIS

Figure 2

Loads:
Load Factor for Vertical Loads= 1.0
Load Factor for Lateral Loads= 1.0
Loads Supported by Pile Cap= 0 %
Shear Condition: Static

(with Load Factor)
Vertical Load, Q= 0.0 -kN
Shear Load, P= 90.0 -kN
Moment, M= 0.0 -kN-m

Profile:
Pile Length, L= 27.0 -m
Top Height, H= 0.000 -m
Slope Angle, As= 0
Batter Angle, Ab= 0

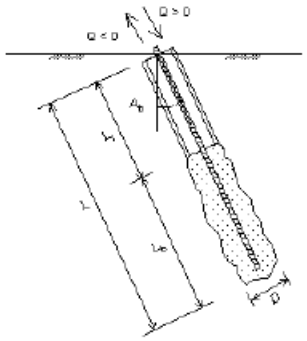

Micropile (MiniPile)

Soil Data:

Depth -m	Gamma -kN/m3	Phi	C -kN/m2	K -MN/m3	e50 or Dr %	Nspt
0	19.5	37.6	11.5	25.9	1.20	5
6	17.9	16.0	52.2	59.3	0.99	8
10	7.9	16.0	52.2	61.7	0.99	8
16	9.7	16.0	29.7	109.2	0.78	12
22	10.0	35.0	0.0	29.4	54.06	20

Pile Data:

Depth -m	Width -cm	Area -cm2	Per. -cm	I -cm4	E -MPa	Weight -kN/m
0.0	30	706.9	94.2	39760.8	20683	1.668
27.0						

Single Pile Lateral Analysis:
Top Deflection, yt= 2.91000-cm
Max. Moment, M= 84.40-kN-m
Top Deflection Slope, St= -0.01970
N/G! Top Deflection, 2.9100-cm, Exceeds the Allowable Deflection= 2.50-cm

Note: If the program cannot find a result or the result exceeds the upper limit. The result will be displayed as 99999.
The Max. Moment calculated by program is an internal force from the applied load conditions. Structural engineer has to check whether the pile has enough capacity to resist the moment with adequate factor of safety. If not, the pile may fail under the load conditions.

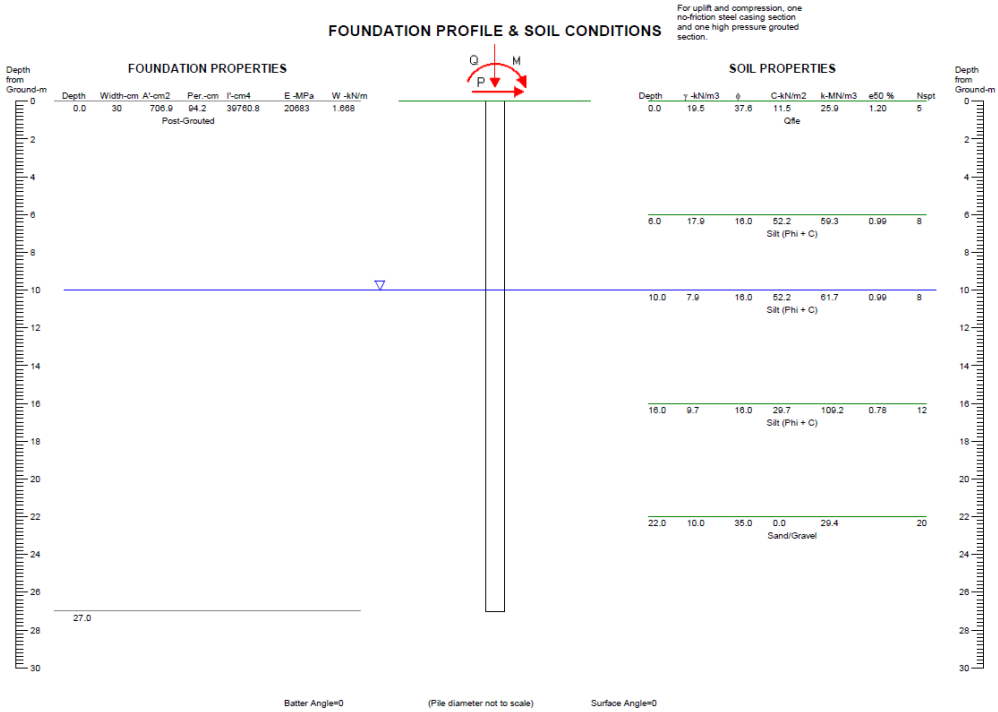

CivilTech Software

Figure 1

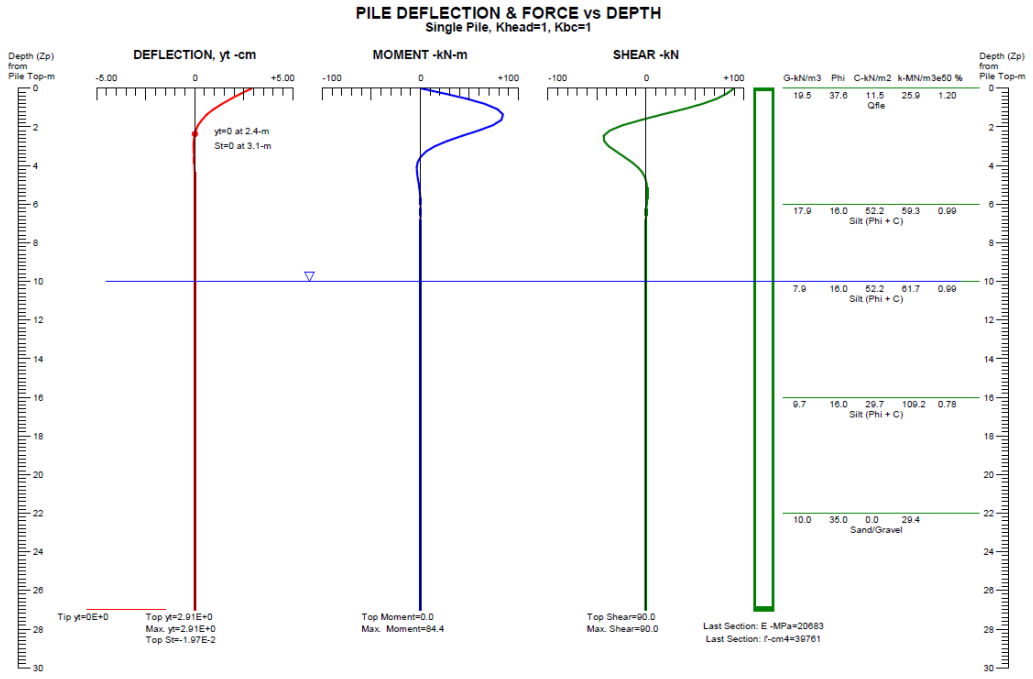

CivilTech Software

Figure 2

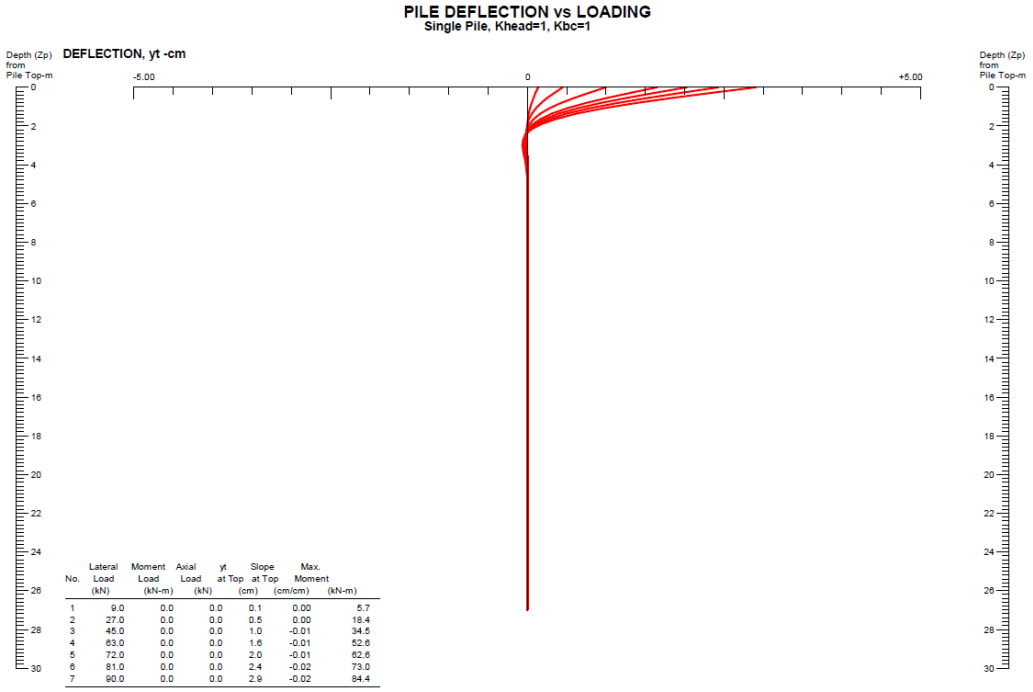

CivilTech Software

Figure 2

LATERAL LOAD vs DEFLECTION & MAX. MOMENT

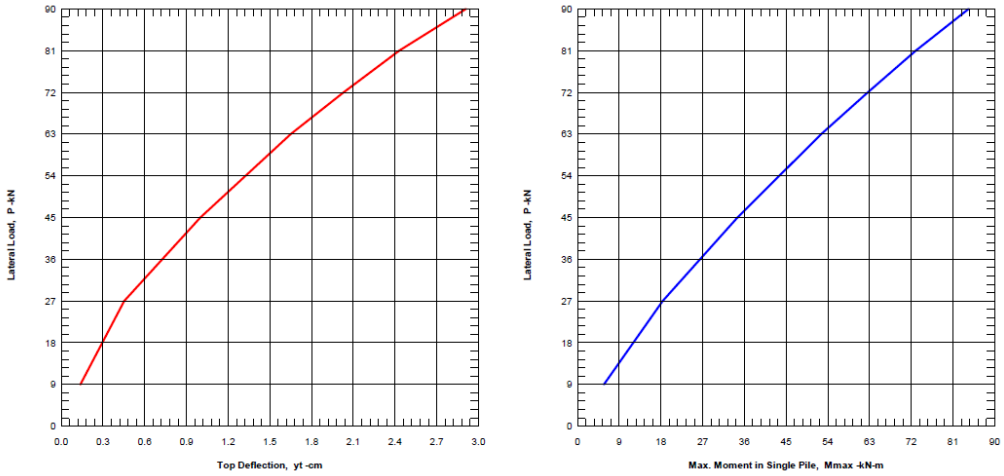

CivilTech Software

Figure 2

Soil Resistance vs. Pile Deflection (p-y)

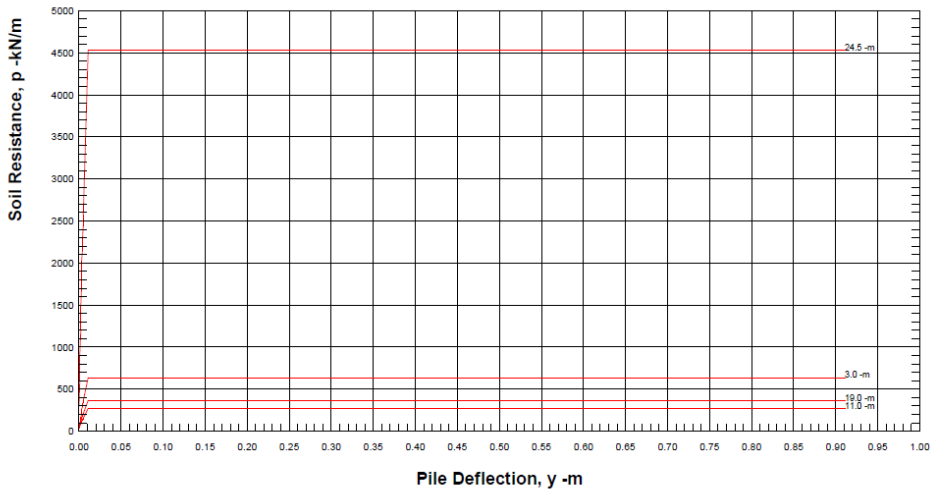

Soil Depth (Zs): 3.0, 11.0, 19.0, 24.5 -m

CivilTech Software

Figure 2

OLoad_L

Soil Resistance vs. Pile Deflection (p-y)

****

Zs -m	p -kN/m	y -m
3.00	0.0	0.000
3.00	32.4	0.000
3.00	64.8	0.001
3.00	97.1	0.001
3.00	129.5	0.002
3.00	161.9	0.002
3.00	194.3	0.003
3.00	226.6	0.003
3.00	259.0	0.003
3.00	291.4	0.004
3.00	323.8	0.004
3.00	343.3	0.005
3.00	361.9	0.005
3.00	637.0	0.011
3.00	637.0	0.311
3.00	637.0	0.611
3.00	637.0	0.911
11.00	0.0	0.000
11.00	34.2	0.000
11.00	52.1	0.001
11.00	66.6	0.001
11.00	79.3	0.002
11.00	90.9	0.002
11.00	101.5	0.003
11.00	111.5	0.003
11.00	120.9	0.003
11.00	129.9	0.004
11.00	138.5	0.004
11.00	146.8	0.005
11.00	154.7	0.005
11.00	272.3	0.011
11.00	272.3	0.311
11.00	272.3	0.611
11.00	272.3	0.911
19.00	0.0	0.000
19.00	46.1	0.000
19.00	70.2	0.001
19.00	89.9	0.001
19.00	107.0	0.002
19.00	122.6	0.002
19.00	137.0	0.003
19.00	150.4	0.003
19.00	163.1	0.003
19.00	175.2	0.004
19.00	186.8	0.004
19.00	198.0	0.005
19.00	208.7	0.005
19.00	367.4	0.011
19.00	367.4	0.311
19.00	367.4	0.611
19.00	367.4	0.911
24.50	0.0	0.000
24.50	300.1	0.000
24.50	600.3	0.001
24.50	900.4	0.001
24.50	1200.5	0.002
24.50	1500.6	0.002
24.50	1689.9	0.003
24.50	1855.9	0.003
24.50	2012.9	0.003
24.50	2162.3	0.004
24.50	2305.4	0.004
24.50	2442.9	0.005
24.50	2575.6	0.005
24.50	4533.1	0.011
24.50	4533.1	0.311
24.50	4533.1	0.611
24.50	4533.1	0.911

Zs - Depth from Soil Top
p - Soil Resistance
y - Pile Deflection

Annex 8. Lateral evaluation using P-Y curves - average case.

LATERAL ANALYSIS

Figure 2

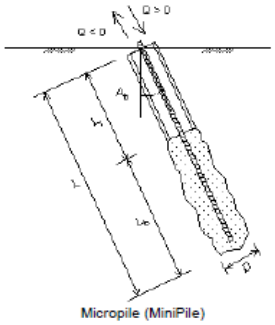

Loads:
Load Factor for Vertical Loads= 1.0
Load Factor for Lateral Loads= 1.0
Loads Supported by Pile Cap= 0 %
Shear Condition: Static

(with Load Factor)
Vertical Load, Q= 0.0 -kN
Shear Load, P= 90.0 -kN
Moment, M= 0.0 -kN-m

Profile:
Pile Length, L= 27.0 -m
Top Height, H= 0.000 -m
Slope Angle, As= 0
Batter Angle, Ab= 0

Soil Data:

Depth -m	Gamma -kN/m3	Phi	C -kN/m2	K -MN/m3	e50 or Dr %	Nspt
0	19	38	27	25.9	0.9	40
6	18	29	53	59.3	1	15
10	8	29	53	61.7	1	15
16	9	31	34	109.2	0.7	35
22	10	41	0	29.4	0.6	45

Pile Data:

Depth -m	Width -cm	Area -cm2	Per. -cm	I -cm4	E -MPa	Weight -kN/m
0.0	30	706.9	94.2	39760.8	20683	1.668
27.0						

Single Pile Lateral Analysis:
Top Deflection, yt= 2.89000-cm
Max. Moment, M= 84.30-kN-m
Top Deflection Slope, St= -0.01960
N/G! Top Deflection, 2.8900-cm, Exceeds the Allowable Deflection= 2.50-cm

Note: If the program cannot find a result or the result exceeds the upper limit. The result will be displayed as 99999.
The Max. Moment calculated by program is an internal force from the applied load conditions. Structural engineer has to check whether the pile has enough capacity to resist the moment with adequate factor of safety. If not, the pile may fail under the load conditions.

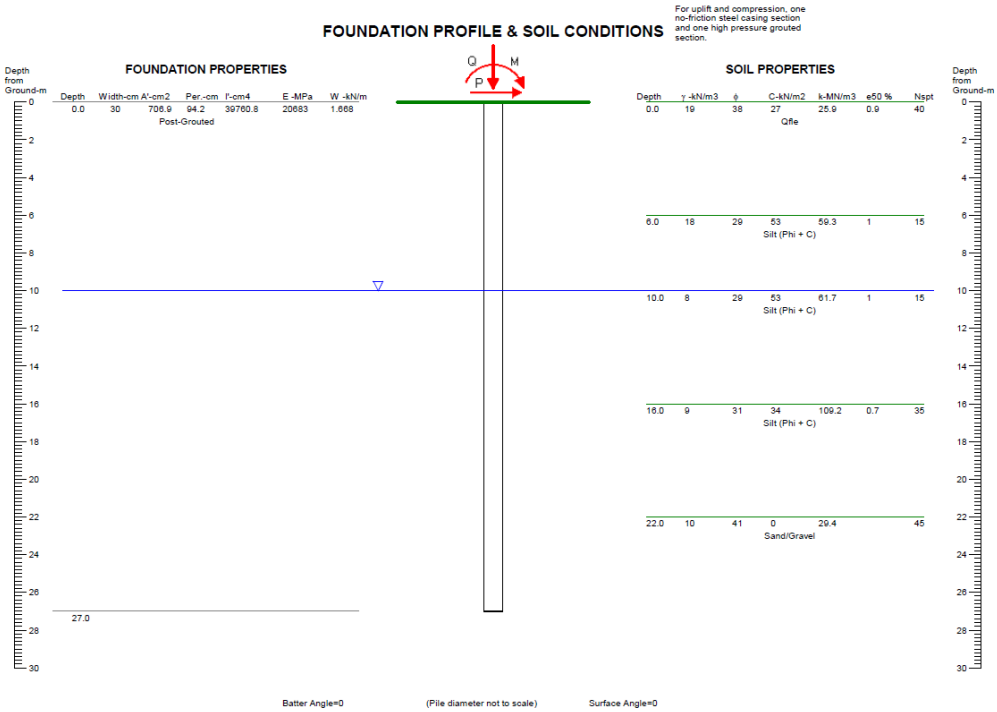

CivilTech Software

Figure 1

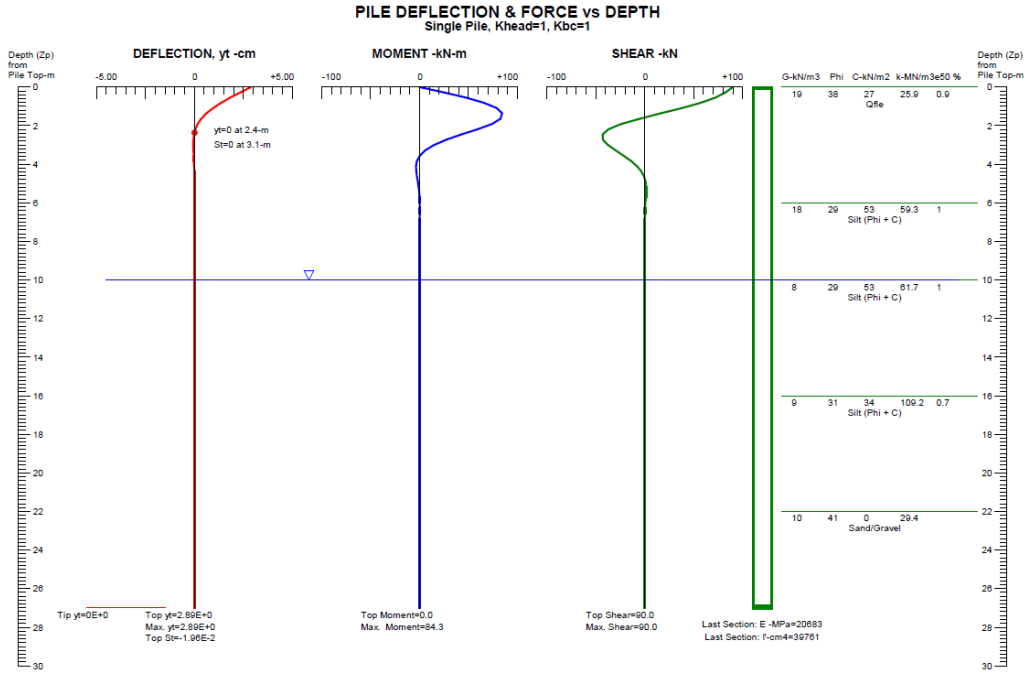

CivilTech Software

Figure 2

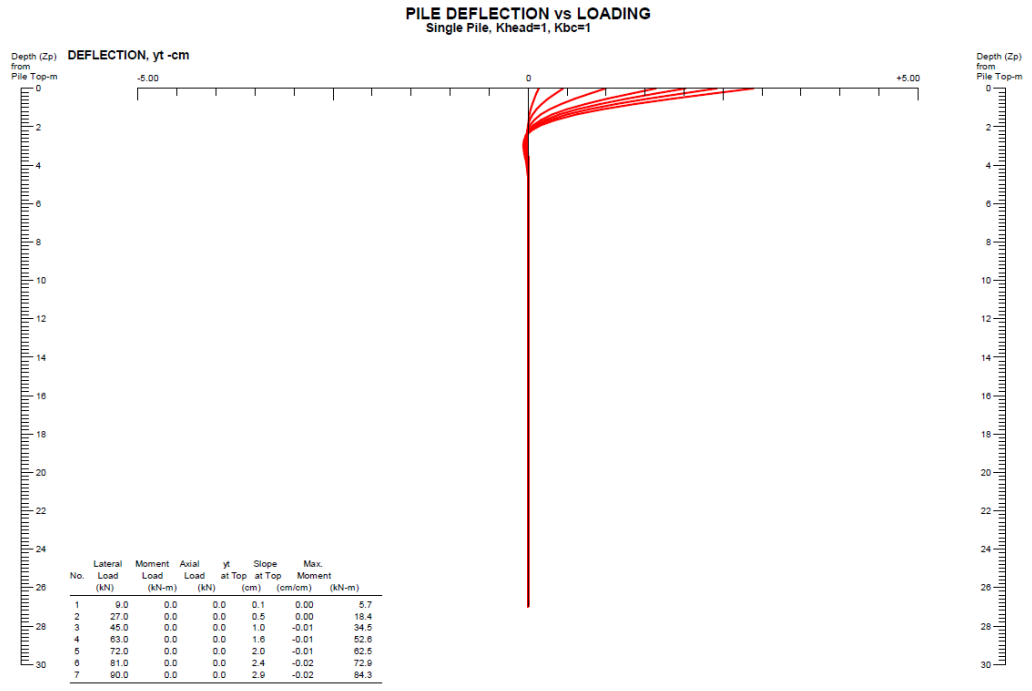

No.	Lateral Load (kN)	Moment Load (kN-m)	Axial Load (kN)	yt at Top (cm)	Slope at Top (cm/cm)	Max. Moment (kN-m)
1	9.0	0.0	0.0	0.1	0.00	5.7
2	27.0	0.0	0.0	0.5	0.00	18.4
3	45.0	0.0	0.0	1.0	-0.01	34.5
4	63.0	0.0	0.0	1.6	-0.01	52.6
5	72.0	0.0	0.0	2.0	-0.01	62.5
6	81.0	0.0	0.0	2.4	-0.02	72.9
7	90.0	0.0	0.0	2.9	-0.02	84.3

CivilTech Software

Figure 2

LATERAL LOAD vs DEFLECTION & MAX. MOMENT

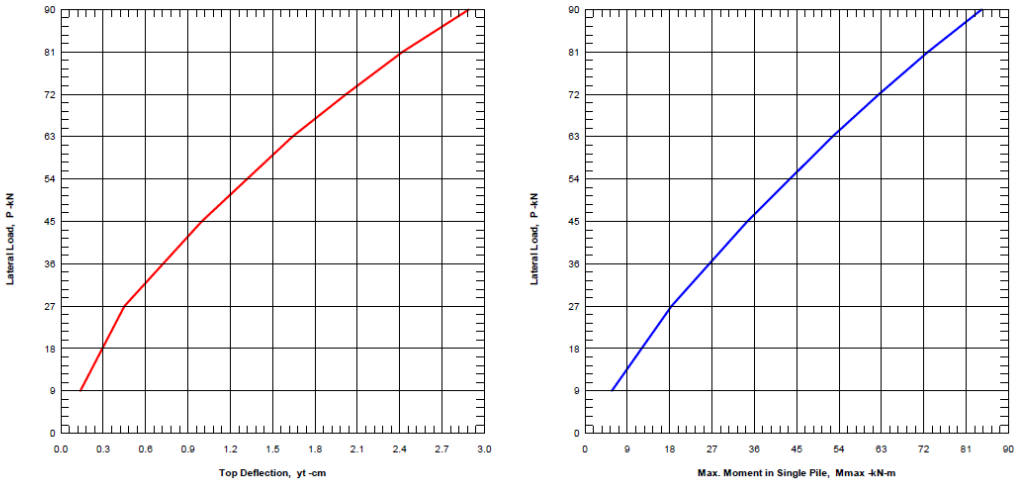

CivilTech Software

Figure 2

Soil Resistance vs. Pile Deflection (p-y)

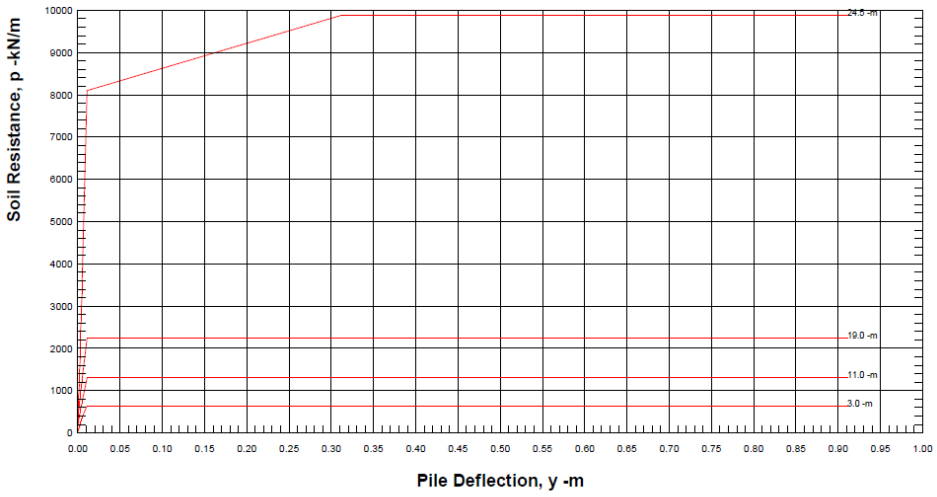

Soil Depth (Zs): 3.0, 11.0, 19.0, 24.5 -m

CivilTech Software

Figure 2

OLoad_L

Soil Resistance vs. Pile Deflection (p-y)

****

Zs -m	p -kN/m	y -m
3.00	0.0	0.000
3.00	32.4	0.000
3.00	64.8	0.001
3.00	97.1	0.001
3.00	129.5	0.002
3.00	161.9	0.002
3.00	194.3	0.003
3.00	226.6	0.003
3.00	259.0	0.003
3.00	291.4	0.004
3.00	323.8	0.004
3.00	346.0	0.005
3.00	364.8	0.005
3.00	642.1	0.011
3.00	642.1	0.311
3.00	642.1	0.611
3.00	642.1	0.911
11.00	0.0	0.000
11.00	163.4	0.000
11.00	249.0	0.001
11.00	318.6	0.001
11.00	379.5	0.002
11.00	434.6	0.002
11.00	485.6	0.003
11.00	533.3	0.003
11.00	578.4	0.003
11.00	621.4	0.004
11.00	662.5	0.004
11.00	702.0	0.005
11.00	740.1	0.005
11.00	1302.6	0.011
11.00	1302.6	0.311
11.00	1302.6	0.611
11.00	1302.6	0.911
19.00	0.0	0.000
19.00	281.0	0.000
19.00	428.3	0.001
19.00	548.0	0.001
19.00	652.7	0.002
19.00	747.6	0.002
19.00	835.2	0.003
19.00	917.3	0.003
19.00	994.8	0.003
19.00	1068.7	0.004
19.00	1139.4	0.004
19.00	1207.4	0.005
19.00	1273.0	0.005
19.00	2240.4	0.011
19.00	2240.4	0.311
19.00	2240.4	0.611
19.00	2240.4	0.911
24.50	0.0	0.000
24.50	300.1	0.000
24.50	600.3	0.001
24.50	900.4	0.001
24.50	1200.5	0.002
24.50	1500.6	0.002
24.50	1800.8	0.003
24.50	2100.9	0.003
24.50	2401.0	0.003
24.50	2701.1	0.004
24.50	3001.3	0.004
24.50	3301.4	0.005
24.50	3601.5	0.005
24.50	8103.4	0.011
24.50	9873.1	0.311
24.50	9873.1	0.611
24.50	9873.1	0.911

Zs - Depth from Soil Top
p - Soil Resistance
y - Pile Deflection

Annex 9. Lateral evaluation using P-Y curves – highest case.

HS - model evaluation:

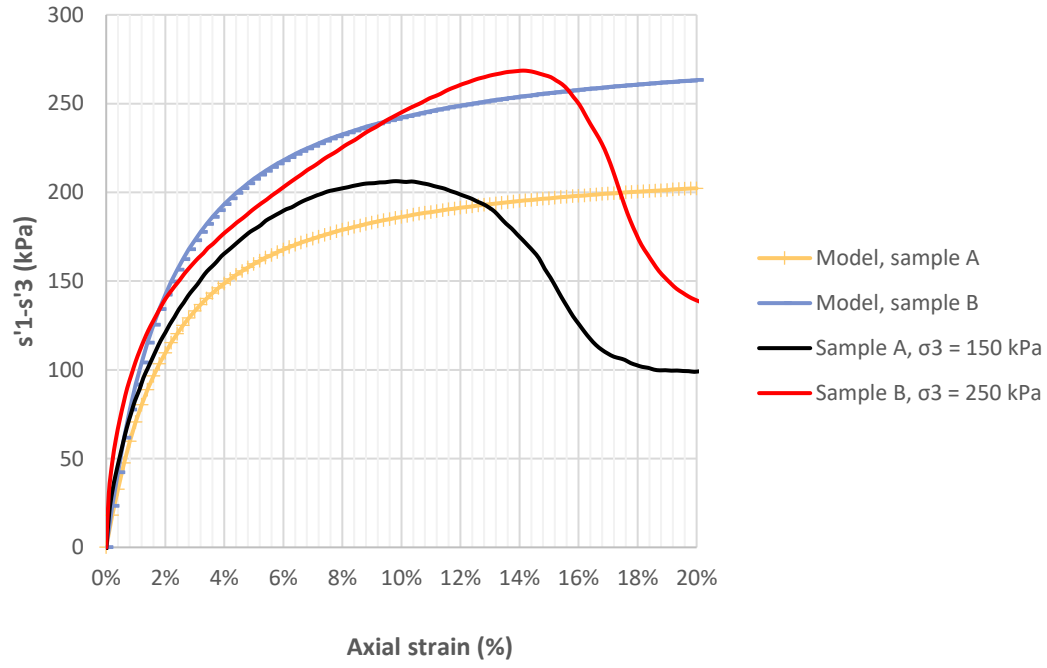

Annex 10. Res. V. HS Model calibration.

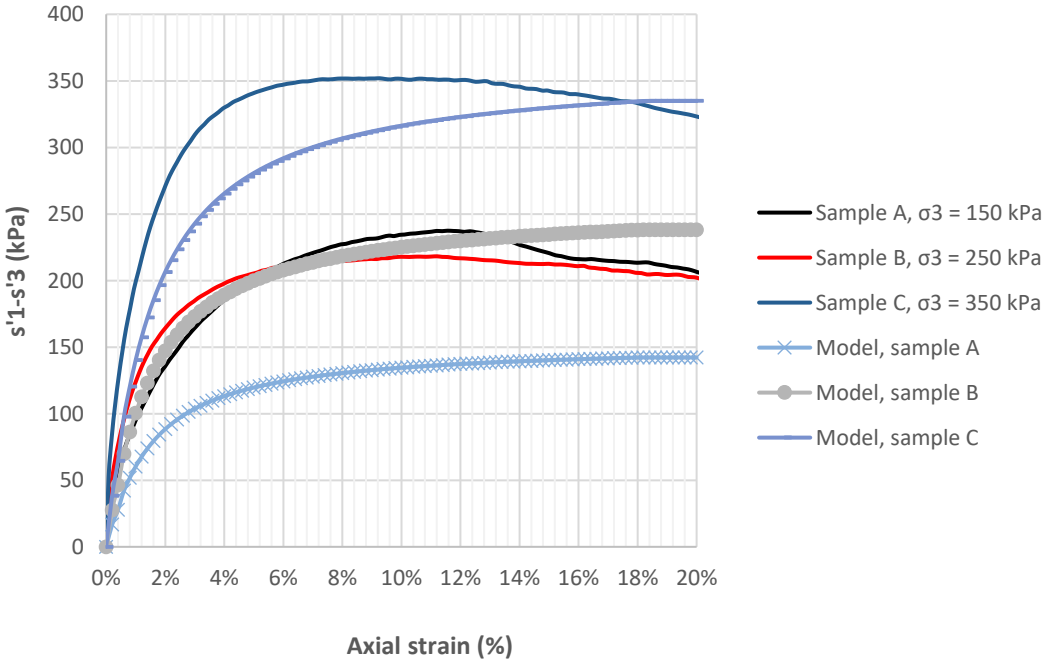

Annex 11. Res. V (2). HS Model calibration.